1,2,4-Triazolyl 5-Azaspiro[2.4]heptanes: Lead Identification and Early Lead Optimization of a New Series of Potent and Selective Dopamine D3 Receptor Antagonists

13 August 2025

1,2,4-Triazolyl 5-Azaspiro[2.4]heptanes: Lead Identification and Early Lead Optimization of a New Series of Potent and Selective Dopamine D3 Receptor Antagonists.

Fabrizio Micheli[*,a], *Alessia Bacchi*[#], *Simone Braggio*[a], *Laura Castelletti*[a], *Palmina Cavallini*[a], *Paolo Cavanni*[a], *Susanna Cremonesi*[a], *Michele Dal Cin*[a], *Aldo Feriani*[a], *Sylvie Gheanne*[a], *Mahmoud Kajbaf*[a], *Luciano Marchió*[#], *Selena Nola*[a], *Beatrice Oliosi*[a], *Annalisa Pellacani*[a], *Elisabetta Perdona'* [a], *Anna Sava*[a], *Teresa Semeraro*[a], *Luca Tarsi*[a], *Silvia Tomelleri*[a], *Andrea Wong*[a], *Filippo Visentini*[a], *Laura Zonzini*[a], *and Christian Heidbreder*[b].

[a] Aptuit s.r.l., Via Fleming 4, 37135 Verona (Italy), [b]Indivior Inc, The Fairfax Building, 10710 Midlothian Turnpike, Suite 430, Richmond VA 23235, USA, [#] Dipartimento di Chimica, Universita' di Parma, Viale delle Scienze, 17A - Campus, I-43124 Parma, Italy

[d]AUTHOR EMAIL ADDRESS*: fabrizio.micheli@aptuit.com; Aptuit s.r.l., Via Fleming 4, 37135 Verona (Italy); Tel. +39-045-8218515; Fax. +39-045-8219111

---

[d] Abbreviations: hERG, human Ether-à-go-go Related Gene; NCE, novel chemical entity; PK, pharmacokinetic; CYP P450, cytochrome P450; hCli, human intrinsic clearance; rCli, rat intrinsic clearance; MW, molecular weight; cLogP, calculated logP; PSA, polar surface area; F%, bioavailability; Fa, Fraction Absorbed; Eh, hepatic extraction B/B, brain/blood; Clb, blood clearance; Vs, distribution.

ABSTRACT. A novel series of 1,2,4-Triazolyl 5-Azaspiro[2.4]heptanes with high affinity and selectivity at the Dopamine (DA) D3 receptor (D3R) is described. Some of these compounds also have high selectivity over the hERG channel and were characterized with respect to their pharmacokinetic properties both *in vitro* and *in vivo* during lead identification and early lead optimization phases. A few derivatives with overall favorable developability characteristics were selected for further late lead optimization studies.

Introduction

Long-lasting adaptations in the brains of individuals addicted to drugs support the concept of addiction as a chronically relapsing disorder that is characterized by the compulsion to seek and take the drug, the loss of control in limiting drug intake, and the emergence of a negative emotional state when access to the drug is withdrawn. The inherent complexity of these neuroadaptations makes the therapeutic management of substance use disorder (SUD) a major challenge for the discovery and development of safe and efficacious pharmacotherapeutic strategies ensuring satisfactory patient compliance and promoting drug abstinence and recovery.

Half a century of research has pointed towards activation of the mesolimbic dopamine (DA) system as a common denominator in response to virtually all drugs of abuse that are voluntarily self-administered by laboratory animals and humans. It is thus quite natural that DA receptors were considered as reasonable targets for the development of SUD medications. Of particular interest is the restricted high-density expression of the DA D3 receptor (D3R) subtype into key elements of the mesolimbic DA system such as the ventral striatum, midbrain, and pallidum, which have all been associated with behaviors

---

volume at steady state; DA, Dopamine. ER, ethoxyresorufin; FCA, 7-methoxy-4-triflouromethylcoumarin-3-acetic acid; BMC, 3-butyryl-7-methoxycoumarin; MMC, 4-methylaminomethyl-7-methoxycoumarin; DEF, diethoxyflourescein; 7-BQ, 7-benzyloxyquinoline

controlled by the presentation of drug-associated cues[1-3]. The strategic localization of the D3R together with changes in its expression following acute, sub-chronic or chronic exposure to drugs of abuse have triggered research efforts leading to the discovery, synthesis and characterization of highly potent and selective D3R antagonists[1-4]. Nonclinical evidence clearly supports the contention that selective D3R antagonists show promise for the treatment of SUD as reflected by their potential to (1) regulate the motivation to self-administer drugs under schedules of reinforcement that require an increase in work demand, and (2) disrupt the responsiveness to drug-associated stimuli that play a key role in reinstatement of drug-seeking behavior triggered by re-exposure to the drug itself, re-exposure to environmental cues that had been previously associated with drug-taking behavior, or stress.[1-3]

GlaxoSmithKline (GSK) reported compounds[5,6] with high *in vitro* and *in vivo* selectivity at the D3R, which can attenuate or block the effects of drugs of abuse in a wide range of animal models of addiction. Additional compounds were also disclosed by the pharmaceutical industry and academic centers[7].

The scope of the present work was to identify potential replacements of the "amino portion" of the above mentioned scaffolds. Two attempts of "amino portion" substitution were recently disclosed [8,9] through a mixed computational and medicinal chemistry strategy that identified both morpholines and octahydropyrrolo[2,3-b]pyrroles.

Using a similar approach, the present work describes a new series of 5-Azaspiro[2.4]heptanes with a detailed Structure Activity Relationship (SAR) in lead identification and early lead optimization phases; a detailed *in vitro* and *in vivo* pharmacokinetic (PK) strategy to selected compounds for the subsequent late lead optimization phase is also presented.

Results and discussion

Since the discovery of the D3R in 1990, both industrial and academic researchers have been trying to identify novel chemical entities (NCEs) that selectively modulate the D3R[4,7]. Among the most characterized derivatives, both *in vitro* and *in vivo*, **SB-277011**, **1**[10] represents one of the prototypical

selective D3R antagonists. In 2010, GSK presented a full characterization of **GSK598809A**, **2**[5] which was progressed to clinical study in humans[11]. Examples of structurally unrelated templates are **PG01037**, **3**[12] the tranylcypromine substituted *cis*-hydroxycyclobutylnaphthamides (**CJ-1882**, **4**)[13], and **YQA14** (**5**)[14], all shown in Figure 1. The octahydropyrrolo[2,3-b]pyrrole derivatives series[9] (**6**) is also reported in the same figure.

Figure 1 goes here

All these structures can, at least theoretically, fit the general "pharmacophore model" for D3R antagonists originally described by Hackling and Stark[15]. In Figure 2, **SB-277011** was pictorially positioned along such a model, which requires an aryl region, an H-bond acceptor, a spacer, the "amino" region and another aryl moiety.

Figure 2 goes here

The tridimensional representation of this theoretical space in a D3R model clearly highlights the medicinal chemistry challenges associated with the identification of an appropriate "amino portion". Such a scaffold must be compliant with specific criteria including appropriate basicity to interact with $Asp^{3.32}$ in the orthosteric binding site[16]; contribution to the overall selectivity of the molecule vs. the DA D2 receptor (D2R), and novelty from an intellectual property perspective. Last, but not least, new molecules must have the appropriate "developability"[17] profile to be progressed towards clinical trials.
Mixed approaches based on the D3R crystal structure[18] were attempted for the identification of the previously mentioned NCEs[8,9]. As described more than 10 years ago[19], "scaffold hopping" is also used by medicinal chemists to identify structurally novel molecules starting from known active compounds and modifying their central core structure.

This approach can lead to completely different core structures that can then be characterized through screening cascades. In this manuscript, our efforts led to the identification of the 5-azaspiro[2.4]heptane moiety as the novel "amino portion".

Based on our previous experience[8,9] the new molecules identified in this exploratory process were initially characterized for their binding activity at the human D3R and D2R, while a few selected derivatives were also evaluated in functional assays to determine their agonist and antagonist properties at the same receptors. The aim of this approach was to identify potent D3R antagonists (pKi ≥ 8), endowed with high selectivity (ideally ≥ 100-fold) vs. the D2R, high (≥ 100-fold or hERG fpKi < 6.0) selectivity vs. the hERG ion channel (for preventing potential cardiovascular liability) as well as a ≥ 50-fold selectivity vs. muscarinic M1-3 receptors (based on previous liability shown by some D3R antagonists reported in literature).

To ensure appropriate developability, all NCEs went through *in vitro* pharmacokinetic (PK) assays such as CYPEX bactosome P450 inhibition and rat and human *in vitro* clearance (rCli and hCli, respectively) in liver microsomes early in the screening cascade.

The synthesis of the new scaffolds is described in Scheme 1, while all the new compounds identified (**7-85a**) are reported in Tables 1 to 11. **SB-277011** (**1**) was used as internal standard for biological assays, while literature data[5] were reported for **GSK598809A** (**2**).

Scheme 1 goes here

Since the 5-azaspiro[2.4]heptane template contains two stereogenic centers, the relative stereochemistry of the compounds can lead to the isolation of both "*cis*" and "*trans*" isomers. Early in the process, the racemate was submitted to test and promising results resulted in each single enantiomer being tested after chromatographic separation. Later on in the exploration, only specific isomers were tested; the X-rays of a few key intermediates were obtained as well as described later on.

The exploration of the newly designed "amino portion" started with an unsubstituted phenyl ring (see Table 1 for derivatives **7** and **8**). Derivative **8b**, which showed nanomolar affinity at the D3R, had about 140-fold selectivity vs. the D2R and more than 500-fold selectivity vs. the hERG channel. This compound was further profiled and proved to be fully inactive as an agonist at the D3R; it behaved as an antagonist (fpKi = 8.18 ± 0.09) with 100-fold selectivity vs. the D2R (fpKi = 6.17 ± 0.16) when tested in a functional DA D2 assay (see Table 8 for a comparison between binding and functional data). In addition, derivative **8b** was completely inactive (fpKi < 4.0) at the DA D1 receptor (D1R) and DA D4 receptor (D4R)), whereas 100-fold selectivity was also observed at the M1 and M3 receptors (fpKi = 6.13 ± 0.11 and 5.69 ± 0.25, respectively) suggesting that the new scaffold could be a promising starting point for exploration. Considering its in *vitro* PK properties, compound **8b** showed IC_{50} values greater than 50 μM on all CYP P450 isoforms (namely CYP1A2, CYP2C9, CYP2C19, CYP3A4 DBOMF and CYP3A4 7BQ) tested with the exception of CYP2D6 (IC_{50} = 0.13 μM).

The introduction of a $–CF_3$ moiety on the *para* position of the phenyl ring (**9**, **10**) of the "amino portion" increased the lipophilicity (cLogP)[20] of the overall molecule of about one unit. This increase led to an improvement in the affinity at the D3R of about one log unit on the best enantiomers both in the *trans* (**9a**) and in the *cis* (**10a**) configurations of the 5-azaspiro[2.4]heptane moiety. The difference in affinity between the two enantiomers was greater for the cis vs. the *trans* isomer. The substitution had no effect on the functional activity of the compounds, which continued to behave as full antagonists (Table 8). No modification on the muscarinic profile of compound **10a** was observed (fpKi = 6.51 ± 0.04 and 6.56 ± 0.11 respectively for M1 and M3 receptors) maintaining the selectivity at about 400-fold over these receptors. Selectivity vs. the D2R was increased by about 350-fold, while selectivity vs. the hERG channel was greater than 600-fold, even if the affinity for the channel was also slightly increased to 0.4 μM.

Both compounds were also tested for *in vitro* PK properties. Compound **9a** showed IC_{50} values greater than 17 μM on all CYP P450 isoforms tested with the exception of CYP2D6 (IC_{50} = 1.3 μM), while

compound **10a** showed IC_{50} values greater than 17 μM on all CYP P450 isoforms tested with the exception of CYP2D6 and CYP3A4 7BQ (IC_{50} = 1.3 μM and 0.30 μM, respectively). Derivative **9a** showed relatively low human intrinsic clearance (hCli) on microsomes (22 μL/min/mg protein) and high clearance in rat (rCli) microsomes (161 μL/min/mg protein). However, derivative **10a** showed relatively high Cli in both species (hCli= 86 and rCli= 83 μL/min/mg protein, respectively). The last *in vitro* parameter to be considered (based on the need for brain penetration)[17e] was the blood and tissue (rodent) protein binding. Both derivatives had excellent fraction unbound (Fu) both in brain (Fu_{br}) and blood (Fu_{bl}). For **9a** the Fu_{br} was 4.8%, while its Fu_{bl} was 12%. Derivative **10a** showed Fu_{br} equal to 9.5% and Fu_{bl} equal to 10.2%. Altogether these data suggested that these molecules are endowed with *in vitro* properties that are suitable for further optimization. Selected PK data are reported in Tables 9 and 10.

In agreement with previously reported procedures[9,16], derivative **10a** was fitted in a D3R model based on x-ray crystal structure using MOE[21]. As clearly shown in Figure 3, derivative **10a** (red) can adopt similar conformations to compound **2**. One may appreciate, with the obvious limitation of reproducing in two dimensions a 3D interaction, that the basic nitrogen of the new "amino portion" can interact with $Asp^{3,32}$. Both derivative **10a** and derivative **2** (in yellow) formed a salt bridge with the aspartic acid in the receptor. Furthermore, the aromatic portion (the oxazole in both compounds) clearly pointed towards the extracellular loop (EL) of the receptor in agreement with literature data. Finally, the new template was able to direct the $–CF_3$ moiety of the phenyl ring of derivative **10a** in a similar hydrophobic region common with compound **2**.

Figure 3 goes here

Keeping constant the p-CF_3 substitution on the phenyl ring and shortening the linker chain (from C3 to C2, derivatives **11** and **12**) led to a reduction in affinity at the D3R; an increase in length (from C3 to C4) also had a detrimental effect on the affinity at the D3R (**13**). The change in the linker length (**12**, **13**) did not modify the functional behavior of the compounds as reported in Table 8.

To verify whether the rotation of the phenyl group of the "amino portion", i.e. whether a change in the amount of that dihedral angle, had any effect on the affinity of the compounds both at the D3R receptor and at the hERG channel, the $-CF_3$ substituent was added in *ortho* position (without changing the cLogP, **14**, **15**). Although the impact on affinity was not obvious for the *trans* isomer, basically maintaining nanomolar affinity at the D3R, a more pronounced effect was observed with the cis isomer with a reduction in affinity of about 10-fold at the D3R. The affinity of the best compound at the hERG channel was not affected.

To verify if the cLogP itself had a role in driving the affinity at the D3R, the $-CF_3$ moiety was replaced by a single –F atom (**16**, **17**; cLogP moved from 3.4 to 2.7). Comparing the most potent compound in each series (i.e. **10a** vs. **17b**) no major difference was observed in terms of affinity and selectivity vs. the D2R and hERG targets. Furthermore, the functional profile (full antagonism, Table 8) remained unchanged. The *in vitro* PK profiling for **17b** showed IC_{50} values greater than 17 μM on all CYP P450 isoforms tested with the exception of CYP2D6 and CYP3A4 7BQ (IC_{50}= 0.7 μM and 3.4 μM, respectively). The compound showed relatively low hCli on microsomes (37 μL/min/mg protein) and moderate rCli (73 μL/min/mg protein). Finally, both Fu_{br} and Fu_{bl} were exceptionally high with values of 27% and 38%, respectively supporting a promising profile to interact with the D3R in the brain.

The introduction of a second –F atom (**18**, **19**) led to a slight change in the overall cLogP, but had no major impact on the affinity at the D3R and the selectivity profile of the best enantiomer (**19b**). Furthermore, also the functional profile remained unchanged as reported in Table 8.

The *in vitro* PK profile of **19b** revealed IC_{50} values greater than 17 μM on all CYP P450 isoforms tested with the exception of CYP2D6 (IC_{50}= 1.2 μM). Although hCli on microsomes was relatively high (53 μL/min/mg protein), rCli was definitely higher (161 μL/min/mg protein). Both Fu_{br} and Fu_{bl} were high with values of 28% and 33%, respectively, suggesting again a promising profile to interact with the D3R in the brain.

A slight increase in cLogP with respect to compound **10a** was achieved with the introduction of a single –F on the already $-CF_3$ substituted phenyl ring (cLogP from 3.4 to 3.6 in derivatives **20**-**23**). The

introduction of the –F in position 2, keeping the $–CF_3$ in position 4 of the phenyl ring, did not change significantly the affinity of the best enantiomer (**21b**) at the D3R and at the hERG channel with still more than 500-fold selectivity vs. the D2R while increasing selectivity vs. the hERG channel to more than 1250-fold. The cis enantiomer showed greater affinity at the D3R compared to the *trans* enantiomer. As reported in Table 8, functional antagonism was confirmed for compounds **20b** and **21b**. A slightly lower selectivity window with high D2R functional activity was observed for **21b** (Table 8). With regards to *in vitro* PK properties. **20b** showed an improved profile at CYP2D6 (IC_{50}= 5.7 μM) with IC_{50} values greater than 17 μM on all CYP P450 isoforms tested with the exception of CYP1A2 (IC_{50}= 0.8 μM). Compound **21b** showed IC_{50} values greater than 17 μM on all CYP P450 isoforms tested with the exception of CYP2D6 (IC_{50}= 0.6 μM). Considering a marked difference in the Cli of the two derivatives, with **20b** showing low hCli and rCli (20 and 23 μL/min/mg protein, respectively) and **21b** showing high hCli and moderate rCli (107 and 59 μL/min/mg protein, respectively), the two compounds were selected to validate *in vitro* data with rodent *in vivo* data[22, 23]. Therefore, both compounds were tested in a portal vein-cannulated rat model[23]. Compound **20b** showed a fraction absorbed (F_a%) of 70% with moderate distribution volume (V_{ss}= 4.9 L/kg) and moderate clearance in blood as expected from the *in vitro* parameters (Cl_b= 32.9 mL/min/kg) leading to moderate half-life ($T_{1/2}$ = 2.3 h) and good bioavailability (F% = 49%) given the relatively low hepatic extraction (E_H = 0.31). Compound **21b** had a fraction absorbed (F_a%) of 8.6% with low distribution volume (V_{ss}= 0.49 L/kg), clearance in blood in relative agreement with the *in vitro* parameters (Cl_b= 15.1 mL/min/kg) although lower than expected. The half-life was short ($T_{1/2}$ = 0.41 h) and bioavailability was low (F%= 4%) because of the poor fraction absorbed and a doubled E_H (0.56). This head to head comparison therefore demonstrated a relatively good reliability of the Cli parameters, but also highlighted a striking difference in terms of the *in vivo* PK properties of the diastereoisomers. Brain penetration was also assessed and a brain to blood (B/B) ratio was achieved using the area under the curve (AUC) values. Both compounds had good ratios, namely 1.6 and 0.8 for **20b** and **21b,** respectively.

Interestingly enough, when the –F was kept in position 4 of the phenyl ring and the $–CF_3$ moiety was in position 2, the most active enantiomer resulted in the *trans* derivative **22a**; neither the overall affinity of this compound at the D3R nor its selectivity vs. off-targets changed significantly. The *in vitro* PK parameters of this derivative did not change either. **22a** showed a Fu_{br}= 8.9% and a Fu_{bl}= 12.3%, while both hCli and rCli were moderate (65 and 51 µL/min/mg protein, respectively). In contrast, derivative **23b** showed Fu_{br} and Fu_{bl} values that were comparable to the other geometric isomer (8.6 and 13.5% respectively), both hCli and rCli significantly increased (320 and 151 µL/min/mg protein, respectively) suggesting a role of the 2-CF_3 moiety in the relative conformation of the phenyl ring, potentially through a change in dihedral angle in the *cis* derivative to a more metabolically unstable situation.

The introduction of a hydroxyl moiety in the side chain (C3 side chain, derivative **24**) to look for additional interaction within the receptor and to reduce the cLogP ever further, was detrimental for the affinity profile. Finally, the introduction of a 3,5 di-chloro substitution on the phenyl (**25**,**26**) had no major effect on the affinity at the D3R, but was clearly detrimental for the selectivity vs. the D2R and vs. the hERG channel.

Based on the preliminary results of this early exploration, it was decided to maintain the *p*–CF_3 phenyl moiety of the "amino portion", but to replace the methyl oxazole ring of **10** with different aromatic or heteroaromatic moieties.

The results for 5-membered heteroaromatics are reported in Table 2. The introduction of a methyl thiazole (**27, 28**) despite an increase in cLogP and in PSA[20] led to a slight decrease in affinity at the D3R when compared to the racemic *cis* derivatives (**28** vs. **10**). The removal of the methyl group and a change in relative orientation of the heteroatoms (**29**, **30**) led to equipotent derivatives (**30** vs. **10**) with about 300-fold selectivity over the D2R and the hERG channel, but with more than one log unit increase in cLogP. The introduction of one extra nitrogen atom in the system (**31**, **32**), despite a significant increase in PSA, left the primary affinity almost unchanged, but produced an unexpected drop in affinity at the hERG channel in the *cis* racemate (**32**), which did not match the significant increase in affinity observed for the *trans* derivative (**31**). The functional profile of **32** was unchanged (Table 8).

Unfortunately, and in contrast with other compounds in this series, **32** was not progressed since it showed a significantly reduced selectivity vs. the M1 receptor (fpKi= 6.77 ± 0.18).

The introduction of a 2 thiophene (**33**) further increased lipophilicity while reducing PSA. This had a beneficial effect on the affinity at the D3R leading to a sub-nanomolar derivative on the racemate, but this change also had a detrimental effect on the hERG affinity. Its regioisomers (**34**) was equivalent both in terms of potency and selectivity. The same behavior was also observed in the case of the furane moiety (**35**, **36**), but high affinity at the hERG channel was observed for derivative **36**. The introduction of a pyrazole moiety (**37**, **38**) led to compounds with high affinity at the D3R and high selectivity. Derivative **37** showed about 200-fold selectivity vs. the D2R and the hERG channel, while **38** increased such window to more than 450-fold. To complete the 5-membered preliminary heterocyclic replacement, the isoxazole **39** was prepared. In this case, the affinity at the D3R was maintained, but with a slight reduction of selectivity as well as an increase in the hERG affinity. None of these derivatives were tested for *in vitro* PK properties because of their racemic nature and their suboptimal profile for further progression through the screening cascade.

The exploration of the oxazole replacement (**10**) was pursued with substituted phenyl rings, so that some of the original oxazole polarity/charge distribution was present (see Table 3 with only the best enantiomer of the derivatives with *cis* configuration).

Derivative **40a** (*p*-$CONH_2$ phenyl) achieved a 2200-fold selectivity over the D2R and a 5000-fold selectivity over the hERG channel, thus supporting the potential of this sub-series. The compounds showed no activity at the D1R and D4R (pKi < 4.50) and a more than 2500-fold selectivity was also achieved vs. M1 and M3 receptors (fpKi= 6.34 ± 0.05 and 6.37 ± 0.08, respectively). The i*n vitro* PK profile revealed IC_{50} values greater than 5 μM on all CYP P450 isoforms tested. hCli on microsomes was high (155 μL/min/mg protein), rCli was moderate (41 μL/min/mg protein); Fu_{br} was equal to 4.4% and Fu_{bl} resulted 14.1%. The modelling studies performed on the compound (Figure 4) suggested the possibility for the amide to positively interact with additional groups present in the secondary binding pocket (SBP)[16] of the D3R.

Moving the amide portion to position 3 of the aromatic ring (*m*-$CONH_2$ phenyl; **41a**) led to about half a log unit reduction in the affinity at the D3R, but also led to a similar reduction in affinity at the other off-targets. Consequently, selectivity vs. the D2R was greater than 1300-fold and selectivity over the hERG channel was 6000-fold; more importantly the absolute hERG value was 3 μM compared with a 0.4 nM affinity at the D3R. The compound showed no affinity at the D1R and only low affinity at the D4R (fpKi= 5.23 ± 0.03); affinity at the M1 and M3 receptors was also moderately low (fpKi= 6.58 ± 0.16 and 6.42 ± 0.10, respectively) leading to more than 550-fold selectivity at these receptors. When tested for *in vitro* PK properties, **41a** showed IC_{50} values greater than 3 μM on all CYP P450 isoforms tested. hCli on microsomes was comparable to derivative **40a** (187 μL/min/mg protein), while rCli was higher (92 μL/min/mg protein) suggesting an increased metabolic transformation of the now unprotected position 4 of the phenyl ring in rodents. Conversely, both Fu_{br} and Fu_{bl} were quite similar to the previous compound (3.7 and 6.7%, respectively). Both **40a** and **41a** were tested in a functional D3R assay, confirming an unchanged antagonist behavior (Table 8).

The insertion of the amide moiety in position 2 of the phenyl ring (*o*-$CONH_2$ phenyl; **42a**) led to a significant decrease in affinity at the D3R (about 100-fold when compared to **40a**) as well as a decrease in selectivity vs. the D2R. It was hypothesized that the change in the dihedral angle induced by the *o*-amide insertion disfavored the interactions with key residues within the D3R and the SBP, leaving the residues within the D2R unchanged. Alternatively, one may hypothesize that such a substituent may have generated steric clashes preventing the best fitting within the binding pocket. To find additional hints which could help to explain better the observed SAR, all the three structures were modeled within the D3R model (Figure 4) as previously reported[9], and the GBVI/WSA dG scoring function as implemented in MOE[21] was used. Subsequently the "lowest score" poses were submitted to conformational search using LowModeMD (MOE) and the lowest energy conformations obtained were further minimized. The ligand-protein affinity was re-calculated and the analysis of the values observed (data in the experimental part), suggested a trend in line with the binding affinity of the derivatives (**40a**,

41a, **42a**), even if the absolute difference in energy did not fully justify the differences observed in the binding affinities for **42a**.

Figure 4 goes here

The introduction of a *p*-SO_2NH_2 phenyl (**43a**) slightly decreased cLogP, but greatly increased the PSA value; the affinity at the D3R was maintained and the selectivity over the D2R and the hERG channel remained high (about 700-fold). Unfortunately, the absolute affinity at the hERG channel was about 0.2 μM and the compound was not progressed. The replacement of the sulphonamide group with an acetyl moiety (**44a**) increased cLogP reducing the PSA value. The affinity at the D3R was unaltered leading to a selectivity vs. the D2R greater than 2000-fold. Unfortunately, the fpKi observed at the hERG channel was similarly high. The nitrile derivative **45a** behaved similarly with very high affinity at the D3R and high selectivity vs. the D2R, but with a comparably high hERG affinity. In contrast, the introduction of a *p*–CH_2CONH_2 (**46a**) group on the phenyl group led to a slight decrease in affinity at the D3R with respect to derivative **10a**. Selectivity vs the D2R remained greater than 500-fold and the selectivity vs. the hERG channel was increased to about 8900-fold with an absolute value of 7.5 μM, leading to one of the lowest hERG affinity up to that point of the exploration. Accordingly, *in vitro* PK data were generated and the compound showed IC_{50} values greater than 7 μM on all CYP P450 isoforms tested; hCli on microsomes was moderate (58 μL/min/mg protein), while rCli was low (22 μL/min/mg protein). In terms of free fraction, both Fu_{br} and Fu_{bl} were relatively high (5.2 and 14.1 %, respectively).

In light of the promising results achieved with derivatives **40a** and **41a**, a minimal bio-isosteric replacement of the primary amide was attempted and the oxazole derivatives **47a** and **48a** were prepared. Derivative **47a** reached sub-nanomolar affinity (0.07 nM) at the D3R with a more than 5300-fold selectivity window vs. the D2R and more than 2200-fold selectivity over the hERG channel. The compound showed no affinity at the D1R and D4R; the affinity at the M1 and M3 receptors was also moderately low (fpKi= 6.17 ± 0.01 and 6.52 ± 0.11, respectively) leading to about 4500-fold selectivity

at these muscarinic receptors. The functional activity confirmed the antagonistic activity at the D3R. Despite a relatively high cLogP, the *in vitro* PK profile of **47a** showed IC_{50} values greater than 3 μM on all CYP P450 isoforms tested. In line with our expectations, however, this high value was also reflected in a reduction of free compound both in brain and blood (Fu_{br} and Fu_{bl}= 1.0 and 1.2 %, respectively). In addition, Cli values reflected the increased lipophilicity: hCli and rCli were increased to 352 and 276 (μL/min/mg protein), respectively. Comparable results were obtained with derivative **48a** (Table 9). No further bio-isosteric replacement exercise was performed at that stage of the project and this activity was postponed to a subsequent lead optimization phase. Functional data for these two derivatives are reported in Table 8.

A rapid exploration of the tolerability of the scaffold to basic 6-membered heteroaromatics was performed using racemic mixtures (and consequently both *trans* and *cis* isomers were also assayed). The results of this exploration are reported in Table 4. For the pyridine moiety (**49**-**54**), the *cis* pyridin-2-yl substituent (**54**) showed the best affinity at the D3R and a 660-fold selectivity vs. the D2R. The *cis* derivative **52** (pyridine-3-yl moiety) showed a more balanced profile with increased selectivity at the hERG up to 680-fold and a 1.2 μM absolute hERG value vs. a 0.2 μM hERG value for derivative **54**. Although the introduction of a second nitrogen atom (**55**-**62**) in the six-membered ring system proved to be efficient for the reduction in overall lipophilicity, it failed to show any major advantage in terms of affinity at the D3R and overall selectivity. One of the most balanced derivatives was the pyridazine-4-yl (**62**), which showed (once again on the *cis* isomer) good affinity at the D3R and 390- and 630-fold selectivity over the D2R and the hERG channel, respectively (the absolute hERG value of 2.5 μM was observed for **62**).

In light of the overall balanced profile of the *cis* 3-pyridinyl derivative **52**, the unsubstituted derivative **63** was prepared (Table 5). The direct comparison between the two racemic compounds clearly show that the removal of the 4-CF_3 group in the phenyl derivative of the "amino portion" led to a decrease in affinity greater than one log unit. For compound **64b** (the best *cis* single enantiomer), such substitution was re-introduced adding an additional 2-F substitution. The result was a derivative showing almost 1.2

nM affinity at the D3R and a selectivity greater than 600-fold at the D2R and hERG channel. The *in vitro* PK revealed IC_{50} values greater than 7 μM on all CYP P450 isoforms tested with the exception of CYP2D6, which was greater than 1 μM. Both Fu_{br} and Fu_{bl} were relatively high with 7.7 % and 16.1 %, respectively. As clearly expected for a non-substituted 3-pyridine, the *in vitro* clearance was characterized by high values (namely, hCli and rCli= 485 and 278 μL/min/mg protein, respectively).

A 2,4-F di-substitution, i.e. the replacement of the 4-CF_3 group with a –F atom (**65b**), led to a slight reduction in the affinity at the D3R with the advantage of a more than half one log unit decrease in cLogP. While maintaining a 1.2 nM affinity at the D3R and a 400-fold selectivity vs. the D2R, this compound increased selectivity vs. hERG to over 2100-fold with an absolute 2.8 μM hERG affinity. Its functional behavior was also confirmed (Table 8). A slight improvement was observed with respect to the CYP P450 profile, while a large increase in the free fraction was seen both in brain and blood (Fu_{br} and Fu_{bl}= 25 and > 50 %, respectively). Similar to the previous compound, Cli data were high (namely, hCli and rCli = 258 and 253 μL/min/mg protein, respectively). Finally, the decision to leave a single 4-F substituent (**66b**) on the aromatic ring further reduced cLogP almost to the original value of the unsubstituted derivative. This reduction had no major impact on the affinity at the D3R, keeping the selectivity profile comparable to the previous derivatives. The fraction unbound of the compound was high (Fu_{br} and Fu_{bl}= 26 and > 50 %, respectively) and, most probably because of the decrease in lipophilicity and despite the presence of an unsubstituted 3 pyridine, Cli values were markedly reduced with respect to the previously analyzed compounds leading to hCli value equal to 91 μL/min/mg protein. Given the results of this very rapid exploration and to maintain homogeneous comparison with the previously synthesized compounds, a further analysis of the aromatic pattern of substitution of this part of the molecule was postponed to the lead optimization phase. The 4-CF_3 group was kept as a reference while substituting the 3-pyridine with groups that, based on Cli data, were hypothesized to prevent the metabolic degradation of the ring.

The insertion of a methyl group in position 2 of the pyridine system (**67a**) was slightly less potent than the corresponding unsubstituted racemate (**52**), but was also less active at off-targets leading to 450- and

1900-fold selectivity vs. the D2R and the hERG channel; derivative **67a** showed a 6.3 μM hERG activity. According to the working hypothesis, the methyl group should have increased the dihedral angle formed by the pyridine ring with the triazole moiety, hence reducing the conjugation of the two rings. Compound **67a** was inactive at the D1R and D4R and the activity at the M1 and M3 muscarinic receptors was quite reduced leading to a selectivity greater than 350-fold at both receptors (fpKi= 5.78 ± 0.14 and 5.91 ± 0.07, respectively). The impact on the CYP P450 profile was positive with IC_{50} values greater than 7 μM on all CYP P450 isoforms tested with the exception of CYP3A4 7BQ, which was greater than 2 μM. Both Fu_{br} and Fu_{bl} were moderate with values of 6.2 and 18.6 %, respectively. A clear reduction in Cli was also observed with hCli and rCli equivalent to 80 and 103 μL/min/mg protein, respectively).

When this methyl was replaced by a trifluoromethyl group (**68a**) cLogP was clearly increased; a decrease in affinity at the D3R and a reduced selectivity profile were also observed. In contrast, this manipulation had a positive effect on the CYP P450 profile; on all the CYP P450 isoforms tested, compound **68a** had IC_{50} values greater than 6 μM. However, the increased lipophilicity had a detrimental effect on free fraction (Fu_{br} and Fu_{bl}= 2.2 and 7.5 %, respectively) as well as on intrinsic clearance; hCli and rCli reverted to 302 and 114 (μL/min/mg protein), respectively.

A reduction in cLogP and a slight increase in PSA were calculated for the replacement of the $–CF_3$ with an electron-donating group such as the methoxy one (**69a**). Potency and selectivity vs. the D2R were comparable to the methyl derivative **67a**, while the affinity at the hERG channel increased by one log unit.

When derivative **70a** (cyano derivative) was prepared to probe the other position close to the pyridine nitrogen, an increase in affinity at the D3R was observed and a good selectivity vs. the D2R was maintained. The affinity at the hERG channel, however, also increased and it was decided not to progress this compound along the screening cascade. The transformation of the nitrile into a primary amide (**71a**) produced a one log unit increase in the affinity at the D3R and the selectivity vs. the secondary targets was greater than 1600-fold. The *in vitro* PK profile of **71a** revealed IC_{50} values greater

than 17 μM on all CYP P450 isoforms and it was therefore decided to investigate its profile further. The reduction in lipophilicity (cLogP= 3.4) had a beneficial effect on free fraction (Fu_{br} and Fu_{bl}= 2.2 and 18.4 %, respectively) and on intrinsic clearance (hCli and rCli were 106 and 29 μL/min/mg protein, respectively). Compound **71a** behaved as a competitive antagonist at the D3R with no activity at the D1R and the D4R, and a 550-fold selectivity over muscarinic M1 and M3 receptors (fpKi= 6.65 ± 0.05 and 6.72 ± 0.04 on M1 and M3, respectively); this compound was therefore tested *in vivo*[22,23] to validate correlation with *in vitro* PK data. Compound **71a** had a relatively good fraction absorbed (F_a= 40%) with moderate distribution volume (V_{ss}= 3.2 L/kg), and relatively low clearance in blood as expected from the *in vitro* parameters (Cl_b= 19.4 mL/min/kg) leading to moderate half-life ($T_{1/2}$ = 2.2 h) and relatively good bioavailability (F%= 40%) given low hepatic extraction (E_H= 0.35). As expected from increased PSA values, the B/B ratio was slightly lower than the previously tested compounds (B/B= 0.3). The overall parameters for this compound constituted an excellent starting point for further exploration in the lead optimization phase.

The exploration of the substitution of the 3 pyridine ring continued with the introduction of two methyl groups (**72a**) to assess whether the contemporary substitution of the two positions alpha to the nitrogen was tolerated. No major differences with the mono substituted methyl derivative **67a** were observed, suggesting that the second methyl was relatively "neutral" to the overall molecule in terms of affinity. The slight increase in lipophilicity had no major impact on the CYP P450 profile (all isoforms had IC_{50} values greater than 9 μM) or on free fraction (Fu_{br} and Fu_{bl}= 4.5 and 12.6 %, respectively), but affected Cli with increased values (hCli and rCli were 299 and 98 μL/min/mg protein, respectively).

Replacing one of the two methyls with the primary amide of **71a** led to the synthesis of compound **73a**. This derivative showed a balanced affinity profile with 1.2 nM affinity at the D3R and 900-fold and 2150-fold vs. the D2R and the hERG channel, respectively. Moreover, the absolute affinity at the hERG channel was about 3 μM. The compound had a "clean" CYP P450 profile showing IC_{50} values greater than 10 μM on all isoforms tested. The rCli was greatly reduced with respect to **72a** (rCli= 38

μL/min/mg protein), while hCli values remained unexpectedly high (hCli = 299 μL/min/mg protein). High free fraction values were also observed (Fu_{br} and Fu_{bl}= 7.8 and 19 %, respectively).

The compound was further profiled *in vitro* for selectivity and functional activity was also assessed. The compound was an antagonist with 0.7 nM affinity at the D3R thus increasing the selectivity vs. the hERG channel to more than 4000-fold; no activity at the D1R and the D4R was observed and a 270-fold selectivity was achieved over the muscarinic M1 and M3 receptors (fpKi= 6.29 ± 0.08 and 6.73 ± 0.08 on M1 and M3, respectively). Given the balanced profile of **73a**, its PK profile was assessed *in vivo*[22, 23]. Compound **73a** showed a good fraction absorbed (F_a= 54%) with moderate-high distribution volume (V_{ss}= 5.5 L/kg) and low clearance in blood as expected from the *in vitro* parameters (Cl_b= 21.1 mL/min/kg). Given the low hepatic extraction (E_H= 0.28), the parameters showed a good half-life ($T_{1/2}$ = 4.3 h) and relatively good bioavailability (F%= 53%). Brain penetration was also assessed showing a B/B ratio equal to 1.5. Similar to 7**1a,** this compound was selected as a starting point for further characterization.

Finally, the transformation of the primary amide into the corresponding carboxylic acid (**74a**) caused an overall reduction in affinity across all targets, and IC_{50} on all CYP P450 isoforms tested greater than 38 μM. Quite unexpectedly for a free carboxylic acid, very high free fractions were observed (Fu_{br} and Fu_{bl}= 22.9 and 29.9 %, respectively) and Cli values were both very low (r, hCli < 11 μL/min/mg protein). Further exploration of this compound during the lead optimization phase of this project was deemed worthy based on its overall selectivity that was greater than 100-fold vs. both the D2R and hERG channel (10 μM affinity).

The exploration of the pyridine moieties **50** and **52** was continued (Table 7) with the introduction of a hydroxyl substituent on the ring leading to the pyridone derivatives **75** and **76**. Only data on the most active *cis* stereoisomers are reported. Both compounds were originally prepared as racemates showing promising selectivity profiles and nanomolar affinity at the D3R. Since **75** had an IC_{50} at the hERG channel greater than 10 μM, its most active enantiomer (**75a**) was further profiled showing selectivity greater than 4300-fold vs. the hERG channel. No affinity at the D1R and the D4R was observed whereas

selectivity vs. muscarinic M1 and M3 receptors was higher than 200-fold (fpKi= 6.31 ± 0.01 and 6.01 ± 0.16 on M1 and M3, respectively). Given its IC_{50} greater than 5 μM on all CYP P450 isoforms tested, its high free fraction (Fu_{br} and Fu_{bl}= 8.0 and 19.1 %, respectively) and low Cli both in rat and human (hCli= 28 and rCli = 14 μL/min/mg protein, respectively), it was decided to assess its PK profile *in vivo*[22,23]. Unfortunately, because of its low membrane permeability (assessed in Caco-2 cell lines)[24] the fraction absorbed of **75a** was negligible (F_a≈ 1%); this problem, associated with high Clb (48 mL/min/kg) and very high distribution volume (V_{ss}= 9.2 L/kg), led to negligible bioavailability (F%≈ 2%). For this reason, compound **76** was not even separated in its enantiomers and the N-methylated version of both compounds was prepared (**77a**, **78a**). Both derivatives showed an excellent affinity and selectivity profile, especially at the hERG channel showing 1800- and 1300-fold hERG selectivity, respectively. Their overall *in vitro* properties were similar: IC_{50} values on all CYP P450 isoforms tested was greater than 9 μM and greater than 17 μM for **77a** and **78a**, respectively. High free fraction was observed for both compounds (Fu_{br} and Fu_{bl}= 10.8 and 25 %, respectively for **77a**, and Fu_{br} and Fu_{bl}= 14.6 and 16.7 %, respectively for **78a**). Both compounds also showed comparable Cli profiles (see Table 9). The medium permeability in the Caco-2 assay for both **77a** and **78a** was slightly better than **75a**. The latter observation was critical considering the *in vivo*[22, 23] PK profile. As expected by the *in vitro* results reported in Table 9, Clb values (reported with the full profiles in Table 10) were almost identical with moderate clearance in rat, as well as V_{ss} and $T_{1/2}$. The difference in bioavailability of the two compounds (10 vs. 30%) perfectly reflected and matched their difference in fraction absorbed (17 vs. 40%). Functional data for **78a** are available in Table 8.

The full removal of the aromaticity from the pyridine ring led to the piperidinyl derivatives **79a** and **80a**. The compounds both showed affinity at the D3R of about 10 nM with 100-fold selectivity vs. the D2R and a 1000-fold selectivity vs. the hERG channel (10 μM). The introduction of a lactam ring, especially on derivative **79a**, reduced cLogP and PSA values, which translated into the CYP P450 profile (IC_{50} of **79a** greater than 21 μM on all isoforms tested). The free fraction (Fu_{br} and Fu_{bl}= 17.8 and 23 %,

respectively) and Cli (hCli= 25 and rCli < 11 μL/min/mg protein) had benefited from this reduction. Given its low permeability the compound was not progressed in that phase of the project.

To pursue the exploration, the carbonyl group of the lactams (**79a**, **80a**) was made exocyclic by preparing derivative **81a**; the system was then further elongated with the cyclohexyl amide **82a**. Neither of the two corresponding "free" amines were prepared and tested since previous explorations on related compounds[8,9] and literature data[25] demonstrated that di-basic compounds, especially on lipophilic scaffolds, usually suffer from very high volumes of distribution, long half-life and high total plasma clearance.

Compound **81a** showed a 7 nM affinity at the D3R with more than 100-fold selectivity vs. the D2R and about 400-fold selectivity vs. the hERG channel (3 μM). **81a** had IC_{50} values greater than 17 μM on all CYP P450 isoforms tested with high free fraction both in brain and blood (Fu_{br} and Fu_{bl}= 11.8 and 20.0 %, respectively; intrinsic clearance values were moderate to low (hCli= 61 and rCli= 17 μL/min/mg protein, respectively). A change in the nature of the thiotriazole substituent did not change the functional profile of the compound (Table 8). Based on medium cLogP and PSA and medium permeability in the Caco-2 assay, this compound was selected to further assess its PK properties *in vivo*[22,23]. **81a** showed good fraction absorbed (F_a= 28%) with moderate-high distribution volume (V_{ss}= 6.0 L/kg) and moderate clearance in blood as expected from the *in vitro* parameters (Cl_b= 39.8 mL/min/kg). Hepatic extraction was unexpectedly low (E_H= 0.0) leading to moderate half-life ($T_{1/2}$= 2.5 h) and a relatively good bioavailability (F%= 33 %). Brain penetration was also assessed with a B/B ratio equal to 0.5.

The acetamide **82a** was well tolerated by the D3R showing an affinity of about 3 nM at the D3R and a very good selectivity vs. the hERG channel (2500-fold). Although lipophilicity was not significantly increased, IC_{50} values on the CYP P450 2D6 decreased with respect to the previous compounds (IC_{50}= 2 μM; all other isoforms > 6 μM).

Following the observation that hydrophilicity was well tolerated in this region of the receptor, the piperidine moiety was replaced by a tetrahydropyrane template (**83a**). This compound showed an excellent affinity at the D3R (1.7 nM), 480-fold selectivity vs. the D2R and 1700-fold selectivity vs. the

hERG channel. Marked reduction in PSA and high permeability in Caco-2 cell lines were observed. The affinity of **83a** was also confirmed functionally (Table 8) with no activity at both the D1R and the D4R. A good selectivity over muscarinic M1 and M3 receptors (> 100-fold) was also achieved (fpKi= 6.60 ± 0.09 and 6.05 ± 0.06 on M1 and M3, respectively). The CYP P450 profile was excellent with IC_{50} values greater than 10 μM on all isoforms tested; free fraction was high (Fu_{br} and Fu_{bl}= 9.7 and 18.8 %, respectively). Intrinsic clearance values in rat were higher than the ones in humans (hCli= 34 and rCli= 59 μL/min/mg protein, respectively). Therefore, the compound was selected to profile its PK properties *in vivo*[22, 23]. **83a** had good fraction absorbed (F_a= 57%) with moderate distribution volume (V_{ss}= 3.7 L/kg), and high clearance in blood as expected from the *in vitro* parameters (Cl_b= 87.3 mL/min/kg). Hepatic extraction was high (E_H= 0.8) leading to short half-life ($T_{1/2}$= 0.6 h) and low bioavailability (F%= 11 %). Brain penetration was also assessed with B/B ratio equal to 0.3, potentially dictated by decreased PSA.

In an attempt to reduce Clb values masking the carbons alpha to the oxygen to prevent their oxidation, the bridged derivative **84a** was prepared. No major differences were observed in the affinity/selectivity profile, while permeability was slightly lower. The free fraction was also slightly reduced, and the rCli was reduced as expected (from 59 to 21 μL/min/mg protein, Table 9). To quickly test the working hypothesis, the compound was administered intravenously (*i.v.*) *in vivo*[2223] to assess blood clearance in rat. Unfortunately, the difference in Cli was not reflected in a difference in Clb, and the values for the two compounds were comparable (Table 10) and relatively high.

Finally, to complete the exploration, the oxygen of **83a** was replaced by a carbon atom, leading to the cyclohexyl derivative **85a**. A substantial increase in cLogP was calculated and translated into an increase in affinity at the DA D3 receptor. As expected, such increase was also observed on the off targets even if an excellent level of selectivity was still maintained (more than 2000-fold vs. the D2R and 1000-fold vs. hERG). The high lipophilicity led to reduced free fraction and very high Cli (Table 9) as expected for such derivative. For both **84a** and **85a**, functional data were generated too, confirming the antagonist profile of the series.

Some of the compounds reported in Tables 6 and 7 were submitted to an "ExpresSProfile - P1" at CEREP[26], a panel consisting of 55 receptors, ion channels and transporters at the 1 μM concentration. A great selectivity was observed for the compounds tested on the majority of the off-targets (data not reported) and the previously identified hERG/M1/M3 potential liability points were also highlighted, confirming their correct inclusion in the screening cascade.

Finally, to attribute unequivocally the stereochemistry of the compounds and to revise the results of the computational work, an appropriate strategy was set up to determine their absolute configuration. The strategy was divided into two parts and comprised as a first step the preparation of the chiral intermediate, (1R,3S)-[4-(trifluoromethyl)phenyl]-5-azaspiro[2.4]heptane (**86**) by preparation of (1R,3S/1S,3R)-[4-(trifluoromethyl)phenyl]-5-azaspiro[2.4]heptane and resolution of the racemic mixture by using chiral HPLC procedure as reported in the experimental part. The assignment of the absolute configuration of the title compound was determined by a single crystal X-ray structure obtained from a crystal of 5-(4-methylbenzenesulfonyl)-(1R, 3S)-[4-(trifluoromethyl)phenyl]-5-azaspiro[2.4]heptane (**87**) derived from the desired enantiomer and crystallized in EtOH as solvent to obtain a single crystal. For those compounds synthesized from **86** or from its (1S,3R)-enantiomer (**88**) (with known absolute stereochemistry based on X-ray structure) a common trend was recognized between absolute configuration of the 5-azaspiro[2.4]heptane moiety and measured binding activity at the D3R for each pair of enantiomers. Figure 5 reports the crystal structures for derivatives **87** and **89**.

Figure 5 goes here

Given the results achieved in this early part of the exploration and reported in Tables 1-7 some hints about the structure-activity of the new 5-azaspiro[2.4]heptane moiety were identified. On this specific scaffold, and coupled to the thiotriazole system to provide D3R antagonism, the relative configuration of the system played a role in determining the affinity at the primary target. Both stereoisomers were active and selective, and the *cis* one resulted often more active than the *trans* one (e.g. **10a** vs. **9a**; **19b** vs. **18b**;

21b vs. **20a**). Nonetheless, the steric hindrance of the substituents on the aromatic ring of this amino portion also played an important role on the affinity and was able to reverse this general trend (e.g. **22a** vs. **23b**; **14** vs. **15**; **25** vs. **26**). Even if this was not specifically noticed in the molecular modelling calculations performed to support the medicinal chemists, this fact might suggest that a specific dihedral angle in the *cis* configuration is required for a more appropriate fitting of the whole molecule within the primary binding site in the D3R pocket.

An additional observation was related to the very high level of selectivity achieved for all the derivatives prepared in the different series. Differently from other series reported in the literature, a selectivity greater than 1000-fold over the hERG channel was observed for many of the compounds reported in the manuscript. High cLogP values (e.g. **33**, **44a**, **45a, 47a**) led to sub-nanomolar affinity at the D3R, but also caused an increase of potency at the hERG channel. Nonetheless, an optimal range of cLogP to achieve both high D3R affinity and an "ideal" selectivity window with respect to the hERG channel was identified ($3 < cLogP < 4.5$), also in agreement with previously reported data[5].

The introduction of additional H-bond capabilities in the molecule (e.g. **40a**, **44a**, **47a**) led to an increase in the affinity at the D3R suggesting the possibility of additional interactions within the secondary binding pocket (SBP)[16] of the D3R, potentially in the region facing the extracellular loop 2 (EL2) as it might be hypothesized by the docking of compound **40a** reported in Figure 4.

The presence in the scaffold of an additional moderately basic center (**49**-**74**) was generally well tolerated from the affinity point of view and had no major impact on the distribution volume point of view. This, in addition to the previously mentioned H-bond acceptor presence and to appropriate protection of the molecule from the metabolic point of view, led to a series of derivatives with good CYP P450 profile and excellent developability properties (Table 9 and 10).

Conclusions

In summary, a combined medicinal chemistry and computational chemistry strategy led to the identification of a new series of 1,2,4-Triazolyl 5-Azaspiro[2.4]heptanes with high affinity and selectivity at the D3R.

Despite the limited exploration of substituents in this early phase of the project, the newly identified "amino portion" provided a well-defined SAR. The affinity at the D3R reached sub-nanomolar values (e.g. **47a**) with a large selectivity window, both on the D2R but especially on the hERG channel (e.g. **75a**, 5000-fold selective, or **46a**, 10000-fold selective).

The observed pharmacokinetic properties (both *in vitro* and in *vivo*) clearly predict good developability characteristics for these molecules even though additional optimization work together with further *in vivo* testing is now required. Some selected derivatives, which showed an overall balanced *in vitro/in vivo* profile were considered for further progression along the screening cascade for subsequent lead optimization, which will be reported in due course.

Experimental section

Biological Test Methods: In vitro studies

[^{3}H]-Spiperone filtration binding assay on membranes from hD3-CHO cells.

This assay provided *in vitro* affinities (pIC_{50}, pKi) of compounds at the human D3R expressed in CHO-K1 cells. The filtration binding involved the incubation of hD3-CHO cell membranes with the radioligand [^{3}H]-Spiperone in the presence or absence of test compounds. Displacement binding was measured by separation of bound from free radioligand using filtration through Glass Microfiber Filters. The assay was performed at room temperature (23 °C). Equilibrium was reached after 80 min and remained stable for at least 120 minutes. Bound radioactivity was measured using a Top-Count reader (for competition experiments) or ß-Counter reader for saturation experiments), while radioligand concentration was determined by liquid scintillation counting.

Expression plasmids

The human D3R (DRD3), transcript variant (NM_000796.2) was purchased from OriGene Technologies, Inc. (cat # SC124083). The cDNA was cloned into pCMV6-XL4 plasmid vector containing CMV promoter for in vivo expression in mammalian cells. The molecular clone sequence data was matched to the reference identifier above as a point of reference. The complete sequence of the molecular clone may differ from the sequence published for this corresponding reference, e.g., by representing an alternative RNA splicing form or single nucleotide polymorphism (SNP).

Large scale cell transfection and cell pellet preparation

CHO-K1 cells were maintained in F12K medium supplemented with 10% dialyzed fetal bovine serum, in a humidified incubator at 37 °C with 5% CO_2. For transfection, cells were plated in Corning Dish 500cm^2 (20x106 cells /dish) and cultured overnight. Cells were then transfected with hDRD3-pCMV6-XL4 plasmid, following the manufacture's protocol with FuGENE HD with a ratio of

transfection complex of 3:1 (300 µL FuGENE: 100 µg plasmid/dish). After 24 h incubation at 37 °C and 5% CO_2, the medium was removed and cells were washed with 25mL of DPBS (no Ca^{2+}, no Mg^{2+}). Versene was added over the cells and incubated at 37 °C for 5 min. Cells were scraped with a "cell scraper" and the cell suspension was collected in a Costar tubes prior to being put on ice. Cell suspensions were centrifuged in a Beckman GS6R centrifuge for 10 min, 4 °C, 1200 rpm (330 rcf), the supernatant removed and the cell pellets washed and collected in a single tube by re-suspension in PBS and centrifugation cycles. The pellet was weighed and frozen down at -80 °C.

CHO-hDRD3 membrane preparation

The frozen pellet was thawed and homogenized in 10 volumes (w/v) in Membrane Preparation Buffer 1 using an Ultra-turrax (3 times for 10 s each cycle). The homogenate was centrifuged for 20 min, 4 °C, at 18500 rpm (40000 rcf) in a SL-50T Sorvall rotor and the pellet re-suspended in 10 volumes w/v in Buffer 1 and re-homogenized as before. After centrifugation, the pellet was re-suspended in 5 volumes of Membrane Preparation Buffer 2. The resulting suspension was aliquoted and frozen down at -80 °C. Protein concentration was determined according to the instructions provided within the BioRad reagent using a BSA standard curve. (Buffer 1= HEPES 20 mM, EDTA 2 mM pH 7.4, ice cold; Buffer 2= HEPES 20 mM pH 7.4, NaCl 100mM, $MgCl_2$ 10mM, EDTA 1 mM, ice cold).

Competition binding experiments

Competition binding experiments were performed in a 96-deep well plate at room temperature (23 °C) with a final assay volume of 500 µL/well according to the following protocol: a) 300 µL of binding buffer were dispensed into each well of the compound plate; b) [^{3}H]-Spiperone stock was diluted in binding buffer solution to obtain the 5x [^{3}H]- Spiperone solution (1.5 nM); c) 100 µL of 1.5 nM [^{3}H]-Spiperone solution were dispensed into each well of the compound plate; d) the competition reaction was started by adding 100 µL of hDRD3-CHO membrane suspension in binding buffer. The final membrane concentration/well was 3.5 µg and the final [^{3}H]-Spiperone concentration was 0.3 nM. The

plate was then incubated on a shaker at 23 °C for 90 min. The reaction was terminated by rapid filtration through Unifilter-96 GF/B filter plates pre-soaked for one hour in Polyethylenimine (PEI) 0.5% (w/v) solution and washed with 1.0 mL of ice cold 0.9% NaCl before the filtration using a Packard cell Harvester. The filter plate was washed 4 times with 1.0 mL ice-cold 0.9% NaCl and then left to dry for at least one hour at 40 °C. The plate was sealed with a back-seal; 50 µL of Microscint-20 were added to each well and the plate was sealed with a top-seal. Bound radioactivity was measured using a Microplate TopCount. Radioligand concentration was determined as follows: 100 µL of [^{3}H]-Spiperone solution (5x) and 3mL Filter Count were mixed in the total added vial and read in β-Counter TriCarb 2900.

Saturation binding experiments

Saturation binding experiments were performed similarly to the competition binding experiments, with the following deviation: [^{3}H]-Spiperone concentrations were chosen from 0.015 to 4.0 nM in a concentration response curve with 12 points. The reaction was terminated by rapid filtration through GF\B paper filter pre-soaked for one hour in Polyethylenimine (PEI) 0.5% (w/v) solution and washed with 1.0 mL of ice cold 0.9% NaCl before the filtration using a Brandel Harvester. The filter was washed 4 times with 1.0 mL ice-cold 0.9% NaCl. The filter was put into pico-vial (PerkinElmer 600252) and 4 mL of Filter count were added. Bound radioactivity was measured using a β-Counter. Samples of working radioligand solution were taken and measured by traditional liquid scintillation counting in order to determine the actual concentration of radiolabel added.

[^{3}H]-Spiperone filtration binding assay on membranes from hD2-CHO cells.

This assay provided *in vitro* affinities (pIC_{50}, pKi) of compounds at the human DA D2 receptor expressed in CHO-K1 cells. The filtration binding involved the incubation of hD2- Gα16-CHO cell membranes with the radioligand [^{3}H]-Spiperone in the presence or absence of test compounds. Displacement binding was measured by separation of bound from free radioligand using filtration through Glass Microfiber Filterplates. The assay was performed at room temperature (23 °C).

Equilibrium was reached after 90 min and remained stable for at least 150 minutes. Bound radioactivity was measured using a Top-Count reader (for competition experiments) or s-Counter reader (for saturation experiments), while radioligand concentration was determined by liquid scintillation counting.

Competition binding experiments

Competition binding experiments were performed in a 96-deep well plate at room temperature (23 °C) with a final assay volume of 1000 µL/well, according to the following protocol: 800 µL of binding buffer were dispensed into each well of the compound plate. [^{3}H]-Spiperone stock was diluted in binding buffer solution to obtain the 10x [^{3}H]- Spiperone solution (0.8 nM). 100 µL of 0.8 nM [3H]-Spiperone solution were dispensed into each well of the compound plate. The competition reaction was started by adding 100 µL of hD2- Gα16-CHO membrane suspension in binding buffer. The final membrane concentration/well was 2 µg and the final [^{3}H]-Spiperone concentration was 0.08 nM. The plate was then incubated on a shaker at 23 °C for 120 min. The reaction was terminated by rapid filtration through Unifilter-96 GF/B filter plates pre-soaked for at least one hour in Polyethylenimine (PEI) 0.5% (w/v) solution and washed with 1.0 mL of ice cold 0.9% NaCl before the filtration using a Packard cell Harvester. The filter plate was washed 4 times with 1.0 mL ice-cold 0.9% NaCl and then left to dry for at least one hour at 40 °C. The plate was sealed with a back-seal; 50 µL of Microscint-20 were added to each well and the plate was sealed with a top-seal. Bound radioactivity was measured using a Microplate TopCount. Radioligand concentration was determined as follows: 100 µL of [^{3}H]-Spiperone solution (5x) and 3 mL Filter Count were mixed in the total added vial and read in β- Counter TriCarb 2900.

Saturation binding experiments

Saturation binding experiments were performed similarly to the competition binding experiments, with the following deviation: [^{3}H]-Spiperone concentrations were chosen from 0.011 to 3.0 nM in a

concentration response curve with 12 points. The reaction was terminated by rapid filtration through GF\B paper filter pre-soaked for one hour in Polyethylenimine (PEI) 0.5% (w/v) solution and washed with 1.0 mL of ice cold 0.9% NaCl before the filtration using a Brandel Harvester. The filter was washed 4 times with 1.0 mL ice-cold 0.9% NaCl. The filter was put into pico-vial (PerkinElmer 600252) and 4 mL of Filter count were added. Bound radioactivity was measured using a β-Counter. Samples of working radioligand solution were taken and measured by traditional liquid scintillation counting in order to determine the actual concentration of radiolabel added.

Functional calcium assay at hD2 recombinant receptor

CHO cells stably expressing human DA receptor type 2, long variant (hD2L), coupled to Gα16 protein (CHO-Gα16-hD2L) were seeded into black walled clear-base 384-well plates at a density of 8,000 cells per well and grown overnight at 37 °C. After washing with the assay buffer (20 mM HEPES, 145 mM NaCl, 5 mM KCl, 5.5 mM glucose, 1 mM $MgCl_2$ and 2 mM $CaCl_2$, pH 7.4) containing 2.5 mM Probenecid, cells were incubated with the cytoplasmic Ca^{2+} probe Fluo-4 AM at 1 μM (final concentration), 37 °C for 60 min. Plates were washed three times as above and placed into a Fluorometric Imaging Plate Reader (FLIPR Tetra, Molecular Devices) to monitor cell fluorescence (ex= 470-495 nm, em= 515-575 nm) before and after the addition of different concentrations of test compounds. Compounds of invention were dissolved in DMSO and 200-fold diluted with assay buffer plus 0.01% Pluronic F-127. Cells were exposed first to test compounds for 10 min, then to a submaximal concentration of the hD2 receptor agonist dopamine (EC_{80}, 50-140 nM). The fluorescence before compound addition (baseline) and before and after addition of agonist challenge was monitored. The peak of Ca^{2+} stimulation (baseline subtracted) was plotted versus the concentration of test compound and the curve fitted using a four-parameter logistic equation (XLfit) to assess the agonist/antagonist potency and maximal response.

Functional binding assay in cell membranes expressing hD3 receptors. [^{35}S] GTPγS

In vitro functional studies were performed according to the following [^{35}S]-GTPγS protocol. Test compounds were serially diluted 1:3 or 1:4 in neat DMSO, 11-point curves; the final top concentration of test drugs in the assay was 10 µM, 1% DMSO; 0.5 µL of test compound serial dilution were dispensed into the assay plate (white solid 384-well plate format). A suspension containing 3 mg/mL PS-WGA Imaging beads (PerkinElmer, RPNQ0260), 0.01% Pluronic F127, 30 µg/mL saponin, 1 µg/mL GDP and 3.5 µg/mL membranes (PerkinElmer, cat.no ES-173-M400UA) was prepared. 0.5 nM [35S]-GTPγS was added to the mixture just prior plate dispensing of 50 µL per well. In case of the antagonist mode, 3 nM of quinelorane (EC80) was also added to the SPA mixture. The assay plate was then sealed and centrifuged for 1min at 800 rpm. After 90 min incubation at room temperature the plate was counted on a Viewlux reader with 613 nm filter, 6x binning for 10 min. Concentration response curve were analyzed using GraphPad or Xlfit for Excel; for agonist mode the pEC_{50} was obtained, while for the antagonist mode the fpKi values of test drug were calculated from the IC_{50} using Cheng and Prusoff equation.

Measure of the effect on hERG channel by tail current recording using in vitro Rapid ICE™

The potency of the compounds in inhibiting human ERG potassium channel (hERG) tail current was assessed in a recombinant HEK293 cell line stably transfected with hERG cDNA, under an inducible promoter, using Rapid ICE™ (Rapid Ion Channel Electrophysiology) assay. Rapid ICE™ is an automated patch-clamp assay utilizing the QPatch HTX system (Sophion Bioscience A/S). Briefly, inducible HEK hERG cells were cultivated in minimum essential medium supplemented with 10% FBS, 1% non-essential amino acids, 1% sodium pyruvate, 2 mM L-glutamine, 15 µg/mL blasticidin and 100 µg/mL hygromycin. hERG channel expression induction was obtained by adding 10 µg/mL tetracycline for 24, 48 or 72 hours before recordings.

The day of the experiment cells were detached with TrypLE and prepared to be loaded on the instrument. Cells were re-suspended in 7 mL Serum-Free Media containing 25 mM Hepes and Soybean

trypsin inhibitor and immediately placed in the cell storage tank of the machine. The composition of the Extracellular Buffer was (mM): NaCl 137; KCl 4; CaCl2 1.8; $MgCl_2$ 1.0; D-glucose 10; N 2 hydroxyethylpiperazine-N'-2-ethanesulfonic acid (HEPES) 10; pH 7.4 with 1 M NaOH. The composition of the pipette solution was (mM): KCl 130; MgCl2 1.0; Ethylene glycol-bis(ß-aminoethyl ether)-N,N,N',N'-tetraacetic acid (EGTA) 5; MgATP 5; HEPES 10; pH 7.2 with 1 M KOH. The voltage protocol included the following steps: step from -80 mV to –50 mV for 200 ms, +20 mV for 4.8 s, step to -50 mV for 5 s then step to the holding potential of -80 mV. Compounds were dissolved in DMSO and diluted in Extracellular Buffer to achieve final test concentrations (0.1, 1 and 10 µM) in 0.1% DMSO. The voltage protocol was run and recorded continuously during the experiment. The vehicle, corresponding to 0.1% DMSO in Extracellular Buffer, was then applied for 3 min followed by the test substance in triplicate. The standard combined exposure time was 5 min. The average of tail current amplitude values recorded from 4 sequential voltage pulses was used to calculate for each cell the effect of the test substance by calculating the residual current (% control) compared with vehicle pre-treatment. Data were reported as % inhibition for each concentration tested and IC50 values were estimated using QPatch software. At least two cells were tested, and even more if results diverge.

Muscarinic M1 and M3 receptor – FLIPR assay

The recombinant human Muscarinic M1 Receptor Cell Line (389 Aptuit CHO h-M1) was generated in-house and pharmacologically validated with reference compounds. Briefly, CHO-KI cells were stably transfected with an expression plasmid encoding for the human Muscarinic M1 receptor (GeneBank accession# NM_000738) following a standard transfection protocol with FuGENE HD (Roche Diagnostic). CHO Muscarinic M1 cells were cultured in a humidified incubator with 5% CO2 in F12K medium containing 10% FBS HI and 450µg/mL of Geneticin (G418). The cells were grown in T175 flasks and split when 90- 100% confluence was reached. The recombinant human Muscarinic M3 Receptor Cell Line (387 Aptuit CHO h-M3) was generated in-house and pharmacologically validated with reference compounds. Briefly, CHO-KI cells were stably transfected with an expression plasmid

encoding for the human Muscarinic M3 receptor (GeneBank accession# NM_000740) following a standard transfection protocol with FuGENE HD (Roche Diagnostic). CHO Muscarinic M3 cells were cultured in a humidified incubator with 5% CO_2 in F12K medium containing 10% FBS HI and 450 ìg/mL of Geneticin (G418). The cells were grown in T175 flasks and split when 90- 100% confluence was reached. This assay provided in vitro agonist (pEC_{50}) and antagonist (pIC_{50}) potency of compounds at the human M1 and M3 receptor stably expressed in CHO cells by modulating intracellular calcium changes using the calcium-sensitive dye Fluo-4 AM and Fluorometric Imaging Plate Reader (FLIPR, Molecular Devices) instrument. A dual read-out FLIPR protocol was applied allowing for agonist and antagonist characterization. In the first part compounds were characterized in a concentration dependent manner (11 point CRC, 1:3 serial dilutions) for their ability to increase intracellular calcium levels with respect to the agonist standard Acetylcholine and a pEC_{50} calculated. After 10 min incubation, a second addition containing the EC_{80} of Acetylcholine followed. Inhibition of the Acetylcholine evoked signal indicated antagonist activity of the compound and enabled the calculation of the compounds pIC_{50}. A quality check (QC) was present in each compound plate. The signal window was monitored performing Z' calculations and evaluating the pharmacology of internal standards. As agonist reference Acetylcholine and Carbachol were characterized, while Atropine and Imipramine served as standards in the antagonist mode. Concentration response curves of compounds were run in duplicate from the same compound stock solution.

Compound plate preparation for 1st FLIPR addition

Serial dilutions 1 to 3 were performed from a compound stock solution by Biomek FX to generate 11-point concentration curve (CRC). 1 µL copy plates were then stamped into V-bottom drug plates at a concentration which was 200-fold the final assay concentration. The copy plates were diluted prior to the experiment with assay buffer containing 0.05% Pluronic F-127 to reach 4 times the final assay concentration (4X, 2% DMSO). The concentration corresponding to the EC_{80} CRCs for acetylcholine-

induced intracellular Ca^{2+} increase was measured during the 1st FLIPR addition. The EC80 corresponded to 4 times the EC_{50} if the Hill-Slope was not different from 1.

Compound plate preparation for 2nd FLIPR addition

Acetylcholine stock in DMSO was diluted in assay buffer containing 0.05% Pluronic F-127 to obtain an agonist stimulus solution (DMSO < 0.02%) corresponding to 5-fold the final EC_{80} concentration.

Intracellular calcium response measurement

The cells were washed in washing buffer using the EMBLA 384 instrument leaving 20 µL/well of buffer after the final aspiration. Cells were then incubated in washing buffer with the cytoplasmic Ca^{2+} indicator Fluo-4 AM at 2 µM and 0.02% Pluronic F-127 final concentrations for 1 hour in a 37 °C incubator (cell loading). After cells were washed three times in washing buffer using the EMBLA 384 instrument, 30 µL of buffer was left in each well at the end of the last wash. The loaded cell plates were transferred to the FLIPR machine and calcium response monitored during the 2 on-line addition protocols:

- First addition: 10 µL/well of the test compound (4X concentration) or buffer were added to the loaded cells and Ca^{2+} mobilization response was measured.
- Second addition: after 10 minutes, 10 µL/well of Acetylcholine EC_{80} (5X concentration) were added as agonist challenge and Ca^{2+} mobilization responses were followed on line.

The final DMSO concentration in the assay was 0.5% w/v after the two FLIPR additions.

P450 CYPEX assay

The described assays measured *in vitro* inhibitory effects (pIC_{50}) of compounds at the human P450 isoforms (1A2, 2C9, 2C19, 2D6, 3A4) expressed in recombinant microsomes. Pro-fluorescent probe substrates were metabolized to fluorescent products by the enzymes. Fluorescence was measured in kinetic mode (1 read/min for 10 min) and the fluorescence rate was calculated. Data were normalized to

controls: DMSO represented 0% effect (i.e. no inhibition), while 10µM Miconazole was set to 100% effect (i.e. complete inhibition). Inhibition of the fluorescent signal determined by P450 activation indicated antagonist activity of the compound and allowed for the calculation of the compound pIC_{50}.

Inhibition (IC_{50}) of human CYP1A2, 2C9, 2C19, 2D6 and 3A4 was determined using Cypex™ Baculosomes expressing the major human P450s. Test compounds serial dilutions 1 to 3 were performed from a 10 mM stock solution in DMSO by Biomek FX to generate 10-point CRC of test compound. A reference compound (e.g. miconazole) was included in each compound plate. The reference compound was diluted and stamped together with test compounds. The final concentrations of the 10-point CRCs of test compounds in the assay plate were 5.00E-05 M; 1.67E-05 M; 5.56E-06 M; 1.85E-06 M; 6.17E-07 M; 2.06E-07M; 6.86E-08 M; 2.29E-08 M; 7.62E-09 M and 2.54E-09 M, respectively. 10µL/well of the test compounds were transferred from compound plate to assay plate using Biomek FX with the appropriate protocol. The assay plate was then incubated at 37 °C for 10 min on a shaker to allow for the interaction between compounds and enzymes. After that, 10µl/well of the cofactor were added to the assay plate using a Multidrop pipette before placing the assay plate in the plate reader EnVision to measure fluorescence. The plate was read every minute for 10 min according to the P450 isoform specific protocol. CYP450 isoform substrates used were ethoxyresorufin (ER; 1A2; 0.5 µM), 7-methoxy-4-triflouromethylcoumarin-3-acetic acid (FCA; 2C9; 50 µM), 3-butyryl-7-methoxycoumarin (BMC; 2C19; 10 µM), 4-methylaminomethyl-7-methoxycoumarin (MMC; 2D6; 10 µM), diethoxyflourescein (DEF; 3A4; 1 µM) and 7-benzyloxyquinoline (7-BQ; 3A4; 25 µM). The test was performed in three replicates

Intrinsic clearance (Cli) assay

Intrinsic clearance (CLi) values were determined in rat and human liver microsomes. Test compounds (0.5 µM) were incubated at 37 °C for 30 min in 50mM potassium phosphate buffer (pH 7.4) containing 0.5 mg microsomal protein/mL. The reaction was started by addition of co-factor (NADPH; 8 mg/mL). The final concentration of solvent was 1% of the final volume. At 0, 3, 6, 9, 15 and 30 min an aliquot

(50 µL) was taken, quenched with acetonitrile containing an appropriate internal standard and analyzed by HPLC-MS/MS. The intrinsic clearance (CLi) was determined from the first order elimination constant by non-linear regression using Grafit v5 (Erithacus software, UK), corrected for the volume of the incubation and assuming 52.5 mg microsomal protein/g liver for all species. Values for CLi were expressed as mL/min/g protein. The lower limit of quantification of clearance was determined to be when <15% of the compound had been metabolized by 30 min and this corresponded to a CLi value of 0.5 mL/min/g protein.

Chemistry

General

Proton Magnetic Resonance (NMR) spectra were recorded either on Varian instruments at 400 or 500 MHz, or on a Bruker instrument at 400 MHz.

Chemical shifts were expressed in parts of million (ppm, δ units). Chemical shifts were reported in ppm downfield (δ) from Me4Si, used as internal standard, and were assigned as singlets (s), broad singlets (br.s.), doublets (d), doublets of doublets (dd), doublets of doublets of doublets (ddd), doublets of triplets (dt), triplets (t), triplets of doublets (td), quartets (q), or multiplets (m).

LC-MS was recorded under the following conditions:

DAD chromatographic traces, mass chromatograms and mass spectra were taken on UPLC/PDA/MS Acquity™ system coupled with Micromass ZQ™ or Waters SQD single quadrupole mass spectrometer operated in positive and/or negative ES ionization mode. The QC methods used were two, one operated under low pH conditions and another one operated under high pH conditions. Details of the method operated under low pH conditions were: column, Acquity BEH C_{18}, 1.7 µm, 2.1 x 50 mm or Acquity CSH C_{18}, 1.7 µm, 2.1 x 50 mm, the temperature column was 40 °C; mobile phase solvent A was milliQ water + 0.1% HCOOH, mobile phase solvent B MeCN + 0.1% HCOOH. The flow rate was 1 mL/min.

The gradient table was t= 0 min 97% A–3% B, t= 1.5 min 0.1% A–99.9% B, t= 1.9 min 0.1% A–99.9% B and t= 2 min 97% A–3% B. The UV detection range was 210–350 nm and the ES^+/ES^- range was 100–1000 amu.

Details of the method operated under high pH conditions were the same as those listed above for the low pH method apart from: column Acquity BEH C_{18}, 1.7 µm, 2.1 x 50 mm; mobile phase solvent A was 10 mM aqueous solution of NH_4HCO_3 adjusted to pH= 10 with ammonia, mobile phase solvent B MeCN.

Semipreparative mass directed autopurifications (MDAP) were carried out using Waters Fractionlynx™ systems operated under low or high pH chromatographic conditions. The stationary phases used were, XTerra C_{18}, XBridge C_{18}, Sunfire C_{18}, XSelect C_{18}, Gemini AXIA C_{18}. The length of the columns was 5, 10 or 15 cm, while the internal diameter was 19, 21 or 30 mm. The particle size of the stationary phases was 5 or 10 µm. The purifications were carried out using low pH or high pH chromatographic conditions. The mobile phase solvent composition was the same used for QC analysis. The combinations stationary/mobile phases used were: XTerra, XBridge, Sunfire, XSelect – low pH mobile phases and XTerra, XBridge, Gemini AXIA – high pH mobile phases. All the purifications were carried out with the column kept at room T. The flow rate used was 17 or 20 mL/min for columns of internal diameter 19 or 21 mm and 40 or 43 mL/min for columns of internal diameter 30 mm. The trigger for the collection of the target species was the presence of the target m/z ratio value in the TIC MS signal. The gradient timetable was customized on the Rt behavior of the target species.

Purification was performed using Biotage® Isolera or Biotage® SP1 flash chromatography systems; these instruments worked with Biotage® KP-SIL cartridges, Biotage® KP-NH cartridges or Biotage® KP-C18 cartridges.

Synthetic procedures.

Unless otherwise stated, all reactions are typically performed under inert atmosphere (for example under Nitrogen). Tlc refers to thin layer chromatography on silica plates, and dried refers to a solution dried over anhydrous sodium sulphate.

The 1,2,4-Triazolyl 5-Azaspiro[2.4]heptanes described here were prepared according to general route provided in Scheme 1. Appropriate protected aryl-5-azaspiro[2.4]heptanes (C) were prepared as follow: the desired aldehydes (1 mmol) were added to a solution of hydrazine hydrate (3 mmol) in EtOH and stirred at room temperature till completion of the reaction. The solution was diluted with water and CH_2Cl_2. Phases were separated; the organic one was dried and concentrated under reduced pressure affording the described hydrazones (A). The protected 3-methylidenepyrrolidine-2,5-diones (B, like the 1-benzyl-3-methylidenepyrrolidine-2,5-dione reported in Scheme 1) were prepared dissolving 1-benzyl-2,5-dihydro-1H-pyrrole-2,5-dione (1 mmol) in AcOH and adding PPh3 (1 mmol). The resulting solution was stirred for 1 hr. at RT then formaldehyde 37% in water (1.8 mmol) was added. The solution was stirred at RT for 2.5 hrs. Volatiles were removed under reduced pressure. The residue was partitioned between water (300 mL) and CH_2Cl_2. The layers were separated and the organic portion was dried; the crude material was purified by flash chromatography.

To obtain compounds (C), to a solution of A (1 mmol) in dioxane at 10 °C, MnO_2 (10 mmol) was added portion wise. The resulting mixture was stirred at RT for 1 h, then it was filtered over a pad of Celite washing with dioxane). This pale yellow solution was then added into a solution of (B) (1 mmol) in dioxane. The resulting orange/red solution was left stirring at RT for 40 hrs. Solvent was removed and the residue was purified by flash chromatography to provide the *cis* and *trans* diastereoisomers of derivatives (C) that were used as such in the next steps.

The separated diastereoisomers (C, 1 mmol) were then dissolved in THF and $LiAlH_4$ 1M in THF (2 mmol) was added dropwise. The resulting orange solution was refluxed for 1 h. Then it was cooled with

an ice bath and quenched with Na_2SO_4 *10 H_2O until gas evolution ceased. The mixture was filtered over a pad of Celite washing with EtOAc, and the solution was concentrated to afford the racemic derivatives (D) that were used as such in the next steps. Subsequently, these compounds were dissolved in MeOH under N_2 and ammonium formate was added. After 2 cycles of vacuum and nitrogen purging, Pd/C was added. The resulting mixture was stirred at reflux for 1 h. After cooling down to RT, it was filtered over a pad of Celite, the solvent was evaporated and the residue was loaded on SCX cartridge (eluting with 1N NH_3 in MeOH) to afford, after evaporation, intermediates (E).

As reported previously[9,10,13,] starting from the carboxylic derivatives (F) it is possible to prepare the desired thiotriazoles (G). In brief, to a solution of the carboxylic acid (1 mmol) in DMF, 4-Methyl-3-thiosemicarbazide (1.1 mmol) was added. Di-isopropyl ethyl amine (1.8 mmol) was added drop wise at RT, then the mixture was cooled with an ice bath before adding T3P (50% w/w in EtOAc) (1.5 mmol). The reaction was stirred at RT overnight. NaOH 4M solution was added (till a resulting pH= 8). The reaction was diluted with EtOAc and the two phases were separated. Additional 4M NaOH was added up to pH 11 and the mixture heated to 70 °C for 40 min. The clear rusty red solution was then cooled down to RT in 3 hours, then 37% HCl was slowly added till pH 5. The clear solution was extracted with CH_2Cl_2, combined organics were dried and concentrated to obtain a brown solid. Crude materials were purified by C_{18} cartridge (eluting from H_2O+0.1% HCOOH to 20% MeCN+0.1% HCOOH). Fractions containing the product were collected and concentrated to reduce the volume, then extracted twice with CH_2Cl_2 to obtain the desired derivatives (G). To a suspension of these derivatives (1 mmol) in a mixture MeOH/Acetone at RT, the appropriate alkylating agents (e.g.1-bromo-3-chloropropane, 1.3 mmol) were added, followed by the addition of K_2CO_3 (1.4 mmol) and the mixture was stirred at RT for 4.5 hrs. It was then partitioned between water and EtOAc and phases were separated. Organic one was washed with brine then dried and concentrated under reduced pressure. Crude material was purified by flash chromatography to achieve the desired compounds (H).

Finally, to achieve the target compounds (T) reported in the Tables 1-7, intermediates (H) and (E) in equimolar quantities were dissolved in DMF and Na_2CO_3 (1.2 mmol) and NaI (1.2 mmol) were added. The suspension was heated at 60 °C overnight. The mixtures were diluted with water and EtOAc and extracted several times with EtOAc. The organic phase was washed with brine, dried and evaporated. The residues were purified by flash chromatography to achieve the above mentioned compounds.

Whenever necessary, the compounds (solids, oils or foams) were taken up with CH_2Cl_2 and a 1.0 M HCl solution in diethylether was added; the solvent was removed under reduced pressure to give the desired compounds as hydrochloride salts.

The enantiomeric purity of each single enantiomer obtained after preparative chromatography on chiral columns, was always verified on the analytical column.

All the structures of the new compounds were confirmed by ^{1}H NMR, MS, HRMS and ^{13}C NMR where necessary. All general chemicals were the highest available grade, and the purity of all synthetic compounds was determined by HPLC analysis and was greater than 95%. As reported in the text, X-rays data were generated on selected intermediates.

(1S,3S/1R,3R)-5-(3-{[4-methyl-5-(4-methyl-1,3-oxazol-5-yl)-4H-1,2,4-triazol-3-yl]sulfanyl}propyl)-1-phenyl-5-azaspiro[2.4]heptane **(7)**

Following the general procedure, the crude residue was purified by flash chromatography to give **7** as a foam. Yield 11%. ^{1}H NMR (*Acetone-d$_6$*) δ: 8.26 (s, 1 H), 7.33 - 7.09 (m, 5 H), 3.78 (s, 3 H), 3.36 - 3.27 (m, 2 H), 2.76 - 2.47 (m, 6 H), 2.41 (s, 3 H), 2.15 - 2.09 (m, 1 H), 2.00 - 1.87 (m, 2 H), 1.65 - 1.37 (m, 2 H), 1.17 - 1.04 (m, 2 H). MS *m/z*: 410.3 $[M+H]^+$.

7 was separated into the single enantiomers by preparative chiral HPLC, using the following details: Column: Chiralcel OJ-H (25 x 2 cm), 5 µm; Mobile phase: n-Hexane/ (Ethanol + 0.1 % isopropyl alcohol) 25/75 % v/v; flow rate: 14 mL/min; DAD detection: 220 nm; loop: 750 µL affording **7a** (enantiomer 1), retention time= 10.5 min and **7b** (enantiomer 2), retention time= 12.1 min.

***(1R,3S/1S,3R)-5-(3-{[4-methyl-5-(4-methyl-1,3-oxazol-5-yl)¬-4H-1,2,4-¬triazol-3-yl]-sulfanyl}propyl)-1-phenyl-5-azaspiro[2.4]heptane* (8)**

Following the general procedure, the crude residue was purified by flash chromatography to give **8** as a foam. Yield 23%. ^{1}H NMR (*Acetone-d_6*) *δ*: 8.26 (s, 1 H) 7.33 - 7.09 (m, 5 H) 3.78 (s, 3 H) 3.36 - 3.27 (m, 2 H) 2.76 - 2.47 (m, 6 H) 2.41 (s, 3 H) 2.15 - 2.09 (m, 1 H) 2.00 - 1.87 (m, 2 H) 1.65 - 1.37 (m, 2 H) 1.17 - 1.04 (m, 2 H). MS *m/z*: 410.3 $[M+H]^+$.

8 was separated into the single enantiomers by preparative chiral HPLC, using the following details: Column: Chiralpak AD-H (25 x 2 cm), 5 µm; mobile phase: n-Hexane/(Ethanol + 0.1 % isopropyl alcohol) 55/45 % v/v; flow rate: 14 mL/min; DAD detection: 220 nm; loop: 750 µL affording **8a** (enantiomer 1) retention time= 7.9 min and **8b** (enantiomer 2), retention time= 9.3 min.

(1S,3S/1R,3R)-5-(3-{[4-methyl-5-(4-methyl-1,3-oxazol-5-yl)-4H-1,2,4-triazol-3-yl]sulfanyl}propyl)-1-[4-(trifluoromethyl)phenyl]-5-azaspiro[2.4]heptane (9)

Following the general procedure, the crude residue was purified by flash chromatography to give **9** as pale yellow foam. Yield 37%. ^{1}H NMR (*$CDCl_3$*) *δ*: 7.95 (s, 1H), 7.54 (d, *J* = 8.03 Hz, 2H), 7.23 (br. s., 2H), 3.73 (s, 3H), 3.37 (m, 2H), 2.94 - 2.59 (m, 5H), 2.55 (s, 3H), 2.31 - 1.97 (m, 3H), 1.63 (br. s., 4H), 1.36 - 1.25 (m, 1H), 1.19 - 1.11 (m, 1H). MS *m/z*: 478.3 $[M+H]^+$.

9 was separated into the single enantiomers by preparative chiral HPLC, using the following details: Column: Chiralpak AD-H (25 x 2 cm), 5 µm; mobile phase: n-Hexane/Ethanol 50/50 % v/v; flow rate: 14 mL/min; DAD detection: 220 nm; loop: 875 µL affording **9a** (enantiomer 1) retention time = 8.5 min and **9b** (enantiomer 2), retention time= 10.9 min.

(1R,3S/1S,3R)-5-(3-{[4-methyl-5-(4-methyl-1,3-oxazol-5-yl)-4H-1,2,4-triazol-3-yl]sulfanyl}propyl)-1-[4-(trifluoromethyl)phenyl]-5-azaspiro[2.4]heptane (10)

Following the general procedure, the crude residue was purified by flash chromatography to give **10** as yellow oil. Yield 31%. ^{1}H NMR (*Acetone-d_6*) δ: 8.28 (s, 1H), 7.63 (d, J = 8.03 Hz, 2H), 7.40 (d, J = 8.28 Hz, 2H), 3.77 (s, 3H), 3.36 - 3.16 (m, 2H), 2.69- 2.46 (m, 5H), 2.44 (s, 3H), 2.30 - 2.22 (m, 1H), 2.03 - 1.79 (m, 5H), 1.35 - 1.26 (m, 1H), 1.26 - 1.19 (m, 1H). MS *m/z*: 478.3 $[M+H]^+$.

10 was separated into the single enantiomers by preparative chiral HPLC, using the following details: Column: Chiralcel OJ-H (25 x 2 cm), 5 µm; mobile phase: n-Hexane/Ethanol 50/50 % v/v; flow rate: 14 mL/min; DAD detection: 220 nm; loop: 750 µL affording **10a** (enantiomer 1) retention time= 7.3 min and **10b** (enantiomer 2), retention time= 9.7 min.

(1S,3S/1R,3R)-5-(2-{[4-methyl-5-(4-methyl-1,3-oxazol-5-yl)-4H-1,2,4-triazol-3-yl]sulfanyl}ethyl)-1-[4-(trifluoromethyl)phenyl]-5-azaspiro[2.4]heptane (11)

Following the general procedure, the crude residue was purified by flash chromatography to give **11** as yellow foam. Yield 51%. ^{1}H NMR (*Acetone-d_6*) δ: 8.27 (s, 1H), 7.62 (d, J = 8.28 Hz, 2H), 7.34 (d, J = 8.28 Hz, 2H), 3.81 (s, 2H), 3.39 (m, 2H), 2.87 (m, 2H), 2.83 - 2.75 (m, 3H), 2.73 - 2.61 (m, 3H), 2.43 (s, 2H), 2.29 - 2.21 (m, 1H), 1.70 - 1.61 (m, 1H), 1.44 (s, 1H), 1.26 (m, 1H), 1.23 - 1.17 (m, 1H). MS *m/z*: 464.3 $[M+H]^+$.

11 was separated into the single enantiomers by preparative chiral HPLC, using the following details: Column: Chiralpak AD-H (25 x 2 cm), 5 µm; mobile phase: n-Hexane/Ethanol 55/45 % v/v; flow rate: 14 mL/min; DAD detection: 220 nm; loop: 750 µL affording **11a** (enantiomer 1) retention time= 11.7 min and **11b** (enantiomer 2), retention time = 13.1 min.

(1R,3S/1S,3R)-5-(2-{[4-methyl-5-(4-methyl-1,3-oxazol-5-yl)-4H-1,2,4-triazol-3-yl]sulfanyl}ethyl)-1-[4-(trifluoromethyl)phenyl]-5-azaspiro[2.4]heptane (12)

Following the general procedure, the crude residue was purified by flash chromatography to give **12** as pale yellow foam. Yield 22%. ^{1}H NMR (*$CDCl_3$*) δ: 7.95 (s, 1H), 7.54 (d, J = 8.03 Hz, 2H), 7.20 (d, J = 8.03 Hz, 2H), 3.68 (s, 3H), 3.44 - 3.28 (m, 2H), 2.85 (s, 3H), 2.76 - 2.68 (m, 1H), 2.57 - 2.51 (m, 3H),

2.50- 2.43 (m, 1H), 2.25 - 2.19 (m, 1H), 2.18 - 2.11 (m, 1H), 2.05 - 1.94 (m, 2H), 1.24 - 1.15 (m, 2H). MS *m/z*: 464.3 $[M+H]^+$.

(1R,3S/1S,3R)-5-(4-{[4-methyl-5-(4-methyl-1,3-oxazol-5-yl)-4H-1,2,4-triazol-3-yl]sulfanyl}butyl)-1-[4-(trifluoromethyl)phenyl]-5-azaspiro[2.4]heptane (13)

Following the general procedure, the crude residue was purified by flash chromatography to give **13** as pale yellow foam. Yield 15%. ^{1}H NMR (*$CDCl_3$*) *δ*: 7.95 (s, 1H), 7.55 (d, *J* = 8.03 Hz, 2H), 7.22 (d, *J* = 7.78 Hz, 2H), 3.74 - 3.65 (m, 3H), 3.33 - 3.20 (m, 2H), 2.94 (br. s., 1H), 2.70 (br. s., 1H), 2.54 (s, 6H), 2.27 - 2.14 (m, 2H), 2.05 (d, *J* = Hz, 2H), 1.82 (m, 3H), 1.32 -1.19 (m, 3H). MS *m/z*: 492.3 $[M+H]^+$.

(1S,3S/1R,3R)-5-(3-{[4-methyl-5-(4-methyl-1,3-oxazol-5-yl)-4H-1,2,4-triazol-3-yl]sulfanyl}propyl)-1-[2-(trifluoromethyl)phenyl]-5-azaspiro[2.4]heptane hydrochloride (14)

Following the general procedure, the crude residue was purified by flash chromatography to give **14** subsequently transformed in corresponding hydrochloride. Yield 13%. ^{1}H NMR (*DMSO-d_6*) *δ*: 10.56 - 10.13 (m, 1H), 8.58 (s, 1H), 7.77 (d, *J* = 8.03 Hz, 1H), 7.64 (t, *J* = 7.40 Hz, 1H), 7.48 (t, *J* = 7.65 Hz, 1H), 7.36 (d, *J* = 7.78 Hz, 1H), 3.71 (s, 3H), 3.68 - 3.49 (m, 2H), 3.28 (m, 4H), 3.22-3.12 (m, 1H), 3.07 - 2.93 (m, 1H), 2.48 (br. s., 2H), 2.39 (s, 3H), 2.10 (br. s., 2H), 1.72 - 1.52 (m, 2H), 1.50 - 1.32 (m, 2H). MS *m/z*: 478.4 $[M+H]^+$.

14 was separated into the single enantiomers by preparative chiral HPLC, using the following details: Column: Chiralpak AD-H (25 x 2 cm), 5 μm; mobile phase: n-Hexane/(Ethanol + 0.1 % isopropylamine) 70/30 % v/v; flow rate: 16 mL/min; DAD detection: 220 nm; loop: 500 μL affording **14a** (enantiomer 1) retention time = 7.2 min and **14b** (enantiomer 2), retention time= 8.4 min.

(1R,3S/1S,3R)-5-(3-{[4-methyl-5-(4-methyl-1,3-oxazol-5-yl)-4H-1,2,4-triazol-3-yl]sulfanyl}propyl)-1-[2-(trifluoromethyl)phenyl]-5-azaspiro[2.4]heptane (15)

Following the general procedure, the crude residue was purified by flash chromatography to give **15** as a light yellow foam. Yield 45%. ^{1}H NMR (*Acetone-d$_6$*) δ: 8.29 (s, 1H), 7.78 - 7.71 (m, 1H), 7.62 - 7.54 (m, 1H), 7.47 - 7.38 (m, 1H), 7.33 - 7.27 (m, 1H), 3.77 (s, 3H), 3.37 - 3.17 (m, 3H), 3.06 - 2.83 (m, 2H), 2.60 (br. s., 4H), 2.44 (s, 3H), 2.41 (br. s., 1H), 2.02 - 1.80 (m, 4H), 1.60 - 1.51 (m, 1H), 1.25 - 1.14 (m, 1H). MS *m/z*: 478.4 $[M+H]^+$.

(1S,3S/1R,3R)-1-(4-fluorophenyl)-5-(3-{[4-methyl-5-(4-methyl-1,3-oxazol-5-yl)-4H-1,2,4-triazol-3-yl] sulfanyl}propyl)-5-azaspiro[2.4]heptane (16)

Following the general procedure, the crude residue was purified by flash chromatography to give **16** as a foam. Yield 38%. ^{1}H NMR (*Acetone-d$_6$*) δ: 8.31 - 8.25 (m, 1H), 7.21 - 7.11 (m, 2H), 7.11 - 7.00 (m, 2H), 3.80 (s, 3H), 3.37 - 3.29 (m, 2H), 2.75 - 2.66 (m, 1H), 2.66 - 2.50 (m, 5H), 2.44 (s, 3H), 2.17 - 2.10 (m, 1H), 2.02 - 1.90 (m, 2H), 1.63 - 1.48 (m, 1H), 1.47 - 1.35 (m, 1H), 1.19 - 1.11 (m, 1H), 1.08-1.04 (m, 1H). MS *m/z*: 428.4 $[M+H]^+$.

16 was separated into the single enantiomers by preparative chiral HPLC, using the following details: Column: Chiralpak AD-H (25 x 2.1 cm), 5 µm; modifier: (Methanol+0.1% isopropylamine) 20 %; flow rate: 45 mL/min; DAD detection: 220 nm; loop: 700 µL affording **16a** (enantiomer 1) retention time= 11.7 min and **16b** (enantiomer 2), retention time= 16.3 min.

(1R,3S/1S,3R)-1-(4-fluorophenyl)-5-(3-{[4-methyl-5-(4-methyl-1,3-oxazol-5-yl)-4H-1,2,4-triazol-3-yl] sulfanyl}propyl)-5-azaspiro[2.4]heptane (17)

Following the general procedure, the crude residue was purified by flash chromatography to give **17** as foam. Yield 46%. ^{1}H NMR (*Acetone-d$_6$*) δ: 8.26-8.30 (m, 1H), 7.21-7.16 (m, 2H), 7.08-7.00 (m, 2H), 3.77 (s, 3H), 3.31-3.15 (m, 2H), 2.75-2.62 (m, 2H), 2.50 (t, *J* = 6.65 Hz 2H), 2.43 (s, 3H), 2.37 (d, *J* = 8.0 Hz, 1H), 2.13-2.09 (m, 2H), 1.99-1.89 (m, 2H), 1.88-1.79 (m, 2H), 1.14-1.06 (m, 2H). MS *m/z*: 428.4 $[M+H]^+$.

17 was separated into the single enantiomers by preparative chiral HPLC, using the following details: Column: Chiralpak AD-H (25 x 2.1 cm), 5 µm; modifier: (Methanol+0.1% isopropylamine) 17 %; flow rate: 46 mL/min; DAD detection: 220 nm; loop: 700 µL affording **17a** (enantiomer 1) retention time = 12.1 min and **17b** (enantiomer 2), retention time= 15.0 min.

(1R,3S/1S,3R)-1-(2,4-difluorophenyl)-5-(3-{[4-methyl-5-(4-methyl-1,3-oxazol-5-yl)-4H-1,2,4-triazol-3-yl]sulfanyl}propyl)-5-azaspiro[2.4]heptane (18)

Following the general procedure, the crude residue was purified by flash chromatography to give **18** as foam. Yield 42%. ^{1}H NMR (*Acetone-d$_6$*) δ: 8.28 (s, 1H), 7.20 -6.87 (m, 3H), 3.81 (s, 2H), 3.33 (t, *J* = 7.15 Hz, 2H), 2.73 -2.50 (m, 7H), 2.43 (s, 3H), 2.15 (br. s., 1H), 2.01 -1.91 (m, 2H), 1.60-1.51 (m, 1H), 1.38-1.30 (m, 1H), 1.24-1.12 (m, 2H). MS *m/z*: 446.4 $[M+H]^+$.

18 was separated into the single enantiomers by preparative chiral HPLC, using the following details: Column: Chiralpak AD-H (25 x 2 cm), 5 µm; mobile phase: (Methanol+0.1% isopropylamine) 18 %; flow rate: 45 mL/min; DAD detection: 220 nm; loop: 700 µL affording **18a** (enantiomer 1) retention time= 11.5 min and **18b** (enantiomer 2), retention time= 15.5 min.

(1S,3S/1R,3R)-1-(2,4-difluorophenyl)-5-(3-{[4-methyl-5-(4-methyl-1,3-oxazol-5-yl)-4H-1,2,4-triazol-3-yl]sulfanyl}propyl)-5-azaspiro[2.4]heptane (19)

Following the general procedure, the crude residue was purified by flash chromatography to give **19** as foam. Yield 49%. ^{1}H NMR (*Acetone-d$_6$*) δ: 8.28 (s, 1H), 7.19-7.09 (m, 1H), 7.04 - 6.88 (m, 2H), 3.77 (s, 5H), 3.31-3.19 (m, 2H), 2.78-2.73 (m, 1H), 2.65 - 2.57 (m, 1H), 2.55 - 2.46 (m, 2H), 2.43 (s, 3H), 2.39-2.34 (m, 1H), 2.14-2.09 (m, 1H), 2.01 - 1.93 (m, 3H), 1.84 (m, 2H), 1.25 - 1.18 (m, 1H), 1.16-1.11 (m, 1H). MS *m/z*: 446.4$[M+H]^+$.

19 was separated into the single enantiomers by preparative chiral HPLC, using the following details: Column: Chiralpak AD-H (25 x 2.1 cm), 5 µm; mobile phase: (Methanol+0.1% isopropylamine) 12 %;

flow rate: 45 mL/min; DAD detection: 220 nm; loop: 700 µL affording **19a** (enantiomer 1) retention time= 14.1 min and **19b** (enantiomer 2), retention time= 18.5 min.

(1R,3S/1S,3R)-1-[2-fluoro-4-(trifluoromethyl)phenyl]-5-(3-{[4-methyl-5-¬(4-methyl-1,3-oxazol-5-yl)-4H-1,2,4-triazol-3-yl]sulfanyl}propyl)-5-azaspiro[2.4]heptane (20)

Following the general procedure, the crude residue was purified by flash chromatography to give **20** as foam. Yield 62%. ^{1}H NMR (*Acetone-d$_6$*) δ: 8.27 (s, 1H), 7.49 (m, 2H), 7.37-7.29 (m, 1H), 3.80 (s, 3H), 3.38-3.32 (m, 2H), 3.12 - 2.47 (m, 6H), 2.42 (s, 3H), 2.35 (m, 1H), 1.69 (br. s., 1H), 1.42 (br. s., 1H), 1.39 - 1.28 (m, 3H). MS *m/z*: 496.3[M+H]$^+$.

20 was separated into the single enantiomers by preparative chiral HPLC, using the following details: Column: Chiralpak AD-H (25 x 2 cm), 5 µm; mobile phase: n-Hexane / (Ethanol+0.1 % isopropyl alcohol) 55/45 % v/v; flow rate: 14 mL/min; DAD detection: 220 nm; loop: 500 µL affording **20a** (enantiomer 1) retention time = 7.7 min and **20b** (enantiomer 2), retention time = 9.3 min.

(1S,3S/1R,3R)-1-[2-fluoro-4-(trifluoromethyl)phenyl]-5-(3-{[4-methyl-5-(4-methyl-1,3-oxazol-5-yl)-4H-1,2,4-triazol-3-yl]sulfanyl}propyl)-5-azaspiro[2.4]heptane (21)

Following the general procedure, the crude residue was purified by flash chromatography to give **21** as foam. Yield 41%. ^{1}H NMR (*Acetone-d$_6$*) δ: 8.27 (s, 1H), 7.49 (d, *J* = 9.03 Hz, 2H), 7.43-7.38 (m, 1H), 3.76 (s, 3H), 3.35 - 3.20 (m, 2H), 3.19 - 2.87 (m, 3H), 2.42 (s, 3H), 2.39-2.33 (m, 1H), 2.19-2.10 (m, 1H), 2.02 - 1.92 (m, 2H), 1.50 - 1.42 (m, 1H), 1.36 - 1.27 (m, 2H). MS *m/z*: 496.3[M+H]$^+$.

21 was separated into the single enantiomers by preparative chiral HPLC, using the following details: Column: Chiralpak AD-H (25 x 2 cm), 5 µm; mobile phase: n-Hexane/(Ethanol+0.1 % isopropyl alcohol) 70/30 % v/v; flow rate: 14 mL/min; DAD detection: 220 nm; loop: 500 µL affording **21a** (enantiomer 1) retention time= 7.6 min and **21b** (enantiomer 2), retention time= 8.8 min.

(1S,3S or 1R,3R)-1-[4-fluoro-2-(trifluoromethyl)phenyl]-5-(3-{[4-methyl-5-(4-methyl-1,3-oxazol-5-yl)-4H-1,2,4-triazol-3-yl]sulfanyl}propyl)-5-azaspiro[2.4] heptane hydrochloride (22a)

The compound was prepared following the general procedure, but using the single *trans* enantiomer 1 and not the racemic mixture; the crude residue was purified by flash chromatography and the hydrochloride made as reported in the general procedure to give **22a** as a yellow solid. Yield 47%. ^{1}H NMR (*DMSO-d$_6$*) δ: 10.30 - 9.93 (m, 1H), 8.57 (s, 1H), 7.70 - 7.61 (m, 1H), 7.55 - 7.46 (m, 1H), 7.44 - 7.36 (m, 1H), 3.71-3.64 (m, 4H), 3.62 - 3.48 (m, 2H), 3.39 - 3.34 (m, 1H), 3.27 - 3.11 (m, 4H), 3.08 - 2.94 (m, 1H), 2.47 - 2.41 (m, 1H), 2.38 (s, 3H), 2.09 (br. s., 2H), 1.70 - 1.51 (m, 2H), 1.49 - 1.39 (m, 1H), 1.39 - 1.30 (m, 1H). MS *m/z*: 496.4[M+H]$^+$.

(1R,3R or 1S,3S)-1-[4-fluoro-2-(trifluoromethyl)phenyl]-5-(3-{[4-methyl-5-(4-methyl-1,3-oxazol-5-yl)-4H-1,2,4-triazol-3-yl]sulfanyl}propyl)-5-azaspiro[2.4]heptane hydrochloride (22b)

The compound was prepared following the general procedure, but using the single *trans* enantiomer 2 and not the racemic mixture; the crude residue was purified by flash chromatography and the hydrochloride made as reported in the general procedure to give **22b** as a yellow solid. Yield 57%. ^{1}H NMR (*DMSO-d$_6$*) δ: 10.15-9.88 (m, 1H), 8.57 (s, 1H), 7.68-7.62 (m, 1H), 7.54-7.48 (m, 1H), 7.46 - 7.38 (m, 1H), 3.71-3.64 (m, 4H), 3.63 - 3.47 (m, 2H), 3.46 - 3.35 (m, 1H), 3.27 - 3.11 (m, 4H), 3.08 - 2.94 (m, 1H), 2.47 - 2.41 (m, 1H), 2.38 (s, 3H), 2.15 - 2.02 (m, 2H), 1.68 - 1.52 (m, 2H), 1.50 - 1.40 (m, 1H), 1.38 -1.28 (m, 1H). MS *m/z*: 496.4[M+H]$^+$.

(1R,3S or 1S,3R)-1-[4-fluoro-2-(trifluoromethyl)phenyl]-5-(3-{[4-methyl-5-(4-methyl-1,3-oxazol-5-yl)-4H-1,2,4-triazol-3-yl]sulfanyl}propyl)-5-azaspiro[2.4]heptane hydrochloride (23a)

The compound was prepared following the general procedure, but using the single *cis* enantiomer 1 and not the racemic mixture; the crude residue was purified by flash chromatography and the hydrochloride made as reported in the general procedure to give **23a** as a yellow solid. Yield 58%. ^{1}H NMR (*DMSO-d$_6$*) δ: 10.12 (br. s., 1H), 8.57 (s, 1H), 7.68-7.63 (m, 1H), 7.49 (m., 1H), 7.42 - 7.33 (m, 1H), 3.84 - 3.72

(m, 1H), 3.69 - 3.61 (m, 3H), 3.39-3.25 (m, 6H), 3.00 - 2.84 (m, 1H), 2.62 - 2.52 (m, 2H), 2.37 (s, 3H), 2.27 - 1.91 (m, 4H), 1.75 - 1.61 (m, 1H), 1.42 - 1.22 (m, 1H). MS *m/z*: 496.4[M+H]$^+$.

(1S,3R or 1R,3S)-1-[4-fluoro-2-(trifluoromethyl)phenyl]-5-(3-{[4-methyl-5-(4-methyl-1,3-oxazol-5-yl)-4H-1,2,4-triazol-3-yl] sulfanyl}propyl)-5-azaspiro[2.4]heptane hydrochloride (23b)

The compound was prepared following the general procedure, but using the single *cis* enantiomer 2 and not the racemic mixture; the crude residue was purified by flash chromatography and the hydrochloride made as reported in the general procedure to give **23b** as a yellow solid. Yield 58%. ^{1}H NMR (*DMSO-d$_6$*) δ: 10.29 - 9.84 (m, 1H), 8.57 (s, 1H), 7.68-7.63 (m, 1H), 7.54 - 7.44 (m, 1H), 7.42 - 7.32 (m, 1H), 3.82 - 3.71 (m, 1H), 3.70 - 3.61 (m, 3H), 3.24 - 3.04 (m, 6H), 2.99 - 2.85 (m, 1H), 2.62 - 2.52 (m, 2H), 2.37 (s, 3H), 2.11-2.01 (m, 4H), 1.74 - 1.61 (m, 1H), 1.26 (m, 1H). MS *m/z*: 496.4 [M+H]$^+$.

1-{[4-methyl-5-(4-methyl-1,3-oxazol-5-yl)-4H-1,2,4-triazol-3-yl]¬sulfanyl}-3-{1-[4-(trifluoromethyl)phenyl]-5-azaspiro[2.4]¬heptan-5-yl}propan-2-ol (24) diastereoisomeric mixture

Following the general procedure, the crude residue was purified by flash chromatography to give **24** as an oil. Yield 9%. ^{1}H NMR (*Acetone-d$_6$*) δ: 8.28 (s, 1H), 7.61 (d, *J* = 8.03 Hz, 2H), 7.43 - 7.31 (m, 2H), 3.77 (d, *J* = 3.76 Hz, 3H), 3.59 - 3.52 (m, 1H), 3.49 - 3.41 (m, 1H), 3.24 - 3.11 (m, 2H), 2.57 (br. s., 2H), 2.43 (s, 3H), 2.28 - 2.20 (m, 2H), 2.00 - 1.92 (m, 2H), 1.92 - 1.88 (m, 1H), 1.35 - 1.26 (m, 2H), 1.24 - 1.17 (m, 1H). MS *m/z*: 494.4 [M+H]$^+$.

(1S,3S/1R,3R)-1-(3,5-dichlorophenyl)-5-(3-{[4-methyl-5-(4-methyl-1,3-oxazol-5-yl)-4H-1,2,4-triazol-3-yl]sulfanyl}propyl)-5-azaspiro[2.4]heptane (25)

Following the general procedure, the crude residue was purified by flash chromatography to give **25**. Yield 9%. ^{1}H NMR (*Acetone-d$_6$*) δ: 8.30 (s, 1H), 7.32 (s, 3H), 3.82 (s, 3H), 3.53 - 3.37 (m, 3H), 2.84 - 2.79 (m, 2H), 2.44 (s, 3H), 2.41 - 2.33 (m, 1H), 2.22 - 2.13 (m, 2H), 1.90 - 1.79 (m, 2H), 1.72 - 1.51 (m, 3H), 1.44 - 1.28 (m, 3H). MS *m/z*: 478.3 [M+H]$^+$.

(1R,3S/1S,3R)-1-(3,5-dichlorophenyl)-5-(3-{[4-methyl-5-(4-methyl-1,3-oxazol-5-yl)-4H-1,2,4-triazol-3-yl]sulfanyl}propyl)-5-azaspiro[2.4]heptane (26)

Following the general procedure, the crude residue was purified by flash chromatography to give **26**. Yield 34%. ^{1}H NMR (*Acetone-d$_6$*) δ: 8.28 (s, 1H), 7.31 - 7.27 (m, 1H), 7.22 (s, 2H), 3.78 (s, 3H), 3.36 - 3.25 (m, 2H), 2.85 - 2.78 (m, 4H), 2.43 (s, 3H), 2.39 - 2.24 (m, 2H), 2.08 (br. s., 2H), 2.02-1.95 (m, 2H), 1.52 - 1.22 (m, 3H). MS *m/z*: 477.9 $[M+H]^+$.

(1S,3S/1R,3R)-5-(3-{[4-methyl-5-(4-methyl-1,3-thiazol-5-yl)-4H-1,2,4-triazol-3-yl]sulfanyl}propyl)-1-[4-(trifluoromethyl)phenyl]-5-azaspiro[2.4]heptane (27)

Following the general procedure, the crude residue was purified by flash chromatography to give **27**. Yield 55%. ^{1}H NMR (*Acetone-d$_6$*) δ: 9.15 (s, 1H), 7.64 (d, *J* = 8.03 Hz, 2H), 7.39 (d, *J* = 8.03 Hz, 2H), 3.62 (s, 3H), 3.36 (s, 2H), 2.72 (br. s., 5H), 2.50 (s, 3H), 2.36 - 2.28 (m, 1H), 2.06 - 1.97 (m, 3H), 1.79 - 1.67 (m, 1H), 1.53 - 1.41 (m, 1H), 1.35 - 1.23 (m, 3H). MS *m/z*: 494.4 $[M+H]^+$.

(1R,3S/1S,3R)-5-(3-{[4-methyl-5-(4-methyl-1,3-thiazol-5-yl)-4H-1,2,4-triazol-3-yl]sulfanyl}propyl)-1-[4-(trifluoromethyl)phenyl]-5-azaspiro[2.4]heptane (28)

Following the general procedure, the crude residue was purified by flash chromatography to give **28**. Yield 40%. ^{1}H NMR (*Acetone-d$_6$*) δ: 9.15 (s, 1H), 7.67 - 7.60 (m, 2H), 7.42 - 7.37 (m, 2H), 3.58 (s, 3H), 3.25 (m, 2H), 2.77 - 2.72 (m, 2H), 2.67 - 2.60 (m, 1H), 2.56 - 2.46 (m, 6H), 2.26 - 2.21 (m, 1H), 2.03 - 1.95 (m, 2H), 1.92 - 1.82 (m, 2H), 1.30 (m, 1H), 1.22 (m, 1H). MS *m/z*: 494.5 $[M+H]^+$.

(1S,3S/1R,3R)-5-(3-{[4-methyl-5-(1,3-thiazol-2-yl)-4H-1,2,4-triazol-3-yl]sulfanyl}propyl)-1-[4-(trifluoromethyl)phenyl]-5-azaspiro[2.4]heptane (29)

Following the general procedure, the crude residue was purified by flash chromatography to give **29**. Yield 61%. ^{1}H NMR (*Acetone-d$_6$*) δ: 8.04 (d, *J* = 3.26 Hz, 1H), 7.81 (d, *J* = 3.26 Hz,1H), 7.63 (d, *J* =

8.28, Hz, 2H), 7.50 (d, *J* = 7.53 Hz 2H), 4.06 (s, 3H), 3.39 (m, 2H), 2.96 (br. s., 5H), 2.39 - 2.26 (m, 1H), 2.0 5- 2.01 (m, 3H), 1.79 - 1.66 (m, 1H), 1.53 - 1.42 (m, 1H), 1.37 - 1.21 (m, 3H). MS *m/z*: 480.4 $[M+H]^+$.

(1R,3S/1S,3R)-5-(3-{[4-methyl-5-(1,3-thiazol-2-yl)-4H-1,2,4-triazol-3-yl]sulfanyl}propyl)-1-[4-(trifluoromethyl)phenyl]-5-azaspiro[2.4]heptane (30)

Following the general procedure, the crude residue was purified by flash chromatography to give **30**. Yield 48%. ^{1}H NMR (*Acetone-d$_6$*) *δ*: 8.03 (d, *J* = 3.26 Hz, 1H), 7.79 (d, *J* = 3.26 Hz, 1H), 7.61 (d, *J* = 8.03 Hz, 2H), 7.37 (d, *J* = 8.03 Hz, 2H), 4.02 (s, 3H), 3.37 - 3.19 (m, 2H), 2.76 - 2.70 (m, 2H), 2.66-2.56 (m, 1H), 2.57 - 2.44 (m, 3H), 2.26 - 2.19 (m, 1H), 2.02 - 1.92 (m, 2H), 1.91 - 1.82 (m, 2H), 1.28 (m, 1H), 1.20 (m, 1H). MS *m/z*: 480.0$[M+H]^+$.

(1S,3S/1R,3R)-5-(3-{[4-methyl-5-(1,2,3-thiadiazol-4-yl)
4H-1,2,4-triazol-3-yl]sulfanyl}propyl)-1-[4-(trifluoromethyl)phenyl]-5-azaspiro[2.4]heptane hydrochloride (31)

Following the general procedure, the crude residue was purified by flash chromatography and the free base transformed into the hydrochloride to give **31**. Yield 22%. ^{1}H NMR (*DMSO-d$_6$*) *δ*: 10.58 (br. s., 1H), 9.79 (s, 1H), 7.67 (m, 2H), 7.46 (m, 2H), 3.90 (s, 3H), 3.70 - 3.50 (m, 4H), 3.40 - 3.16 (m, 6H), 3.12 - 3.00 (m, 1H), 2.48 - 2.37 (m, 1H), 1.97 - 1.80 (m, 1H), 1.56 - 1.29 (m, 3H). MS *m/z*: 481.4 $[M+H]^+$.

(1R,3S/1S,3R)-(3-{[4-methyl-5-(1,2,3-thiadiazol-4-yl)-4H-1,2,4-triazol-3-yl]sulfanyl}propyl)-1-[4-(trifluoromethyl)phenyl]-5-azaspiro[2.4]heptane (32)

Following the general procedure, the crude residue was purified by flash chromatography to give **32**. Yield 9%. ^{1}H NMR (*CDCl$_3$*) *δ*: 9.34 (s, 1H), 7.54 (d, *J* = 8.28 Hz, 2H), 7.22 (d, *J* = 8.03 Hz, 2H), 4.04 (s, 3H), 3.38-3.25 (m, 2H), 2.90 - 2.80 (m, 1H), 2.74 - 2.63 (m, 1H), 2.58 (br. s., 2H), 2.49 - 2.42 (m, 1H), 2.16 (d, *J* = Hz, 2H), 2.01 (br. s., 5H), 1.21 (s, 2H). MS *m/z*: 481.4 $[M+H]^+$.

(1R,3S/1S,3R)-5-(3-{[4-methyl-5-(thiophen-2-yl)-4H-1,2,4-triazol-3-yl]sulfanyl}propyl)-1-[4-(trifluoromethyl)phenyl]-5-azaspiro[2.4]heptane (33)

Following the general procedure, the crude residue was purified by flash chromatography to give **33**. Yield 50%. ^{1}H NMR (*Acetone-d$_6$*) δ: 7.69 (dd, *J* = 1.13, 5.14 Hz, 1H), 7.64 - 7.58 (m, 3H), 7.37 (d, *J* = 8.28 Hz, 2H), 7.24 (dd, *J* = 3.64, 5.14 Hz, 1H), 3.79 (s, 3H), 3.29 - 3.10 (m, 2H), 2.76 - 2.69 (m, 2H), 2.65 - 2.57 (m, 1H), 2.57 - 2.43 (m, 3H), 2.25 - 2.19 (m, 1H), 2.03 - 1.92 (m, 2H), 1.87 - 1.77 (m, 2H), 1.30 - 1.25 (m, 1H), 1.23 - 1.17 (m, 1H). MS *m/z*: 479.0 $[M+H]^+$.

(1R,3S/1S,3R)-5-(3-{[4-methyl-5-(thiophen-3-yl)-4H-1,2,4-triazol-3-yl]sulfanyl}propyl)-1-[4-(trifluoromethyl)phenyl]-5-azaspiro[2.4]heptane (34)

Following the general procedure, the crude residue was purified by flash chromatography to give **34**. Yield 45%. ^{1}H NMR (*Acetone-d$_6$*) δ: 7.96 (dd, *J* = 1.38, 2.89 Hz, 1H), 7.68 (dd, *J* = 2.76, 5.02 Hz, 1H), 7.58-7.63 (m, 3H), 7.37 (d, *J* = 8.03 Hz, 2H)), 3.76 (s, 3H), 3.28 - 3.10 (m, 2H), 2.76 - 2.69 (m, 2H), 2.65 - 2.56 (m, 1H), 2.55 - 2.42 (m, 3H), 2.26 - 2.19 (m, 1H), 2.02 - 1.92 (m, 2H), 1.87 - 1.77 (m, 2H), 1.28 (m, 1H), 1.20 (m, 1H). MS *m/z*: 479.0 $[M+H]^+$.

(1R,3S/1S,3R)-5-(3-{[5-(furan-2-yl)-4-methyl-4H-1,2,4-triazol-3-yl]sulfanyl}propyl)-1-[4-(trifluoromethyl)phenyl]-5-azaspiro[2.4]heptane (35)

Following the general procedure, the crude residue was purified by flash chromatography to give **35**. Yield 32%. ^{1}H NMR (*Acetone-d$_6$*) δ: 7.81(dd, *J* = 0.75, 1.76 Hz, 1H), 7.61 (d, *J* = 8.03 Hz, 2H), 7.37 (d, *J* = 8.28 Hz, 2H), 7.03 (dd, *J* = 0.75, 3.51 Hz, 1H), 6.68 (dd, *J*= 1.88, 3.39 Hz, 1H), 3.79 (s, 3H), 3.28 - 3.11 (m, 2H), 2.76 - 2.70 (m, 1H), 2.67 - 2.57 (m, 1H), 2.56 - 2.44 (m, 3H), 2.25 - 2.20 (m, 1H), 2.02 - 1.89 (m, 2H), 1.87 - 1.79 (m, 2H), 1.55 - 1.46 (m, 1H), 1.31 - 1.25 (m, 1H), 1.24 - 1.17 (m, 1H). MS *m/z*: 463.0 $[M+H]^+$.

(1R,3S/1S,3R)-5-(3-{[5-(furan-3-yl)-4-methyl-4H-1,2,4-triazol-3-yl]sulfanyl}propyl)-1-[4-(trifluoromethyl)phenyl]-5-azaspiro[2.4]heptane (36)

Following the general procedure, the crude residue was purified by flash chromatography to give **36**. Yield 45%. ^{1}H NMR (*Acetone-d_6*) δ: 7.69 (dd, J = 1.13, 5.14 Hz, 1H), 7.57-7.64 (m, 3H), 7.37 (d, J = 8.28 Hz, 2H), 7.24 (dd, J = 3.76, 5.27 Hz, 1H), 3.72 (s, 3H), 3.27 - 3.06 (m, 2H), 2.76 - 2.70 (m, 2H), 2.65 - 2.56 (m, 1H), 2.55 - 2.42 (m, 3H), 2.24 - 2.19 (m, 1H), 2.00 -1.92 (m, 2H), 1.81 (m, 2H), 1.30 - 1.24 (m, 1H), 1.24 - 1.17 (m, 1H). MS *m/z*: 463.0 $[M+H]^+$.

(1R,3S/1S,3R) -5-(3-{[4-methyl-5-(1-methyl-1H-pyrazol-4-yl)-4H-1,2,4-triazol-3-yl]sulfanyl}propyl)-1-[4-(trifluoromethyl)phenyl]-5-azaspiro[2.4]heptane (37)

Following the general procedure, the crude residue was purified by flash chromatography to give **37**. Yield 54%. ^{1}H NMR (*Acetone-d_6*) δ: 8.17 - 8.13 (m, 1H), 7.89 - 7.86 (m, 1H), 7.65 - 7.60 (m, 2H), 7.41 - 7.36 (m, 2H), 4.00 (s, 3H), 3.71 (s, 3H), 3.24 - 3.08 (m, 2H), 2.76 - 2.71 (m, 1H), 2.65 - 2.57 (m, 1H), 2.54 - 2.43 (m, 3H), 2.26 - 2.20 (m, 2H), 2.04 - 1.95 (m, 3H), 1.87 - 1.78 (m, 2H), 1.32 - 1.26 (m, 1H), 1.24 - 1.19 (m, 1H). MS *m/z*: 477.5 $[M+H]^+$.

(1R,3S/1S,3R)-5-(3-{[4-methyl-5-(1-methyl-1H-pyrazol-5-yl)-4H-1,2,4-triazol-3-yl]sulfanyl}propyl)-1-[4-(trifluoromethyl)phenyl]-5-azaspiro[2.4]heptane (38)

Following the general procedure, the crude residue was purified by flash chromatography to give **38**. Yield 43%. ^{1}H NMR (*Acetone-d_6*) δ: 7.61 (d, J = 2.01 Hz, 1H), 7.54 (d, J = 8.03Hz, 2H), 7.22 (d, J = 8.28Hz, 2H), 6.51 (d, J = 2.01 Hz, 1H), 4.15 (s, 3H), 3.60 - 3.56 (m, 3H), 3.39 - 3.25 (m, 2H), 2.89 (d, J = Hz, 1H), 2.73 (br. s., 1H), 2.62 (br. s., 2H), 2.50 (d, J = Hz, 1H), 2.25 - 2.13- (m, 2H), 2.12 - 1.91 (m, 4H), 1.27 - 1.18 (m, 2H). MS *m/z*: 477.4 $[M+H]^+$.

(1R,3S/1S,3R)-5-(3-{[4-methyl-5-(3-methyl-1,2-oxazol-5-yl)-4H-1,2,4-triazol-3-yl]sulfanyl}propyl)-1-[4-(trifluoromethyl)phenyl]-5-azaspiro[2.4]heptane (39)

Following the general procedure, the crude residue was purified by flash chromatography to give **39**. Yield 64%. ^{1}H NMR (*Acetone-d_6*) δ: 7.65 - 7.58 (m, 2H), 7.41 - 7.37 (m, 2H), 6.91 - 6.88 (m, 1H), 3.84

(s, 3H), 3.28 (m, 2H), 2.90 - 2.81 (m, 2H), 2.60 (br. s., 3H), 2.38 (s, 3H), 2.30 - 2.23 (m, 1H), 2.03 - 1.84 (m, 5H), 1.34 - 1.29 (m, 1H), 1.23 (m, 1H). MS *m/z*: 478.1 $[M+H]^+$.

4-[4-methyl-5-({3-[(1R,3S)-1-[4-(trifluoromethyl)phenyl]-5-azaspiro[2.4]heptan-5-yl]propyl}sulfanyl)-4H-1,2,4-triazol-3-yl]benzamide (40a)

The compound was prepared following the general procedure, but using (1R,3S)-1-[4-(trifluoromethyl)phenyl]-5-azaspiro[2.4]heptane, *cis* enantiomer 1, and not the racemic mixture; the crude residue was purified by flash chromatography to give **40a**. Yield 72%. ^{1}H NMR (*Acetone-d*$_6$) δ: 8.12 (d, J = 8.53 Hz, 2H), 7.87 (d, J = 8.53Hz, 2H), 7.63 (d, J = 8.03 Hz, 2H), 7.39 (d, J = 8.28 Hz, 2H), 6.76 (br.s., 1H), 3.73 (s, 3H), 3.32 - 3.17 (m, 2H), 2.76 - 2.71 (m, 1H), 2.68 - 2.59 (m, 1H), 2.58 - 2.44 (m, 3H), 2.29 - 2.20 (m, 1H), 2.12 - 2.08 (m, 1H), 2.04 - 1.82 (m, 4H), 1.30 (m, 1H), 1.22 (m, 1H). MS *m/z*: 516.4 $[M+H]^+$.

3-[4-methyl-5-({3-[(1R,3S)-1-[4-(trifluoromethyl)phenyl]-5-azaspiro[2.4]heptan-5-yl]propyl}sulfanyl)-4H-1,2,4-triazol-3-yl]benzamide (41a)

The compound was prepared following the general procedure, but using (1R,3S)-1-[4-(trifluoromethyl)phenyl]-5-azaspiro[2.4]heptane, *cis* enantiomer 1, and not the racemic mixture; the crude residue was purified by flash chromatography to give **41a**. Yield 66%. ^{1}H NMR (*Acetone-d*$_6$) δ: 8.27 (t, J=1.63 Hz, 1H), 8.11 (td, J = 1.47, 7.84 Hz, 1H), 7.92 (td, J = 1.38, 8.03 Hz, 1H), 7.53-7.77 (m, 4H), 7.39 (d, J = 8.28 Hz, 2H), 6.76 (br.s., 1H), 3.72 (s, 3H), 3.32 - 3.16 (m, 2H), 2.77 - 2.70 (m, 1H), 2.68 - 2.59 (m, 1H), 2.58 - 2.42 (m, 3H), 2.29 - 2.21 (m, 1H), 2.07 - 1.93 (m, 3H), 1.91 - 1.81 (m, 2H), 1.34 - 1.26 (m, 1H), 1.25 -1.19 (m, 1H). MS *m/z*: 516.4 $[M+H]^+$.

2-[4-methyl-5-({3-[(1R,3S)-1-[4-(trifluoromethyl)phenyl]-5-azaspiro[2.4]heptan-5-yl]propyl}sulfanyl)-4H-1,2,4-triazol-3-yl]benzamide hydrochloride (42a)

The compound was prepared following the general procedure, but using (1R,3S)-1-[4-(trifluoromethyl)phenyl]-5-azaspiro[2.4]heptane, *cis* enantiomer 1, and not the racemic mixture; the crude residue was purified by flash chromatography and the hydrochloride made as reported in the general procedure to give **42a**. Yield 22%. ^{1}H NMR (*DMSO-d$_6$*) δ: 11.03 - 10.40 (m, 2H), 8.02 - 7.30 (m, 7H), 6.87 (br. s., 1H), 3.82 - 3.60 (m, 3H), 3.47 - 3.05 (m, 5H), 3.05 - 2.61 (m, 4H), 2.48 - 1.82 (m, 4H), 1.56 - 1.22- (m, 2H). MS *m/z*: 516.4 $[M+H]^+$.

4-[4-methyl-5-({3-[(1R,3S)-1-[4-(trifluoromethyl)phenyl]-5-azaspiro[2.4]heptan-5-yl]propyl}sulfanyl)-4H-1,2,4-triazol-3-yl]benzene-1-sulfonamide (43a)

The compound was prepared following the general procedure, but using (1R,3S)-1-[4-(trifluoromethyl)phenyl]-5-azaspiro[2.4]heptane, *cis* enantiomer 1, and not the racemic mixture; the crude residue was purified by flash chromatography to give **43a**. Yield 60%. ^{1}H NMR (Acetone-d$_6$) δ: 8.05 (s, 2H), 7.97 (s, 2H), 7.66 - 7.58 (m, 2H), 7.42 - 7.32 (m, 2H), 6.76 - 6.70 (m, 1H), 3.74 (s, 3H), 3.26 (m, 2H), 2.79 (br. s., 2H), 2.70 - 2.45 (m, 4H), 2.26 - 2.21 (m, 1H), 2.02 - 1.81 (m, 4H), 1.29 (m, 1H), 1.21 (m, 1H). MS *m/z*: 552.3 $[M+H]^+$.

1-{4-[4-methyl-5-({3-[(1R,3S)-1-[4-(trifluoromethyl)phenyl]-5-azaspiro[2.4]heptan-5-yl]propyl}sulfanyl)-4H-1,2,4-triazol-3-yl]phenyl}ethan-1-one hydrochloride (44a)

The compound was prepared following the general procedure, but using (1R,3S)-1-[4-(trifluoromethyl)phenyl]-5-azaspiro[2.4]heptane, *cis* enantiomer 1, and not the racemic mixture; the crude residue was purified by flash chromatography and the hydrochloride made as reported in the general procedure to give **44a**. Yield 62%. ^{1}H NMR (*DMSO-d$_6$*) δ: 10.44 - 10.14 (m, 1H), 8.12 (d, *J* = 8.28 Hz, 2H), 7.88 (d, *J* = 8.53 Hz, 2H), 7.65 (d, *J* = 8.03 Hz, 2H), 7.48 - 7.38 (m, 2H), 3.74 - 3.68 (m, 1H), 3.64 (d, *J* = 4.02 Hz, 3H), 3.47 - 3.38 (m, 1H), 3.21 (d, *J* = 7.28 Hz, 6H), 2.65 (s, 3H), 2.45 - 2.20 (m, 2H), 2.14 - 1.92 (m, 3H), 1.53 - 1.26 (m, 2H). MS *m/z*: 515.4 $[M+H]^+$.

4-[4-methyl-5-({3-[(1R,3S)-1-[4-(trifluoromethyl)phenyl]-5-azaspiro[2.4]heptan-5-yl]propyl}sulfanyl)-4H-1,2,4-triazol-3-yl]benzonitrile (45a)

The compound was prepared following the general procedure, but using (1R,3S)-1-[4-(trifluoromethyl)phenyl]-5-azaspiro[2.4]heptane, *cis* enantiomer 1, and not the racemic mixture; the crude residue was purified by flash chromatography to give **45a**. Yield 78%. ^{1}H NMR (*Acetone-d$_6$*) δ: 8.05 - 7.93- (m, 4H), 7.62 (d, J = 8.03 Hz, 2H), 7.39 (d, J = 8.28 Hz, 2H), 3.76 (s, 3H), 3.34 - 3.19 (m, 2H), 2.77 - 2.72 (m, 1H), 2.68 - 2.60 (m, 1H), 2.57 - 2.45 (m, 3H), 2.28 - 2.20 (m, 1H), 2.13 - 2.08 (m, 1H), 2.04 - 1.81- (m, 4H), 1.32 - 1.26 (m, 1H), 1.22 (m, 1H). MS *m/z*: 498.4 $[M+H]^+$.

2-{4-[4-methyl-5-({3-[(1R,3S)-1-[4-(trifluoromethyl)phenyl]-5-azaspiro[2.4]heptan-5-yl]propyl}sulfanyl)-4H-1,2,4-triazol-3-yl]phenyl}acetamide (46a)

The compound was prepared following the general procedure, but using (1R,3S)-1-[4-(trifluoromethyl)phenyl]-5-azaspiro[2.4]heptane, *cis* enantiomer 1, and not the racemic mixture; the crude residue was purified by flash chromatography to give **46a**. Yield 61%. ^{1}H NMR (*DMSO-d$_6$*) δ: 7.68 - 7.58 (m, 4H), 7.53 (br.s., 1H), 7.45 (d, J = 8.28 Hz, 2H), 7.33 (d, J = 8.28 Hz, 2H), 6.94 (br.s., 1H), 3.58 (s, 3H), 3.48 (s, 2H), 3.16-3.08 (m, 2H), 2.74 - 2.64 (m, 1H), 2.48 - 2.37 (m, 4H), 2.25 - 2.17 (m, 1H), 1.96 (d, 3H), 1.76 (s, 2H), 1.28 (t, J = 5.52 Hz, 1H), 1.18 (m, 1H). MS *m/z*: 530.4 $[M+H]^+$.

(1R,3S)-5-[3-({4-methyl-5-[4-(1,3-oxazol-2-yl)phenyl]-4H-1,2,4-triazol-3-yl}sulfanyl)propyl]-1-[4-(trifluoromethyl)phenyl]-5-azaspiro[2.4]heptane (47a)

The compound was prepared following the general procedure, but using (1R,3S)-1-[4-(trifluoromethyl)phenyl]-5-azaspiro[2.4]heptane, *cis* enantiomer 1, and not the racemic mixture; the crude residue was purified by flash chromatography to give **47a**. Yield 60%. ^{1}H NMR (*Acetone-d$_6$*) δ: 8.25 - 8.19 (m, 2H), 8.11 (d, J = 0.75 Hz, 1H), 7.97 - 7.92 (m, 2H), 7.62 (d, J = 8.03Hz,

2H), 7.44 - 7.37 (m, 3H), 3.76 (s, 3H), 3.34 - 3.20 (m, 2H), 2.72 - 2.47 (m, 6H), 2.28 (br. s., 1H), 2.02 - 1.86 (m, 4H), 1.33 (br. s., 1H), 1.24 (br. s., 1H). MS *m/z*: 540.4 $[M+H]^+$.

(1R,3S)-5-[3-({4-methyl-5-[3-(1,3-oxazol-2-yl)phenyl]-4H-1,2,4-triazol-3-yl}sulfanyl)propyl]-1-[4-(trifluoromethyl)phenyl]-5-azaspiro[2.4]heptane (48a)

The compound was prepared following the general procedure, but using (1R,3S)-1-[4-(trifluoromethyl)phenyl]-5-azaspiro[2.4]heptane, *cis* enantiomer 1, and not the racemic mixture; the crude residue was purified by flash chromatography to give **48a**. Yield 57%. ^{1}H NMR (*Acetone-d$_6$*) δ: 8.43 (t, *J* = 1.63 Hz, 1H), 8.22 (td, *J* = 1.32, 7.91 Hz, 1H), 8.11 (d, *J* = 0.5 Hz, 1H), 7.91 (td, *J* = 1.32, 7.91 Hz, 1H), 7.75 (t, *J* = 7.78 Hz, 1H), 7.63 (d, *J* = 8.03 Hz, 2H), 7.43 (d, *J* = 8.03 Hz, 2H), 7.38 (d, *J* = 0.5 Hz, 1H), 3.77 (s, 3H), 3.38 - 3.19 (m, 2H), 3.04 - 2.64 (m, 6H), 2.37 - 2.28 (m, 2H), 2.05 - 1.93 (m, 3H), 1.41 - 1.35 (m, 1H), 1.30 - 1.25 (m, 1H). MS *m/z*: 540.4 $[M+H]^+$.

(1S,3S/1R,3R)-5-(3-{[4-methyl-5-(pyridin-4-yl)-4H-1,2,4-triazol-3-yl]sulfanyl}propyl)-1-[4-(trifluoromethyl)phenyl]-5-azaspiro[2.4]heptane (49)

Following the general procedure, the crude residue was purified by flash chromatography to give **49**. Yield 62%. ^{1}H NMR (*Acetone-d$_6$*) δ: 8.74-8.80 (m, 2H), 7.75-7.80 (m, 2H), 7.63 (d, *J* = 8.03 Hz, 2H), 7.36 (d, *J* = 8.03Hz, 2H), 3.81 (s, 3H), 3.35 (m, 2H), 2.64 (br. s., 6H), 2.24-2.32 (m, 1H), 2.09-2.13 (m, 1H), 1.99 (m, 2H), 1.62-1.75 (m, 1H), 1.38-1.50 (m, 1H), 1.29-1.21 (m, 2H). MS *m/z*: 474.4 $[M+H]^+$.

(1S,3S/1R,3R)-5-(3-{[4-methyl-5-(pyridin-4-yl)-4H-1,2,4-triazol-3-yl]sulfanyl}propyl)-1-[4-(trifluoromethyl)phenyl]-5-azaspiro[2.4]heptane hydrochloride (50)

Following the general procedure, the crude residue was purified by flash chromatography and the hydrochloride made as reported in the general procedure to give **50**. Yield 30%. ^{1}H NMR (*DMSO-d$_6$*) δ: 11.35 - 11.13 (m, 1H), 8.92 (d, *J* = 6.53 Hz, 2H), 8.07 (d, *J* = 6.53 Hz, 2H), 7.65 (dd, *J* = 5.14, 7.91 Hz, 2H), 7.45 (m, 2H), 3.73 (d, *J* = 4.02 Hz, 3H), 3.70 - 3.61 (m, 1H), 3.45 - 3.35 (m, 1H), 3.35 - 3.23 (m,

3H), 3.22 - 3.03 (m, 2H), 2.65 - 2.56 (m, 1H), 2.98 - 2.56 (m, 1H), 2.49 - 2.36 (m, 1H), 2.34 - 1.94 (m, 4H), 1.51 - 1.25 (m, 2H). MS *m/z*: 474.4 $[M+H]^+$.

(1S,3S/1R,3R)-5-(3-{[4-methyl-5-(pyridin-3-yl)-4H-1,2,4-triazol-3-yl]sulfanyl}propyl)-1-[4-(trifluoromethyl)phenyl]-5-azaspiro[2.4]heptane (51)

Following the general procedure, the crude residue was purified by flash chromatography to give **51**. Yield 59%. ^{1}H NMR (*Acetone-d$_6$*) δ: 8.96 (d, *J* = 2.26Hz, 1H), 8.73 (dd, *J* = 1.51, 5.02 Hz, 1H), 8.15 (td, *J* = 1.98, 7.84 Hz 1H), 7.63 (d, *J* = 8.03 Hz, 2H), 7.60 - 7.54 (m, 1H), 7.35 (d, *J* = 8.03 Hz, 2H), 3.76 (s, 3H), 3.33 (m, 2H), 2.73-2.77 (m, 1H), 2.68 - 2.54 (m, 6H), 2.31 - 2.24 (m, 1H), 1.97 (s, 2H), 1.72 - 1.62 (m, 1H), 1.49 - 1.38 (m, 1H), 1.27 (m, 1H), 1.24 - 1.19 (m, 1H). MS *m/z*: 474.4 $[M+H]^+$.

(1R,3S/1S,3R)-5-(3-{[4-methyl-5-(pyridin-3-yl)-4H-1,2,4-triazol-3-yl]sulfanyl}propyl)-1-[4-(trifluoromethyl)phenyl]-5azaspiro[2.4]heptane dihydrochloride (52)

Following the general procedure, the crude residue was purified by flash chromatography and the compound transformed into the hydrochloride to give **52**. Yield 34%. ^{1}H NMR (*DMSO-d$_6$*) δ: 11.38 - 11.12 (m, 1H), 8.94 (d, *J* = 2.01 Hz, 1H), 8.77 (dd, *J* = 1.51, 5.02 Hz, 1H), 8.21 (td, *J* = 1.88, 7.78 Hz, 2H), 7.76-7.54 (m, 3H), 7.65 (m, 2H), 7. 7.44 (d, *J* = 7.78, 2H), 3.72 - 3.60 (m, 4H), 3.46 - 2.89 (m, 7H), 2.66 - 2.56 (m, 1H), 2.48 - 2.18 (m, 2H), 2.16 - 1.94 (m, 3H), 1.48 (s, 2H). MS *m/z*: 474.5 $[M+H]^+$.

(1S,3S/1R,3R)-5-(3-{[4-methyl-5-(pyridin-2-yl)-4H-1,2,4-triazol-3-yl]sulfanyl}propyl)-1-[4-(trifluoromethyl)phenyl]-5-azaspiro[2.4]heptane (53)

Following the general procedure, the crude residue was purified by flash chromatography to give **53**. Yield 58%. ^{1}H NMR (*Acetone-d$_6$*) δ: 8.71 (d, *J*=5.02 Hz, 1H), 8.22 (d, *J* = 8.03 Hz, 1H), 7.98 (dt, *J* = 1.63, 7.72 Hz, Hz, 1H), 7.62 (d, *J* = 9.28Hz, 2H), 7.51 - 7.45 (m, 1H), 7.35 (d, *J* = 8.28 Hz, 2H), 4.05 (s, 3H), 3.39 - 3.30 (m, 2H), 2.77 - 2.71 (m, 2H), 2.68 - 2.54 (m, 5H), 2.31 - 2.23 (m, 1H), 2.02 - 1.93 (m, 2H), 1.71 - 1.61 (m, 1H), 1.47 - 1.37 (m, 1H), 1.29 - 1.23 (m, 1H), 1.23 - 1.18-(m, 1H). MS *m/z*: 474.5 $[M+H]^+$.

(1R,3S/1S,3R)-5-(3-{[4-methyl-5-(pyridin-2-yl)-4H-1,2,4-triazol-3-yl]sulfanyl}propyl)-1-[4-(trifluoro methyl)phenyl]-5-azaspiro[2.4]heptane dihydrochloride (54)

Following the general procedure, the crude residue was purified by flash chromatography and the compound transformed into the hydrochloride to give **54**. Yield 30%. ^{1}H NMR (*DMSO-d_6*) δ: 10.84 - 10.54 (m, 1H), 8.73 (d, *J* = 4.52 Hz, 1H), 8.12 (d, *J* = 7.78Hz, 1H), 8.01 (t, *J*= 7.78 Hz 1H), 7.66 (d, *J* = 8.03 Hz, 2H), 7.56-7.51 (m, 1H), 7.44 (d, *J* = 8.03 Hz,2H), 4.00-3.84 (m, 3H), 3.75 - 3.65 (m, 1H), 3.46 - 2.92 (m, 7H), 2.70 - 2.59 (m, 1H), 2.43 - 2.18 (m, 2H), 2.16 - 1.92 (m, 3H), 1.53 - 1.25 (m, 2H). MS *m/z*: 474.5 $[M+H]^+$.

(1S,3S/1R,3R)-5-(3-{[4-methyl-5-(pyrazin-2-yl)-4H-1,2,4-triazol-3-yl]sulfanyl}propyl)-1-[4-(trifluoro methyl)phenyl]-5-azaspiro[2.4]heptane (55)

Following the general procedure, the crude residue was purified by flash chromatography to give **55**. Yield 25%. ^{1}H NMR (*Acetone-d_6*) δ: 9.38 (d, *J* = 1.25 Hz, 1H), 8.72 (m, 2H), 7.63 (d, *J* =8.03 Hz, 2H), 7.52 - 7.33 (m, 2H), 4.02 (s, 3H), 3.50 - 3.40 (m, 2H), 3.15 - 2.89 (m, 3H), 2.47 - 2.31 (m, 1H), 2.19 - 2.11 (m, 1H), 2.02 (br. s., 1H), 1.86 - 1.72 (m, 2H), 1.65 - 1.43 (m, 2H), 1.41 - 1.25 (m, 3H). MS *m/z*: 475.1 $[M+H]^+$.

(1R,3S/1S,3R)-5-(3-{[4-methyl-5-(pyrazin-2-yl)-4H-1,2,4-triazol-3-yl]sulfanyl}propyl)-1-[4-(trifluoro methyl)phenyl]-5-azaspiro[2.4]heptane (56)

Following the general procedure, the crude residue was purified by flash chromatography to give **56**. Yield 54%. ^{1}H NMR (*Acetone-d_6*) δ: 9.39 (d, *J* = 1.51 Hz, 1H), 8.76 - 8.69 (m, 2H), 7.62 (d, *J* = 8.03 Hz, 2H), 7.39 (d, *J* = 8.28 Hz, 2H), 4.00 (s, 3H), 3.38 - 3.21 (m, 2H), 2.77 - 2.72 (m, 2H), 2.68 - 2.60-(m,

1H), 2.57 - 2.47 (m, 3H), 2.28 - 2.21 (m, 1H), 2.03 - 1.93 (m, 2H), 1.93 - 1.83 (m, 2H), 1.32 - 1.25 (m, 1H), 1.24 - 1.19 (m, 1H). MS *m/z*: 475.1 $[M+H]^+$.

(1S,3S/1R,3R)-5-(3-{[4-methyl-5-(pyrimidin-4-yl)-4H-1,2,4-triazol-3-yl]sulfanyl}propyl)-1-[4-(trifluoromethyl)phenyl]-5-azaspiro[2.4]heptane (57)

Following the general procedure, the crude residue was purified by flash chromatography to give **57**. Yield 19%. ^{1}H NMR (*Acetone-d*$_6$) δ: 9.28 (d, J = 1.51 Hz, 1H), 8.95 (d, J = 5.27 Hz, 1H), 8.23 (dd, J = 1.51, 5.27 Hz 1H), 7.63 (d, J = 8.28 Hz, 2H), 7.45 - 7.31 (m, 2H), 4.09 (s, 3H), 3.47 - 3.34 (m, 2H), 2.75 - 2.56 (m, 4H), 2.39 - 2.26 (m, 1H), 2.05 - 1.97 (m, 3H), 1.80 - 1.63 (m, 1H), 1.55 - 1.40 (m, 1H), 1.37 - 1.19 (m, 3H). MS *m/z*: 475.5 $[M+H]^+$.

(1R,3S/1S,3R)-5-(3-{[4-methyl-5-(pyrimidin-4-yl)-4H-1,2,4-triazol-3-yl]sulfanyl}propyl)-1-[4-(trifluoromethyl)phenyl]-5-azaspiro[2.4]heptane (58)

Following the general procedure, the crude residue was purified by flash chromatography to give **58**. Yield 55%. ^{1}H NMR (*Acetone-d*$_6$) δ: 9.31 - 9.27 (m, 1H), 8.99 - 8.92 (m, 1H), 8.26 - 8.22 (m, 1H), 7.65 - 7.59 (m, 2H), 7.42 - 7.36 (m, 2H), 4.07 (s, 3H), 3.39 - 3.22 (m, 2H), 2.76 - 2.71 (m, 2H), 2.68 - 2.59 (m, 1H), 2.56 - 2.46 (m, 3H), 2.27 - 2.21 (m, 1H), 2.03 - 1.83 (m, 4H), 1.32 - 1.26 (m, 1H), 1.22 (m, 1H). MS *m/z*: 475.1 $[M+H]^+$.

(1S,3S/1R,3R)-5-(3-{[4-methyl-5-(pyridazin-3-yl)-4H-1,2,4-triazol-3-yl]sulfanyl}propyl)-1-[4-(trifluoromethyl)phenyl]-5-azaspiro[2.4]heptane (59)

Following the general procedure, the crude residue was purified by flash chromatography to give **59**. Yield 39%. ^{1}H NMR (*Acetone-d*$_6$) δ: 9.36 - 9.27 (m, 1H), 8.40 (dd, J = 1.63, 8.66 Hz, 1H), 7.89 (dd, J = 1.63, 8.66 Hz,, 1H), 7.63 (d, J = 8.03 Hz, 2H), 7.36 (d, J = 8.28 Hz, 2H), 4.13 (s, 3H), 3.49 - 3.33 (m, 2H), 2.79 - 2.74 (m, 2H), 2.68 - 2.56 (m, 4H), 2.31 - 2.24 (m, 1H), 2.13 - 2.10 (m, 1H), 2.13 - 2.09 (m,

2H), 2.04 - 1.95 (m, 2H), 1.71 - 1.62 (m, 1H), 1.49 - 1.39 (m, 1H), 1.30 - 1.25 (m, 1H), 1.24 - 1.18 (m, 1H). MS *m/z*: 475.4 $[M+H]^+$.

1R,3S/1S,3R)-5-(3-{[4-methyl-5-(pyridazin-3-yl)-4H-1,2,4-triazol-3-yl]sulfanyl}propyl)-1-[4-(trifluoromethyl)phenyl]-5-azaspiro[2.4]heptane (60)

Following the general procedure, the crude residue was purified by flash chromatography to give **60**. Yield 62%. ^{1}H NMR (*Acetone-d$_6$*) δ: 9.34 - 9.28 (m, 1H), 8.44 - 8.37 (m, 1H), 7.91 - 7.84 (m, 1H), 7.66 - 7.59 (m, 2H), 7.45 - 7.37 (m, 2H), 4.09 (s, 3H), 3.41 - 3.25- (m, 2H), 2.95 - 2.52- (m., 6H), 2.32 - 2.24- (m, 1H), 2.04 - 1.87 (m, 4H), 1.38 - 1.20 (m, 2H). MS *m/z*: 475.4 $[M+H]^+$.

(1S,3S/1R,3R)-5-(3-{[4-methyl-5-(pyridazin-4-yl)-4H-1,2,4-triazol-3-yl]sulfanyl}propyl)-1-[4-(trifluoromethyl)phenyl]-5-azaspiro[2.4]heptane (61)

Following the general procedure, the crude residue was purified by flash chromatography to give **61**. Yield 47%. ^{1}H NMR (*Acetone-d$_6$*) δ: 9.65 (m, 1H), 9.40 (m, 1H), 8.05 (m, 1H), 7.64 (d, J = 8.28 Hz, 2H), 7.36 (d, J = 8.28 Hz, 2H), 3.90 (s, 3H), 3.38 (m, 2H), 2.67 - 2.56 (m, 5H), 2.31 - 2.25 (m, 1H), 2.13 - 2.09 (m, 1H), 2.03 - 1.94 (m, 2H), 1.72 - 1.63 (m, 1H), 1.48 - 1.39 (m, 1H), 1.30 - 1.25 (m, 1H), 1.24 - 1.20 (m, 1H). MS *m/z*: 475.4 $[M+H]^+$.

(1R,3S/1S,3R)-5-(3-{[4-methyl-5-(pyridazin-4-yl)-4H-1,2,4-triazol-3-yl]sulfanyl}propyl)-1-[4-(trifluoromethyl)phenyl]-5-azaspiro[2.4]heptane (62)

Following the general procedure, the crude residue was purified by flash chromatography to give **62**. Yield 63%. ^{1}H NMR (*Acetone-d$_6$*) δ: 9.66 - 9.60 (m, 1H), 9.42 - 9.37 (m, 1H), 8.08 - 8.02 (m, 1H), 7.66 - 7.60 (m, 2H), 7.43 - 7.36 (m, 2H), 3.86 (s, 3H), 3.36 - 3.21 (m, 2H), 2.73 - 2.45 (m, 4H), 2.27 - 2.21 (m, 1H), 2.15 - 2.08 (m, 1H), 2.03 - 1.83 (m, 5H), 1.33 - 1.19 (m, 2H). MS *m/z*: 475.4 $[M+H]^+$.

(1R,3S/1S,3R)-5-(3-{[4-methyl-5-(pyridin-3-yl)-4H-1,2,4-triazol-3-yl]sulfanyl}propyl)-1-phenyl-5-azaspiro[2.4]heptane (63)

Following the general procedure, the crude residue was purified by flash chromatography to give **63**. Yield 47%. ^{1}H NMR (*Acetone-d_6*) δ: 8.97 (d, J = 1.76 Hz, 1H), 8.75 (dd, J = 1.63, 4.89 Hz, 1H), 8.17 (td, J =1.98, 7.84 Hz, 1H),7.62 - 7.54 (m, 1H), 7.33-7.27 (m, 2H), 7.23-7.14 (m, 3H), 3.74 (s, 3H), 3.36 - 3.20 (m, 3H), 3.00 - 2.52 (m, 4H), 2.38 - 2.26 (m, 1H), 2.17 (m 1H), 2.04 - 1.87 (m, 3H), 1.27-1.11 (m, 2H), 1.19 - 1.12 (m, 1H). MS *m/z*: 406.4 $[M+H]^+$.

(1S,3S)-1-[2-fluoro-4-(trifluoromethyl)phenyl]-5-(3-{[4-methyl-5-(pyridin-3-yl)-4H-1,2,4-triazol-3-yl]sulfanyl}propyl)-5-azaspiro[2.4]heptane dihydrochloride (64b)

Following the general procedure, the compound was prepared to give **64** (data not reported) which was separated into the single enantiomers by preparative chiral HPLC (SFC) and the compound transformed into the hydrochloride to give **64b**. Column: Chiralpak AD-H (25 x 2.0 cm), 5 µm; mobile phase: (Methanol+0.1% isopropylamine) 22 %; flow rate: 45 mL/min; DAD detection: 220 nm; loop: 700 µL **64b** (enantiomer 2), retention time = 9.1 min. Yield 49%. ^{1}H NMR (*Acetone-d_6*) δ: 8.96 (d, J = 1.51 Hz, 1H), 8.79 (dd, J = 1.51, 4.77 Hz, 1H), 8.23 (d, J = 8.03 Hz, 1H), 7.60 - 7.56 (m, 1H), 7.49 (d, J = 8.28 Hz, 2H), 7.38 - 7.32 (m, 1H), 3.73 (s, 3H), 3.36 - 3.17 (m, 2H), 2.71 - 2.44 (m, 5H), 2.30 - 2.26 (m, 1H), 2.05 - 1.96 (m, 3H), 1.90 - 1.83 (m, 2H), 1.41 - 1.22 (m, 2H). MS *m/z*: 492.4 $[M+H]^+$.

(1S,3S)-1-(2,4-difluorophenyl)-5-(3-{[4-methyl-5-(pyridin-3-yl)-4H-1,2,4-triazol-3-yl]sulfanyl}propyl)-5-azaspiro[2.4]heptane (65b)

Following the general procedure, the compound was prepared to give **65** (data not reported) which was separated into the single enantiomers by preparative chiral HPLC (SFC). Column: Chiralpak AD-H (25 x 2.0 cm), 5 µm; mobile phase: (Methanol+0.1% isopropylamine) 25 %; flow rate: 45 mL/min; DAD detection: 220 nm; loop: 700 µL **65b** (enantiomer 2), retention time = 11.6 min. Yield 39%. ^{1}H NMR (*Acetone-d_6*) δ: 8.99 - 8.94 (m, 1H), 8.77 - 8.72 (m, 1H), 8.19 - 8.14 (m, 1H), 7.62 - 7.55 (m, 1H), 7.20 - 7.12 (m, 1H), 7.04 - 6.90 (m, 2H), 3.74 (s, 3H), 3.35-3.20 (m, 2H), 2.78 - 2.74 (m, 1H), 2.66 - 2.59 (m,

1H), 2.56 - 2.47 (m, 2H), 2.38 (d, *J* = 9.03 Hz, 1H), 2.15 - 2.09 (m, 1H), 2.02 - 1.95 (m, 3H), 1.92 - 1.82 (m, 2H), 1.25 - 1.20 (m, 1H), 1.19 - 1.12 (m, 1H). MS *m/z*: 442.3 $[M+H]^+$.

(1R,3S)-1-(4-fluorophenyl)-5-(3-{[4-methyl-5-(pyridin-3-yl)-4H-1,2,4-triazol-3-yl]sulfanyl}propyl)-5-azaspiro[2.4]heptane (66b)

Following the general procedure, the compound was prepared to give **66** (data not reported) which was separated into the single enantiomers by preparative chiral HPLC (SFC) to give **66b**. Column: Chiralpak AD-H (25 x 2.0 cm), 5 µm; mobile phase: (Methanol+0.1% isopropylamine) 25 %; flow rate: 45 mL/min; DAD detection: 220 nm; loop: 700 µL **66b** (enantiomer 2), retention time= 15.9 min. Yield 31%. ^{1}H NMR (*Acetone-d$_6$*) δ: 8.97 (d, *J* = 1.76 Hz, 1H), 8.74 (dd, *J* = 1.38, 4.89 Hz, 1H), 1H), 8.16 (d, *J* = 7.78 Hz 1H), 7.58 (m, 1H), 7.24 - 7.17 (m, 2H), 7.09 - 7.01 (m, 2H), 3.76 - 3.72 (m, 3H), 3.32 - 3.18 (m, 2H), 2.78 - 2.62 (m, 2H), 2.52 (m, 2H), 2.44 - 2.36 (m, 1H), 2.15 - 2.09 (m, 2H), 2.02 - 1.82 (m, 4H), 1.16 - 1.06 (m, 2H). MS *m/z*: 424.4 $[M+H]^+$.

(1R,3S)-5-(3-{[4-methyl-5-(2-methylpyridin-3-yl)-4H-1,2,4-triazol-3-yl]sulfanyl}propyl)-1-[4-(trifluoromethyl)phenyl]-5-azaspiro[2.4]heptane dihydrochloride (67a)

The compound was prepared following the general procedure, but using (1R,3S)-1-[4-(trifluoromethyl)phenyl]-5-azaspiro[2.4]heptane, *cis* enantiomer 1, and not the racemic mixture; the crude residue was purified by flash chromatography to give the free base that was transformed into the hydrochloride **67a**. Yield 18%. ^{1}H NMR (*DMSO-d$_6$*) δ: 10.99 - 10.72 (m, 1H), 8.77 - 8.70 (m, 1H), 8.14 - 8.04 (m, 1H), 7.66 (d, *J* = 8.03 Hz, 2H), 7.62 - 7.56 (m, 1H), 7.45 (d, *J* = 7.68 Hz, 2H), 3.73 - 3.63 (m, 2H), 3.48 - 3.36 (m, 4H), 3.34 - 3.07 (m, 6H), 3.01 - 2.91 (m, 1H), 2.71 - 2.59 (m, 1H), 2.44 - 2.17 (m, 2H), 2.09 (br. s., 3H), 1.53 - 1.36 (m, 2H), 1.35 - 1.21 (m, 1H). MS *m/z*: 488.4 $[M+H]^+$.

(1R,3S)-5-[3-({4-methyl-5-[2-(trifluoromethyl)pyridin-3-yl]-4H-1,2,4-triazol-3-yl}sulfanyl)propyl]-1-[4-(trifluoromethyl)phenyl]-5-azaspiro[2.4]heptane dihydrochloride (68a)

The compound was prepared following the general procedure, but using (1R,3S)-1-[4-(trifluoromethyl)phenyl]-5-azaspiro[2.4]heptane, *cis* enantiomer 1, and not the racemic mixture; the crude residue was purified by flash chromatography to give the free base that was transformed into the hydrochloride **68a**. Yield 55%. ^{1}H NMR (*DMSO-d$_6$*) δ: 10.57 - 10.24 (m, 1H), 8.98 (d, J = 4.77 Hz, 1H), 8.25 (d, J = 7.78 Hz, 1H), 7.95 (m, 1H), 7.66 (d, , J = 8.03 Hz, 2H), 7.44 (m, 2H), 3.77 - 3.65 (m, 1H), 3.48 - 3.41 (m, 1H), 3.35 (br. s., 3H), 3.26-3.19 (m, 6H), 3.04 - 2.63 (m, 1H), 2.45 - 2.20 (m, 2H), 2.16 - 1.92 (m, 3H), 1.53 - 1.27 (m, 2H). MS *m/z*: 542.4 $[M+H]^+$.

(1R,3S)-5-(3-{[5-(2-methoxypyridin-3-yl)-4-methyl-4H-1,2,4-triazol-3-yl]sulfanyl}propyl)-1-[4-(trifluoromethyl)phenyl]-5-azaspiro[2.4]heptane dihydrochloride (69a)

The compound was prepared following the general procedure, but using (1R,3S)-1-[4-(trifluoromethyl)phenyl]-5-azaspiro[2.4]heptane, *cis* enantiomer 1, and not the racemic mixture; the crude residue was purified by flash chromatography to give the free base that was transformed into the hydrochloride **69a**. Yield 52%. ^{1}H NMR (*DMSO-d$_6$*) δ: 10.88 -10.39 (m, 1 H), 8.46- 8.34 (m, 1 H), 7.87 (d, J = 7.34 Hz, 1 H), 7.71 - 7.61 (m, 2 H), 7.44 (d, J = 8.31 Hz, 2 H), 7.15 - 7.24 (m, 1 H), 3.97 - 3.86 (m, 3 H), 3.82 - 2.60 (m, 11 H), 2.59- 2.32 (m, 1 H), 2.31 - 1.89 (m, 4 H), 1.54 - 1.26 (m, 2 H), MS *m/z*: 504.4 $[M+H]^+$.

5-[4-methyl-5-({3-[(1R,3S)-1-[4-(trifluoromethyl)phenyl]-5-azaspiro[2.4]heptan-5-yl]propyl}sulfanyl)-4H-1,2,4-triazol-3-yl]pyridine-2-carbonitrile dihydrochloride (70a)

The compound was prepared following the general procedure, but using (1R,3S)-1-[4-(trifluoromethyl)phenyl]-5-azaspiro[2.4]heptane, *cis* enantiomer 1, and not the racemic mixture; the crude residue was purified by flash chromatography to give the free base that was transformed into the hydrochloride **70a**. Yield 30%. ^{1}H NMR (*DMSO-d$_6$*) δ: 10.70 - 10.41 (m, 1H), 9.11 (s, 1H), 8.42 (dd, J=2.01, 8.03 Hz, 1H), 8.27 (d, J=8.28 Hz, 1H), 7.66 (d, J = 7.78 Hz, 2H), 7.49 - 7.38 (m, 2H), 3.67 (d, J = 4.02 Hz, 3H), 3.47 - 3.06 (m, 7H), 3.01 - 2.61 (m, 1H), 2.50 - 2.45 (m, 1H), 2.44 - 2.20 (m, 2H), 2.15 - 1.92 (m, 3H), 1.53 - 1.26 (m, 2H). MS *m/z*: 499.5 $[M+H]^+$.

(1R,3S)-5-[4-methyl-5-({3-[(1R,3S)-1-[4-(trifluoromethyl)phenyl]-5-azaspiro[2.4]heptan-5-yl]propyl}sulfanyl)-4H-1,2,4-triazol-3-yl]pyridine-2-carboxamide (71a)

The compound was prepared following the general procedure, but using (1R,3S)-1-[4-(trifluoromethyl)phenyl]-5-azaspiro[2.4]heptane, *cis* enantiomer 1, and not the racemic mixture; the crude residue was purified by flash chromatography to give **71a**. Yield 26%. ^{1}H NMR (*Acetone-d$_6$*) δ: 9.02 - 8.97 (m, 1H), 8.36 (dd, *J*=2.13, 8.16 Hz, 1H), 8.31 - 8.25 (m, 1H), 8.07 - 7.95 (m, 1H), 7.62 (d, *J* = 8.03 Hz, 2H), 7.39 (d, *J* = 8.03 Hz, 2H), 6.98 - 6.85 (m, 1H), 3.81 - 3.73 (m, 3H), 3.36 - 3.18 (m, 2H), 2.71 - 2.39 (m, 5H), 2.29-2.20 (m, 1H), 2.17 - 2.10 (m, 1H), 2.04 - 1.79 (m, 4H), 1.30 (br. s., 1H), 1.23 (d, *J* = 7.53Hz, 1H). MS *m/z*: 517.5 $[M+H]^+$.

(1R,3S)-5-(3-{[5-(2,6-dimethylpyridin-3-yl)-4-methyl-4H-1,2,4-triazol-3-yl]sulfanyl}propyl)-1-[4-(trifluoromethyl)phenyl]-5-azaspiro[2.4]heptane (72a)

The compound was prepared following the general procedure, but using (1R,3S)-1-[4-(trifluoromethyl)phenyl]-5-azaspiro[2.4]heptane, *cis* enantiomer 1, and not the racemic mixture; the crude residue was purified by flash chromatography to give **72a**. Yield 71%. ^{1}H NMR (*Acetone-d$_6$*) δ: 7.70 - 7.66 (m, 1H), 7.64 - 7.59 (m, 2H), 7.44 - 7.38 (m, 2H), 7.26 - 7.21 (m, 1H), 3.45 (s, 3H), 3.36 - 3.18 (m, 3H), 2.90 - 2.82 (m, 1H), 2.74 - 2.57 (m, 3H), 2.55 (s, 3H), 2.39 (s, 3H), 2.34 - 2.25 (m, 1H), 2.15 - 2.09 (m, 1H), 2.05 - 1.98 (m, 3H), 1.97 - 1.89 (m, 2H), 1.38 - 1.21 (m, 2H). MS *m/z*: 502.4 $[M+H]^+$.

6-methyl-5-[4-methyl-5-({3-[(1R,3S)-1-[4-(trifluoromethyl)phenyl]-5-azaspiro[2.4]heptan-5-yl]propyl}sulfanyl)-4H-1,2,4-triazol-3-yl]pyridine-2-carboxamide (73a)

The compound was prepared following the general procedure, but using (1R,3S)-1-[4-(trifluoromethyl)phenyl]-5-azaspiro[2.4]heptane, *cis* enantiomer 1, and not the racemic mixture; the crude residue was purified by flash chromatography to give **73a**. Yield 51%. ^{1}H NMR (*DMSO-d$_6$*) δ: 8.13 (br. s., 1 H), 8.05 - 8.01 (m, 1 H), 8.00 - 7.96 (m, 1H), 7.76 (br. s., 1 H), 7.60 (d, *J* =

8.20 Hz, 2 H), 7.32 (d, *J* = 8.20 Hz, 2 H), 3.36 (s, 3H), 3.20 - 3.10 (m, 2H), 2.74 - 2.69 (m, 1H), 2.54 - 2.36 (m, 7H), 2.20 (dd, *J* = 8.30, 6.38 Hz, 1H),1.98 - 1.82 (m, 3H), 1.81 - 1.71 (m, 2H), 1.27 (t, *J* = 5.63 Hz, 1 H), 1.20 - 1.14 (m, 1 H). ^{13}C NMR (101 MHz, DMSO) Schift 165.4, 156.7, 152.9, 150.8, 150.6, 145.0, 139.4, 128.0, 125.8, 124.8, 124.6, 124.5, 119.0, 57.2, 54.0, 53.9, 35.5, 30.9, 30.5, 29.9, 28.7, 125.8, 22.7, 18.9. MS *m/z*: 531.4 $[M+H]^+$.

6-methyl-5-[4-methyl-5-({3-[(1R,3S)-1-[4-(trifluoromethyl)phenyl]-5-azaspiro[2.4]heptan-5-yl]propyl}sulfanyl)-4H-1,2,4-triazol-3-yl]pyridine-2-carboxylic acid formate (74a)

The compound was prepared following the general procedure, but using (1R,3S)-1-[4-(trifluoromethyl)phenyl]-5-azaspiro[2.4]heptane, *cis* enantiomer 1, and not the racemic mixture; the crude residue was purified by FC on C_{18} cartridge (eluent water+0.1% FA to 60 % water+0.1% FA 40% MeOH +0.1%) to give **74a**. Yield 18%. ^{1}H NMR (*Acetone-d$_6$*) δ: 8.15 (s, 1H), 8.13 - 8.10 (m, 1H), 7.61 (s, 2H), 7.43 - 7.36 (m, 2H), 3.54 (s, 3H), 3.37 - 3.18 (m, 4H), 2.72 (br. s., 1H), 2.64 - 2.51 (m, 6H), 2.31 - 2.25 (m, 1H), 2.09 (br. s., 2H), 2.02 - 1.93 (m, 2H), 1.90 - 1.86 (m, 1H), 1.35 - 1.28 (m, 1H), 1.26 - 1.21 (m, 1H). MS *m/z*: 532.4 $[M+H]^+$.

5-[4-methyl-5-({3-[(1R,3S/1S,3R)-1-[4-(trifluoromethyl)phenyl]-5-azaspiro[2.4]heptan-5-yl]propyl}sulfanyl)-4H-1,2,4-triazol-3-yl]-1,2-dihydropyridin-2-one (75)

The compound was prepared following the general procedure, and the crude residue was purified by flash chromatography to give **75**. Yield 45%. ^{1}H NMR (*DMSO-d$_6$*) δ: 12.10 - 11.96 (m, 1H), 7.80 - 7.68 (m, 2H), 7.64 - 7.55 (m, 2H), 7.36 - 7.27 (m, 2H), 6.53 - 6.44 (m, 1H), 3.52 (s, 3H), 3.15 - 3.01 (m, 2H), 2.68 (br. s., 1H), 2.48 - 2.33 (m, 4H), 2.26 - 2.16 (m, 1H), 2.02 - 1.81 (m, 3H), 1.73 (m, 2H), 1.27 (m, 1H), 1.18 (m, 1H). MS *m/z*: 490.5 $[M+H]^+$.

5-[4-methyl-5-({3-[(1R,3S)-1-[4-(trifluoromethyl)phenyl]-5-azaspiro[2.4]heptan-5-yl]propyl}sulfanyl)-4H-1,2,4-triazol-3-yl]-1,2-dihydropyridin-2-one (75a)

The compound was prepared following the general procedure, but using (1R,3S)-1-[4-(trifluoromethyl)phenyl]-5-azaspiro[2.4]heptane, *cis* enantiomer 1, and not the racemic mixture; the crude residue was purified by flash chromatography to give **75a**. Yield 31%. ^{1}H NMR (*Acetone-d$_6$*) δ: 7.88 (d, J = 2.51 Hz, 1H), 7.75 (dd, J = 2.51, 9.54 Hz, 1H), 7.61 (d, J = 8.28 Hz 2H), 7.37 (d, J = 8.28 Hz, 2H), 6.52 - 6.46 (d, J = 9.29 1H), 3.66 (s, 3H), 3.27 - 3.10 (m, 3H), 2.78 - 2.68 (m, 2H), 2.65 - 2.56 (m, 1H), 2.47 (s, 3H), 2.27 - 2.18 (m, 1H), 2.02 - 1.92 (m, 2H), 1.87 - 1.75 (m, 2H), 1.30 - 1.25 (m, 1H), 1.22 - 1.17 (m, 1H). MS *m/z*: 490.5 $[M+H]^+$.

4-[4-methyl-5-({3-[(1R,3S/1S,3R)-1-[4-(trifluoromethyl)phenyl]-5-azaspiro[2.4]heptan-5-yl]propyl}sulfanyl)-4H-1,2,4-triazol-3-yl]-1,2-dihydropyridin-2-one (76)

The compound was prepared following the general procedure, and crude residue was purified by flash chromatography to give **76**. Yield 17%. ^{1}H NMR (*DMSO-d$_6$*) δ: 7.61 (d, J = 8.28 Hz, 2H), 7.54 (d, J = 6.78 Hz, 1H), 7.32 (d, J = 8.03 Hz, 2H), 6.63 (d, J = 1.51 Hz, 1H), 6.53 - 6.46 (m, 1H), 3.61 (s, 3H), 3.19 - 3.07 (m, 2H), 2.74 - 2.65 (m, 1H), 2.49 - 2.35 (m, 5H), 2.24 - 2.17 (m, 1H), 1.98 - 1.83 (m, 3H), 1.79 - 1.70 (m, 2H), 1.30 - 1.24 (m, 1H), 1.21 - 1.13 (m, 1H). MS *m/z*: 490.4 $[M+H]^+$.

1-methyl-5-[4-methyl-5-({3-[(1R,3S)-1-[4-(trifluoromethyl)phenyl]-5-azaspiro[2.4]heptan-5-yl]propyl}sulfanyl)-4H-1,2,4-triazol-3-yl]-1,2-dihydropyridin-2-one hydrochloride (77a)

The compound was prepared following the general procedure, but using (1R,3S)-1-[4-(trifluoromethyl)phenyl]-5-azaspiro[2.4]heptane, *cis* enantiomer 1, and not the racemic mixture; the crude residue was purified by flash chromatography and then transformed into the hydrochloride to give **77a**. Yield 58%. ^{1}H NMR (*DMSO-d$_6$*) δ: 10.36 (s, 1H), 10.15 - 10.14 (m, 1H), 8.17 (br. s., 1H), 7.79 - 7.61 (m, 3H), 7.45 (d, J = 7.70 Hz, 2H), 6.55 (d, J = 9.40 Hz, 1H), 3.71 (br. s.,2H), 3.48-3.64 (m, 6H), 3.47 - 3.24 (m, 2H), 3.18 (d, J = 4.6 Hz, 4H), 2.99 (br. s., 1H), 2.26 (d, J = 5.00 Hz, 1H), 2.18 - 1.88 (m, 3H), 1.54 - 1.25 (m, 2H). MS *m/z*: 504.5 $[M+H]^+$.

1-methyl-4-[4-methyl-5-({3-[(1R,3S)-1-[4-(trifluoromethyl)phenyl]-5-azaspiro[2.4]heptan-5-yl]propyl}sulfanyl)-4H-1,2,4-triazol-3-yl]-1,2-dihydropyridin-2-one hydrochloride (78a)

The compound was prepared following the general procedure, but using (1R,3S)-1-[4-(trifluoromethyl)phenyl]-5-azaspiro[2.4]heptane, *cis* enantiomer 1, and not the racemic mixture; the crude residue was purified by flash chromatography and then transformed into the hydrochloride to give **78a**. Yield 82%. ^{1}H NMR (*Acetone-d$_6$*) δ: 7.77 - 7.72 (m, 1H), 7.65 - 7.59 (m, 2H), 7.43 - 7.36 (m, 2H), 6.73 - 6.68 (m, 1H), 6.63 - 6.56 (m, 1H), 3.76 (s, 3H), 3.58 - 3.51 (m, 3H), 3.35 - 3.15 (m, 2H), 2.58 (br. s., 4H), 2.29 - 2.23 (m, 1H), 2.17 (br. s., 1H), 2.02 - 1.81 (m, 5H), 1.35 - 1.29 (m, 1H), 1.26 - 1.20 (m, 1H). MS *m/z*: 504.3 $[M+H]^+$.

4-[4-methyl-5-({3-[(1R,3S)-1-[4-(trifluoromethyl)phenyl]-5-azaspiro[2.4]heptan-5-yl]propyl}sulfanyl)-4H-1,2,4-triazol-3-yl]piperidin-2-one hydrochloride (diastereomeric mixture) (79a)

The compound was prepared following the general procedure, but using (1R,3S)-1-[4-(trifluoromethyl)phenyl]-5-azaspiro[2.4]heptane, *cis* enantiomer 1, and not the racemic mixture; the crude residue was purified by flash chromatography and then transformed into the hydrochloride to give **79a**. Yield 36%. ^{1}H NMR (*DMSO-d$_6$*) δ: 10.25 - 9.96 (m, 1H), 7.68 (d, J = 8.03 Hz, 2H), 7.60 (br. s., 1H), 7.44 (br. s., 2H), 3.76 - 3.59 (m, 2H), 3.50 (s, 3H), 3.40 (br. s., 2H), 3.11 (br. s., 5H), 2.48 - 2.40 (m, 3H), 2.31 - 2.19 (m, 2H), 2.16 - 1.87 (m, 4H), 1.85 - 1.71 (m, 2H), 1.55 - 1.26 (m, 3H). MS *m/z*: 494.5 $[M+H]^+$.

1-methyl-4-[4-methyl-5-({3-[(1R,3S)-1-[4-(trifluoromethyl)phenyl]-5-azaspiro[2.4]heptan-5-yl]propyl}sulfanyl)-4H-1,2,4-triazol-3-yl]piperidin-2-one (diastereomeric mixture) (80a)

The compound was prepared following the general procedure, but using (1R,3S)-1-[4-(trifluoromethyl)phenyl]-5-azaspiro[2.4]heptane, *cis* enantiomer 1, and not the racemic mixture; the crude residue was purified by flash chromatography and then transformed into the hydrochloride to give **80a**. Yield 55%. ^{1}H NMR (*Acetone-d$_6$*) δ: 7.63 (s, 2H), 7.46 - 7.33 (m, 2H), 3.62

(s, 3H), 3.52 - 3.35 (m, 3H), 3.25 - 3.04 (m, 2H), 2.91 (s, 3H), 2.74 - 2.33 (m, 7H), 2.31 - 2.19 (m, 2H), 2.06 - 1.69 (m, 6H), 1.36 - 1.20 (m, 2H). MS *m/z*: 508.4 $[M+H]^+$.

1-{4-[4-methyl-5-({3-[(1R,3S)-1-[4-(trifluoromethyl)phenyl]-5-azaspiro[2.4]heptan-5-yl]propyl}sulfanyl)-4H-1,2,4-triazol-3-yl]piperidin-1-yl}ethan-1-one (81a)

The compound was prepared following the general procedure, but using (1R,3S)-1-[4-(trifluoromethyl)phenyl]-5-azaspiro[2.4]heptane, *cis* enantiomer 1, and not the racemic mixture; the crude residue was purified by flash chromatography on NH cartridge (eluting from cyclohexane to EtOAc 100%, then to MeOH 100%) to give **81a** as a colorless oil. Yield 79%. ^{1}H NMR (*Acetone-d$_6$*) *δ*: 7.60 (d, *J* = 8.19 Hz, 2 H), 7.37 (d, *J* = 8.20 Hz, 2 H), 4.48 (d, *J* = 13.08 Hz, 1 H), 3.99 (d, *J* = 13.45 Hz, 1 H), 3.57 (s, 3 H), 3.32 - 3.21 (m, 1 H), 3.20 -3.01 (m, 3 H), 2.93 - 2.35 (m, 6 H), 2.22 (t, *J* = 7.15 Hz, 1 H), 2.14 - 1.59 (m, 12 H), 1.31 - 1.23 (m, 1 H), 1.23 - 1.16 (m, 1 H), ^{13}C NMR (101 MHz, DMSO) Shift 168.0, 158.0, 149.1, 145.2, 128.0, 126.0, 124.8, 124.5, 57.2, 54.0, 53.9, 45.3, 35.6, 31.6, 30.5, 30.0, 30.0, 29.7, 29.4, 28.8, 28.0, 21.2, 19.0. MS *m/z*: 522.4 $[M+H]^+$.

N-{4-[4-methyl-5-({3-[(1R,3S)-1-[4-(trifluoromethyl)phenyl]-5-azaspiro[2.4]heptan-5-yl]propyl}sulfanyl)-4H-1,2,4-triazol-3-yl]cyclohexyl}acetamide (82a)

The compound was prepared following the general procedure, and crude residue was purified by chiral HPLC to give **82a**. Column: Chiralcel OJ-H (25 x 2.0 cm), 5 μm; mobile phase: n-Hexane/(Ethanol/Methanol + 0.1 % isopropylamine) 85/15 % v/v; flow rate: 16 mL/min; DAD detection: 220 nm; loop: 350 μL **82a** (enantiomer 1), retention time= 8.7 min. Yield 55%. ^{1}H NMR (*Acetone-d$_6$*) *δ*: 7.61 (d, *J* = 8.31 Hz, 2 H), 7.36 (d, *J* = 7.83 Hz, 2 H), 7.13 (br. s., 1 H), 4.04 - 3.89 (m, 1 H), 3.53 (s, 3 H), 3.22 - 3.02 (m, 2 H), 2.99 - 2.90 (m, 1 H), 2.75 - 2.67 (m, 1 H), 2.59 (q, *J* = 7.34 Hz, 1 H), 2.52 - 2.38 (m, 3 H), 2.22 (dd, *J* = 8.31, 6.36 Hz, 1 H), 2.09 - 2.07 (m, 1 H), 2.03 -1.73 (m, 13 H), 1.71 - 1.62 (m, 2 H), 1.27 (t, *J* = 5.62 Hz, 1 H), 1.20 (dd, *J* = 8.56, 5.14 Hz, 1 H), MS *m/z*: 536.5 $[M+H]^+$.

(1R,3S)-5-{3-{[4-methyl-5-(oxan-4-yl)-4H-1,2,4-triazol-3-yl]¬sulfanyl}¬propyl)-1-[4-(trifluoromethyl)phenyl]-5-azaspiro[2.4]heptane (83a)

The compound was prepared following the general procedure, and crude residue was purified by chiral HPLC to give **83a**. Column: Chiralcel OJ-H (25 x 2.0 cm), 5 µm; mobile phase: n-Hexane/Ethanol 65/35 % v/v; flow rate: 14 mL/min; DAD detection: 220 nm; loop: 1000 µL **83a** (enantiomer 1), retention time = 8.4 min. Yield 55%. ^{1}H NMR (*Acetone-d$_6$*) δ: 7.63 (d, J = 8.03 Hz, 2H), 7.41 (s, 2H), 4.07 - 3.93 (m, 2H), 3.58 (s, 3H), 3.56 - 3.47 (m, 2H), 3.35 - 3.31 (m, 1H), 3.23 - 3.05 (m, 3H), 2.71 - 2.42 (m, 5H), 2.30 - 2.20 (m, 1H), 2.02 - 1.76 (m, 8H), 1.35 - 1.28 (m, 1H), 1.26 - 1.19 (m, 1H). MS *m/z*: 481.3 $[M+H]^+$.

(1R,3S)-5-{3-[(4-methyl-5-{8-oxabicyclo[3.2.1]octan-3-yl}¬-4H-1,2,4-triazol-3-yl)sulfanyl]propyl}-1-[4-(trifluoromethyl)phenyl]-5-azaspiro[2.4]heptane (84a)

The compound was prepared following the general procedure, and crude residue was purified by chiral HPLC to give **84a**. Column: Chiralcel OJ-H (25 x 2.0 cm), 5 µm; mobile phase: n-Hexane / (Ethanol + 0.1% isopropylamine) 60/40 % v/v; flow rate: 14 mL/min; DAD detection: 220 nm; loop: 2000 µL **84a** (enantiomer 1), retention time = 6.5 min. Yield 52%. ^{1}H NMR (*Acetone-d$_6$*) δ: 7.62 (d, J = 8.28 Hz, 2H), 7.39 ((d, J = 8.03 Hz, 2H), 4.48 - 4.33 (m, 2H), 3.57 (s, 3H), 3.46 - 3.28 (m, 2H), 3.22 - 3.03 (m, 2H), 2.72 - 2.38 (m, 5H), 2.29 - 2.20 (m, 1H), 1.99-1.93 (m, 7H), 1.86 - 1.69 (m, 5H), 1.35 - 1.27 (m, 1H), 1.25 - 1.17 (m, 1H). MS *m/z*: 507.1 $[M+H]^+$.

(1R,3S)-5-{3-[(5-cyclohexyl-4-methyl-4H-1,2,4-triazol-3-yl)¬sulfanyl]propyl}-1-[4-(trifluoromethyl)phenyl]-5-azaspiro[2.4]heptane hydrochloride (85a)

The compound was prepared following the general procedure, and crude residue was purified by chiral HPLC to give **85a**. Column: Chiralcel OJ-H (25 x 2.0 cm), 5 µm; mobile phase: n-

Hexane/(Ethanol/Methanol 1/1 + 0.1% isopropylamine) 85/15 % v/v; flow rate: 18 mL/min; DAD detection: 220 nm; loop: 1000 µL **85a** (enantiomer 1), retention time= 6.6 min. Yield 32%. ^{1}H NMR (*Acetone-d$_6$*) *δ*: 7.63 (d, *J* = 8.03 Hz, 2H), 7.39 (d, *J* = 7.28 Hz, 2H), 3.54 (s, 3H), 3.42 (m, 1H), 3.23 - 3.02 (m, 2H), 2.66 - 2.37 (m, 4H), 2.67 - 2.35 (m, 1H), 2.31 - 2.18 (m, 2H), 1.96 (br. s., 4H), 1.83 (br. s., 5H), 1.67 - 1.54 (m, 2H), 1.51 - 1.27 (m, 4H), 1.25 - 1.17 (m, 1H). MS *m/z*: 479.5 $[M+H]^+$.

(1R,3S)-1-[4-(trifluoromethyl)phenyl]-5-azaspiro[2.4]heptane (86) and (1S,3R)-1-[4-(trifluoromethyl)phenyl]-5-azaspiro[2.4]heptane (88)

(1S,3R/1R,3S)-5-benzyl-1-[4-(trifluoromethyl)phenyl]-5-azaspiro[2.4]heptane-4,6-dione (Diastereoisomer *CIS*) was dissolved in THF and $LiAlH_4$ 1M in THF was added dropwise at 0 ^{0}C . The resulting orange solution was heated at reflux for 1 h. Then it was cooled with an ice bath and quenched with Na_2SO_4 * 10 H_2O until gas evolution ceased. The mixture was filtered over a pad of Celite® washing with EtOAc, and the solution was concentrated to afford (1R,3S/1S,3R)-5-benzyl-1-[4-(trifluoromethyl)phenyl]-5-azaspiro[2.4]heptane (*CIS*) as oil that submitted to chiral prep HPLC (SFC) to separate the enantiomers. Column: Chiralpak AD-H (25 x 2.1 cm), 5 µm; mobile phase: (Ethanol+0.1 % isopropylamine) 7 %; flow rate: 45 mL/min; DAD detection: 220 nm; loop: 900 µL **86** (enantiomer 1), retention time= 7.9 min, 100% *ee*; **88** (enantiomer 2) retention time 10.2 min, 100% *ee*. Yield 52%. ^{1}H NMR (*$CDCl_3$*) *δ*: 7.54 (d, *J* = 8.03 Hz, 2H), 7.19 (d, *J* = 8.28 Hz, 2H), 3.08 (dt, *J* = 4.39, 6.84 Hz, 2H), 2.70 (d, *J* = 11.04 Hz, 1H), 2.52 (d, *J* = 11.29 Hz, 1H), 2.21 (dd, *J* = 6.15, 8.41 Hz, 1H), 1.93 (dt, *J* = 2.76, 6.78 Hz, 2H), 1.29 (dd, *J* = 5.27, 8.53 Hz, 1H), 1.17 (t, *J*=5.77 Hz, 1H). MS *m/z*: 242.0 $[M+H]^+$.

(1R,3S)-5-(4-methylbenzenesulfonyl)-1-[4-(trifluoromethyl)phenyl]-5-azaspiro[2.4]heptane (87)

86 in dichloromethane (3 mL) was stirred at 0 °C; triethylamine (0.022 mL, 0.15 mmol) was added, followed by 4-methylbenzenesulfonyl chloride (21 mg, 0.11 mmol) and then the mixture was slowly warmed to room temperature and stirred at the same temperature for 1 h. CH_2Cl_2 was added, washed with water and brine, then dried with Na_2SO_4, filtered and concentrated. The residue was

chromatographed by flash chromatography on silica gel (eluent from cyclohexane to 40% Ethyl acetate) affording **87** (33 mg, y= 83%) as white solid.

The latter was suspended in 0.3 mL of EtOH and then heated until dissolution. After slow cooling to RT, crystallization was observed. Crystals were filtered and used for the molecular and crystal structure determination by single crystal high-resolution X-ray diffraction to determine the absolute stereochemistry.

X-ray crystallography

The X-ray data collection was performed on a plate-like crystal of approximate dimensions 0.26x0.22x0.02 mm mounted on a glass capillary. The X-ray intensities were measures on a Bruker Smart system equipped with an APEXII CCD area detector, using the Mo Kα radiation (λ = 0.71073 Å) at T = 293 K. The collected intensities were corrected for Lorentz and polarization factors and empirically for absorption by using the SADABS program[27]. Crystals diffracted weakly and the final collection did not reach high theta values, nevertheless it was possible to determine unambiguously the molecular structure of the compound.

The structure was solved by direct methods using the program Sir2011[28], and was refined with the program SHELXL-2014[29]. Anisotropic thermal displacement parameters were refined for all the non-H atoms, apart from the terminal –Ph-CH_3 and –Ph-CF_3 groups. The trifluoromethyl groups were disordered over two positions. Hydrogen atoms were introduced in calculated positions. Crystal data are reported below:

Empirical formula	$C_{80}H_{80}F_{12}N_4O_8S_4$
Formula weight	1581.72
Temperature/K	293
Crystal system	Orthorhombic
Space group	$P2_12_12_1$
a/Å	11.75(5)
b/Å	17.30(7)
c/Å	41.04(9)

α/°	90
β/°	90
γ/°	90
Volume/Å^3	8342(52)
Z, Z'	16, 4
ρ_{calc}g/cm^3	1.259
μ/mm^{-1}	0.194
F(000)	3296
Crystal size/mm^3	0.26 × 0.22 × 0.02
Radiation/Å	MoKα (λ = 0.71073)
2Θ range for data collection/°	2.540 to 34.540
Index ranges	-9 ≤ h ≤ 9, -14 ≤ k ≤ 12, -33 ≤ l ≤ 28
Reflections collected	17849
Independent reflections	4938 [R_{int} = 0.1815, R_{sigma} = 0.1678]
Data/restraints/parameters	4938/74/686
Goodness-of-fit on F^2	1.003
Final R indexes [I>=2σ (I)]	R_1 = 0.0786, wR_2 = 0.1598
Final R indexes [all data]	R_1 = 0.1766, wR_2 = 0.2100
Largest ΔF max/min / e Å^{-3}	0.20/-0.20
Flack parameter	0.1(2)

The compound crystallizes in the chiral orthorhombic space group $P2_12_12_1$. The asymmetric unit comprises four molecules. The Flack parameter for the present structure is 0.094(322) by classical fit to all intensities and 0.064(210) from 639 selected quotients (Parson's method) strongly supporting the present absolute structure determination.

According to the absolute structure determination, the configuration is **1*R*, 3*S***.

^{1}H NMR (*$CDCl_3$*) *δ*: 7.50-7.64 (m, 2H), 7.46 (d, *J* = 8.03 Hz, 2H), 7.22 (d, *J* = 7.78 Hz, 2H), 6.99 (d, *J* = 8.53 Hz, 2H), 3.55 (ddd, *J* = 4.52, 7.47, 9.35 Hz, 1H), 3.39-3.25 (m, 1H), 3.14 (d, *J* = 10.04 Hz, 1H), 2.74 (d, *J* = 10.04 Hz, 1H), 2.45 (s, 3H), 2.06 (dd, *J* = 5.14, 7.65 Hz, 2H), 1.82 (ddd, *J* = 4.64, 7.09, 12.11 Hz, 1H), 1.19 (dd, *J* = 5.90, 8.91 Hz, 1H), 1.14-1.00 (m, 1H)MS *m/z*: 396.4 $[M+H]^+$.

(1S,3R)-5-(4-methylbenzenesulfonyl)-1-[4-(trifluoromethyl)phenyl]-5-azaspiro[2.4]heptane (89)

88 (3.48 mmol) in dichloromethane (15 mL) was stirred at 0 °C; triethylamine (0.73 mL, 5.22 mmol) was added, followed by 4-methylbenzenesulfonyl chloride (730 mg, 3.83 mmol) and then the reaction mixture was slowly warmed to room temperature and stirred at that temperature for 2 hrs. CH_2Cl_2 was

added, washed with water and brine, then dried with Na_2SO_4, filtered and concentrated. The residue was chromatographed by flash chromatography on silica gel (eluent from cyclohexane to 40% Ethyl acetate) affording **89** as white solid. 100 mg of **89** were suspended in 1 mL of EtOH and then heated until dissolution. After slow cooling to RT, the solution was left standing at RT for 3 days after which time crystallization was observed. Crystals were filtered and used for the molecular and crystal structure determination by single crystal high-resolution X-ray diffraction to determine the absolute stereochemistry.

X-ray crystallography

The X-ray data collection was performed on a plate-like crystal of approximate dimensions 0.31x0.24x0.07 mm mounted on a glass capillary. The X-ray intensities were measures on a Bruker Smart system equipped with an APEXII CCD area detector, using the Mo Kα radiation (λ = 0.71073 Å) at T = 293 K. The collected intensities were corrected for Lorentz and polarization factors and empirically for absorption by using the SADABS program[27]. Crystals diffracted weakly and the final collection did not reach high theta values, nevertheless it was possible to determine unambiguously the molecular structure of the compound.

The structure was solved by direct methods using the program Sir2011[28], and was refined with the program SHELXL-2014[29]. Anisotropic thermal displacement parameters were refined for all the non-H atoms, apart from mthe terminal $–CH_3$ and $-CF_3$ groups. The latter ones were disordered over two positions. Hydrogen atoms were introduced in calculated positions. Crystal data are reported below.

Empirical formula	$C_{80}H_{80}F_{12}N_4O_8S_4$
Formula weight	1581.72
Temperature/K	293
Crystal system	Orthorhombic
Space group	$P2_12_12_1$
a/Å	11.567(7)
b/Å	17.155(9)

c/Å	40.16(2)
α/°	90
β/°	90
γ/°	90
Volume/Å^3	7970(8)
Z, Z'	16, 4
ρ_{calc}g/cm^3	1.318
μ/mm^{-1}	0.203
F(000)	760.0
Crystal size/mm^3	0.31 × 0.24 × 0.07
Radiation/Å	MoKα (λ = 0.71073)
2Θ range for data collection/°	1.291 to 38.640
Index ranges	-10 ≤ h ≤ 10, -15 ≤ k ≤ 15, -37 ≤ l ≤ 37
Reflections collected	47185
Independent reflections	6706 [R_{int} = 0.0941, R_{sigma} = 0.0494]
Data/restraints/parameters	6706/56/926
Goodness-of-fit on F^2	1.013
Final R indexes [I>=2σ (I)]	R_1 = 0.0623, wR_2 = 0.1419
Final R indexes [all data]	R_1 = 0.0993, wR_2 = 0.1665
Largest ΔF max/min / e Å^{-3}	0.26/-0.24
Flack parameter	-0.01(6)

The compound crystallizes in the chiral orthorhombic space group $P2_12_12_1$. The asymmetric unit comprises four molecules. The Flack parameter for the present structure is 0.000(199) by classical fit to all intensities and -0.005(57) from 1566 selected quotients (Parson's method) strongly supporting the present absolute structure determination. According to the absolute structure determination, the configuration is **1*S*, 3*R***.

^{1}H NMR ($CDCl_3$) δ: 7.50-7.64 (m, 2H), 7.46 (d, J = 8.03 Hz, 2H), 7.22 (d, J = 7.78 Hz, 2H), 6.99 (d, J = 8.53 Hz, 2H), 3.55 (ddd, J = 4.52, 7.47, 9.35 Hz, 1H), 3.39-3.25 (m, 1H), 3.14 (d, J = 10.04 Hz, 1H), 2.74 (d, J = 10.04 Hz, 1H), 2.45 (s, 3H), 2.06 (dd, J = 5.14, 7.65 Hz, 2H), 1.82 (ddd, J = 4.64, 7.09, 12.11 Hz, 1H), 1.19 (dd, J = 5.90, 8.91 Hz, 1H), 1.14-1.00 (m, 1H)MS *m/z*: 396.4 $[M+H]^+$.

Crystallographic data (excluding structure factors) for **8**~~9~~7 and ~~89~~ 87 have been deposited with the Cambridge Crystallographic Data Centre as supplementary publications nos CCDC 1489497-1489498. ~~CCDC XXX~~. Copies of the data can be obtained free of charge on application to CCDC, 12 Union Road, Cambridge CB2 1EZ, UK (fax: (+44) 1223-336-033; e-mail: deposit@ccdc.cam.ac.uk).

Formattato: Tipo di carattere: (Predefinito) Times New Roman, 12 pt

Computational Modelling

A model of the DA D3 receptor (D3R) x-ray crystal structure (PDB ID 3PBL), pre-treated using "Structure Preparation application" within MOE[21] was built as described in reference 13. Compounds here described were docked in the minimized model, by a pharmacophore guided induced fit docking protocol, consisting in an H bond donor (to Asp110) and an aromatic center (located into the Ptm23 pocket) features as placement constraints. Ambe12: EHT and "Reaction field" were used as force field and implicit solvent model, respectively. Best poses were further submitted to conformational search using LowModeMD simulation. This docking model and protocol previously described[9] provided good predictive validity in discriminating potent (pKi > 7.5) from relatively weaker (pKi < 7.0) DA D3 receptor antagonists, the latter showing no meaningful poses to the D3R model.

As far as **40a-42a** were concerned, the three molecules were docked into the DA D3 receptor model in agreement with the previously reported protocol[9] using the GBVI/WSA dG scoring function as implemented in MOE[21, 30, 31]. The lowest score poses were submitted to conformational search using LowModeMD (MOE). The lowest energy conformations were further minimized and ligand-protein affinity was re-calculated. Results are reported below in Table 12.

Table 12. GBVI/WSA: free energy of binding of the ligand which uses GB/VI solvation model

		Affinity: GBVI/WSA dg (kcal/mol)	
Entry	**R**	**Docking (lowest pose)**	**LowModeMD (lowes energy complex)**
40a	4-benzamide (Cis, s.e.1)	-10.5	-12.3
41a	3- benzamide (Cis, s.e.1)	-10.5	-11.5
42a	2- benzamide (Cis, s.e.1)	-9.7	-10.8

Acknowledgement

We would like to acknowledge Indivior, Inc. for supporting this project as well as all the colleagues of the Aptuit departments who helped in generating the data reported in this manuscript and for the fruitful discussion during the preparation of this manuscript.

References

(1) Heidbreder, C. A.; Gardner, E. L.; Xi, Z-X.; Thanos, P. K.; Mugnaini, M.; Hagan, J. J.; Ashby, C. R. Jr. The role of central DA D_3 receptors in drug addiction: a review of pharmacological evidence. *Brain Res. Rev.* **2005**, *49*, 77-105

(2) Heidbreder, C. A.; Newman, A. H. Current perspectives on selective dopamine D3 receptor antagonists as pharmacotherapeutics for addictions and related disorders. Ann. N.Y. Acad. Sci. **2010**, 1187:4-34.

(3) Heidbreder, C. Rationale in support of the use of selective dopamine D3 receptor antagonists for the pharmacotherapeutic management of drug addiction. Naunyn-Schmiedeberg's Archives of Pharmacology **201**3, 386: 167-176.

(4) a) Keck,T. M.; John, W. S.; Czoty, P. W.; Nader, M. A. and Newman, A. H. Identifying Medication Targets for Psychostimulant Addiction: Unraveling the Dopamine D3 Receptor Hypothesis *J. Med. Chem.* **2015**, 58, 5361-5380. b) Micheli, F.; Heidbreder, C. Dopamine D3 receptor antagonists: a patent review (2007-2012). *Expert Opin. Ther. Pat.* **2013**, 23, 363-381.

(5) Micheli, F.; Arista, L.; Bonanomi, G.; Blaney, F. E.; Braggio, S.; Capelli, A. M.; Checchia, A.; Damiani, F.; Di-Fabio, R.; Fontana, S.;Gentile, G.; Griffante, C.; Hamprecht, D.; Marchioro, C.; Mugnaini, M.; Piner, J.; Ratti, E.; Tedesco, G.; Tarsi, L.; Terreni, S.; Worby, A.;Ashby, C. R., Jr.; Heidbreder, C. 1,2,4-Triazolyl azabicyclo[3.1.0]-hexanes: a new series of potent and selective dopamine D(3) receptor antagonists. *J. Med. Chem.* **2010**, *53*, 374−391.

(6) Micheli, F.; Bonanomi, G.; Blaney, F. E.; Braggio, S.; Capelli, A. M.; Checchia, A.; Curcuruto, O.; Damiani, F.; Di-Fabio, R.; Donati, D.; Gentile, G.; Gribble, A.; Hamprecht, D.; Tedesco, G.; Terreni, S.; Tarsi, L.; Lightfoot, A.; Pecoraro, M.; Petrone, M.; Perini, O.; Piner, J.; Rossi, T.;

Worby, A.; Pilla, M.; Valerio, E.; Griffante, C.; Mugnaini, M.; Wood, M.; Scott, C.; Andreoli, M.; Lacroix, L.; Schwarz, A.; Gozzi, A.; Bifone, A.; Ashby, C. R. Jr.; Hagan, J. J.; Heidbreder, C. 1,2,4-triazol-3-yl-thiopropyl-tetrahydrobenzazepines: A series of potent and selective dopamine D3 receptor antagonists *J. Med. Chem* **2007**, *50*, 5076-5089.

(7) Micheli, F. Recent advances in the development of dopamine D3 receptor antagonists: a medicinal chemistry perspective. *Chem-MedChem* **2011**, *6*, 1152−1162.

(8) Micheli, F.; Cremonesi, S.; Semeraro, T.; Tarsi, L.; Tomelleri, S.; Cavanni, P.; Oliosi, B.; Perdona', E.; Sava, A.; Zonzini, L.; Feriani, A.; Braggio, S.; Heidbreder, C. Novel morpholine scaffolds as selective dopamine (DA) D3 receptor antagonists. *Bioorg. Med.Chem. Lett.* **2016**, *24* 1329-1332.

(9) Micheli, F.; Bernardelli, A.; Bianchi, F.; Braggio, S.; Castelletti, L.; Cavallini, P.; Cavanni, P.; Cremonesi, S.; Dal Cin, M.; Feriani, A.; Oliosi, B.; Semeraro, T.; Tarsi, L.; Tomelleri, S.; Wong, A.; Visentini, F.; Zonzini, L.; Heidbreder, C. 1,2,4-triazolyl octahydropyrrolo[2,3-b]pyrroles: A new series of potent and selective dopamine D3 receptor antagonists *Bioorg. Med.Chem.* **2016**, *24*, 1619-1636.

(10) Stemp, G.; Ashmeade, T.; Branch, C. L.; Hadley, M. S.; Hunter, A. J.; Johnson, C. N.; Nash, D. J.; Thewlis, K. M.; Vong, A. K.; Austin, N. E.; Jeffrey, P.; Avenell, K. Y.; Boyfield, I.; Hagan, J. J.; Middlemiss, D. N.; Reavill, C.; Riley, G. J.; Routledge, C.; Wood, M. Design and synthesis of trans-N-[4-[2-(6-cyano-1,2,3, 4-tetrahydroisoquinolin-2- yl)ethyl]cyclohexyl]-4-quinolinecarboxamide (SB-277011): a potent and selective dopamine D(3) receptor antagonist with high oral bioavailability and CNS penetration in the rat. *J. Med. Chem*. **2000**, *43*, 1878−1885.

(11) Mugnaini, M.; Iavarone, L.; Cavallini, P.; Griffante, C.; Oliosi, B.; Savoia, C.; Beaver, J.; Rabiner, E. A.; Micheli, F.; Heidbreder, C.; Andorn, A.; Merlo Pich, E.; Bani, M. Occupancy of brain

dopamine D3 receptors and drug craving: a translational approach. *Neuropsychopharmacology* **2013**, *38*, 302-12.

(12) Grundt, P.; Carlson, E. E.; Cao, J.; Bennett, C. J.; McElveen, E.; Taylor, M.; Luedtke, R. R.; Newman, A. H. Novel heterocyclic trans olefin analogues of N-{4-[4-(2,3-dichlorophenyl)piperazin-1-yl]butyl}- arylcarboxamides as selective probes with high affinity for the dopamine D3 receptor. *J. Med. Chem.* **2005**, *48*, 839−848.

(13) Chen, J.; Levant, B.; Jiang, C.; Keck, T. M.; Newman, A. H.; Wang, S. Tranylcypromine Substituted cis-Hydroxycyclobutylnaphthamides as Potent and Selective Dopamine D3 Receptor Antagonists. *J. Med. Chem.* **2014**, *57*, 4962-4968.

(14) Hua, R.; Song, R.; Yang, R.; Su, R.; Li, J. The dopamineD3 receptor antagonist YQA14 that inhibits the expression and drug-primed reactivation of morphine-induced conditioned place preference in rats. *Eur. J. Pharm.* **2013***, 720,* 212-217.

(15) Hackling, A. E.; Stark, H. Dopamine D3 Receptor Ligands with Antagonist Properties *Chembiochem* **2002**, *3*, 946-961.

(16) Newman, A. H.; Beuming, T.; Banala, A. K.; Donthamsetti, P.; Pongetti, K.; LaBounty, A.; Levy, B.; Cao, J.; Michino, M.; Luedtke, R. R.; Javitch,. A.; Shi, L. Molecular Determinants of Selectivity and Efficacy at the Dopamine D3 Receptor *J. Med. Chem.* **2012**, *55*, 6689−6699.

(17) a) Hughes, J. P.; Rees, S.; Kalindjian, S. B.; Philpott, K. L. Principles of early drug discovery *Br. J. Pharmacol*. **2011**, *162,* 1239–1249. b) Saxena, V.; Panicucci, R.; Joshi, Y.; Garad, S. Developability assessment in pharmaceutical industry: An integrated group approach for selecting developable candidates. *J. Pharm. Sci.* **2009**, *98*, 1962-79. c) Han, C.; Wang, B. Factors that impact the developability of drug candidates: an overview Chapter 1 in Drug Delivery: Principles and Applications Edited by Wang, B.; Siahaan, T.; Soltero, R. ISBN 0-471-47489-4 # 2005 John Wiley

& Sons, Inc. d) Keck, T. M.; John, W. S.; Czoty, P. W.; Nader, M. A.; Newman, A. H. Identifying Medication Targets for Psychostimulant Addiction: Unraveling the Dopamine D3 Receptor Hypothesis*, J. Med. Chem.* **2015**, *58*, 5361−5380. e) Watson, J.; Wright, S.; Lucas, A.; Clarke, K. L.; Viggers, J.; Cheetham, S.; Jeffrey, P.; Porter, R.; Read, K. D. Receptor occupancy and brain free fraction. *Drug Metab. Dispos*. **2009**, *37*, 753−760.

(18) a) Keck, T. M.; Burzynski, C.; Shi, L.; Newman, A. H. Beyond small-molecule SAR: using the dopamine D3 receptor crystal structure to guide drug design from Advances in Pharmacology (San Diego, CA, United States) (2014), 69 (Emerging Targets & Therapeutics in the Treatment of Psychostimulant Abuse), 267-300. b) Carlsson, J.; Coleman, R. G.; Setola, V.; Irwin, J. J.; Fan, H.; Schlessinger, A.; Sali, A.; Roth, B. L.; Shoichet, B. K. Ligand discovery from a dopamine D3 receptor homology model and crystal structure *Nature Chemical Biology*, **2011**, *7*, 769-778. c) Vass, M.; Agai-Csongor, E.; Horti, F.; Keseru, G. M. Multiple Fragment Docking and Linking in Primary and Secondary Pockets of Dopamine Receptors *ACS Medicinal Chemistry Letters* **2014**, *5*, 1010-1014.

(19) Böhm, H-J.; Flohr, A.; Stahl, M. Scaffold hopping *Drug Discovery Today: Technologies* **2004**, *1*, 217-224.

(20) MarvinSketch 6.1.6, (build id: 6.1.6_b695) by Chemaxon (www.chemaxon.com).

(21) Molecular Operating Environment (MOE), 2013.08; Chemical Computing Group Inc., 1010 Sherbooke St. West, Suite #910, Montreal, QC, Canada, H3A 2R7, 2015.

(22) The research complied with national legislation and with company policy on the Care and Use of Animals and with related codes of practice.

(23) Matsuda, Y.; Konno, Y.; Satsukawa, M.; Kobayashi, T.; Takimoto, Y.; Morisaki, K.; Yamashita, S. Assessment of intestinal availability of various drugs in the oral absorption process using portal vein-cannulated rats. *Drug Metab Dispos.* **2012**, *40*, 2231-8.

(24) van Breemen, R., B.; Li, Y. Caco-2 cell permeability assays to measure drug absorption. *Expert Opin Drug Metab Toxicol.* **2005**, *1*, 175-85.

(25) a) Hay, T.; Jones, R.; Beaumont, K.; Kemp, M. Modulation of the Partition Coefficient between Octanol and Buffer at pH 7.4 and pKa to Achieve the Optimum Balance of Blood Clearance and Volume of Distribution for a Series of Tetrahydropyran Histamine Type 3 Receptor Antagonists *Drug Metab Dispos.* **2009**, *37*, 1864–1870. b) *Lead Generation: Methods and Strategies, Volume 67*; Holenz, J.; Mannhold, R., Kubinyi, H., Folkers, G. Eds.; Wiley, 2016; c) *Pharmacokinetics and Metabolism in Drug Design, Volume 51, 3rd Ed.;* D. A., Allerton, C., Kalgutkar, A. S. , van de Waterbeemd, H., Walker, D. K. Eds: Wiley, 2012

(26) www.cerep.fr

(27) SAINT: SAX, Area Detector Integration, Siemens Analytical instruments INC., Madison, Wisconsin, USA; SADABS: Siemens Area Detector Absorption Correction Software, G. Sheldrick, 1996, University of Goettingen, Germany.

(28) Burla, M. C.; Caliandro, R.; Camalli, M.; Carrozzini, B.; Cascarano, G. L.; Giacovazzo, C.; Mallamo, M.; Mazzone, A.; Polidori, G.; Spagna, R. SIR2011: A new package for crystal structure determination and refinement *Journal of Applied Crystallography* **2012**, *45*, 357-361.

(29) Sheldrick, G. M. Crystal structure refinement with SHELXL. *Acta Cryst.* **2008**, A64, 112-122.

(30) Naïm, M.; Bhat, S.; Rankin, K. N.; Dennis, S.; Chowdhury, S. F.; Siddiqi, I.; Drabik, P.; Sulea, T.; Bayly, C. I.; Jakalian, A.; Purisima, E. O. Solvated interaction energy (SIE) for scoring protein-ligand binding affinities. 1. Exploring the parameter space. J. Chem. Inf. Model. **2007**, *47*, 122–133.

(31) Labute, P. The Generalized Born / Volume Integral (GB/VI) Implicit Solvent Model: Estimation of the Free Energy of Hydration Using London Dispersion Instead of Atomic Surface Area. *J. Comp. Chem.* **2008**, *19*, 1693–1698.

Table 1. Affinity data at the D3D and D2R and potency data at the hERG ion channel for derivatives **1, 2** and **7-26**.

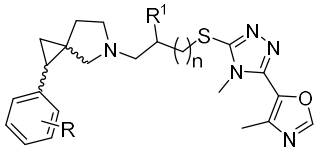

Entry	R	hD3 pKi	hD2 pKi	hERG pIC$_{50}$	n, R1	cLogP	PSA
1	NA	8.19 ± 0.02	6.31 ± 0.01	6.17 ± 0.03	NA	4.6	69.0
2	NA	8.9*	6.2*	6.1*	NA	3.2	85.3
7	H (Trans, rac.)	7.60 ± 0.21	6.00 ± 0.17	NT	1, H	2.5	85.3
7a	H (Trans, s.e. 1)	7.55 ± 0.31	6.29 ± 0.11	5.40 ± 0.13	1, H	2.5	85.3
7b	H (Trans, s.e. 2)	7.38 ± 0.20	6.15 ± 0.18	5.44 ± 0.06	1, H	2.5	85.3
8	H (Cis, rac.)	7.75 ± 0.08	6.03 ± 0.07	NT	1, H	2.5	85.3
8a	H (Cis, s.e. 1)	6.10 ± 0.28	4.77 ± 0.18	5.33 ± 0.20	1, H	2.5	85.3
8b	H (Cis, s.e. 2)	8.26 ± 0.20	6.10 ± 0.11	5.54 ± 0.02	1, H	2.5	85.3
9	4-CF_3 (Trans, rac.)	8.04 ± 0.10	6.18 ± 0.01	NT	1, H	3.4	85.3
9a	4-CF_3 (Trans, s.e. 1)	8.40 ± 0.03	6.05 ± 0.08	6.72 ± 0.13	1, H	3.4	85.3
9b	4-CF_3 (Trans, s.e. 2)	7.91 ± 0.15	6.20 ± 0.11	6.43 ± 0.04	1, H	3.4	85.3
10	4-CF_3 (Cis, rac.)	8.78 ± 0.18	6.53 ± 0.05	NT	1, H	3.4	85.3
10a	4-CF_3 (Cis, s.e. 1)	9.20 ± 0.12	6.67 ± 0.04	6.39 ± 0.09	1, H	3.4	85.3
10b	4-CF_3 (Cis, s.e. 2)	6.89 ± 0.20	NT	NT	1, H	3.4	85.3
11	4-CF_3 (Trans, rac.)	7.56 ± 0.11	6.29 ± 0.09	NT	0	3.2	85.3
11a	4-CF_3 (Trans, s.e. 1)	7.11 ± 0.13	6.01 ± 0.10	6.50 ± 0.18	0	3.2	85.3
11b	4-CF_3 (Trans, s.e. 2)	7.65 ± 0.05	6.10 ± 0.07	6.87 ± 0.06	0	3.2	85.3
12	4-CF_3 (Cis, rac.)	7.02 ± 0.20	6.28 ± 0.04	6.28 ± 0.08	0	3.2	85.3
13	4-CF_3 (Cis, rac.)	7.34 ± 0.04	6.01 ± 0.05	6.25 ± 0.06	2	3.9	85.3
14	2-CF_3 (Trans, rac.)	8.82 ± 0.16	6.91 ± 0.14	5.71 ± 0.02	1, H	3.4	85.3
14a	2-CF_3 (Trans, s.e. 1)	7.05 ± 0.15	6.14 ± 0.10	NT	1, H	3.4	85.3
14b	2-CF_3 (Trans, s.e. 2)	9.26 ± 0.05	7.20 ± 0.18	6.05 ± 0.01	1, H	3.4	85.3

15	2-CF_3 (Cis, rac.)	7.58 ± 0.20	5.80 ± 0.07	NT	1, H	3.4	85.3
16	4-F (Trans, rac.)	7.60 ± 0.03	6.01 ± 0.04	NT	1, H	2.7	60.0
16a	4-F (Trans, s.e. 1)	7.38 ± 0.07	5.96 ± 0.01	NT	1, H	2.7	60.0
16b	4-F (Trans, s.e. 2)	7.54 ± 0.05	6.10 ± 0.02	NT	1, H	2.7	60.0
17	4-F (Cis, rac.)	8.49 ± 0.03	6.37 ± 0.08	NT	1, H	2.7	60.0
17a	4-F (Cis, s.e. 1)	6.54 ± 0.09	5.09 ± 0.18	NT	1, H	2.7	60.0
17b	4-F (Cis, s.e. 2)	9.04 ± 0.12	6.62 ± 0.01	6.22 ± 0.06	1, H	2.7	60.0
18	2,4-F (Trans, rac.)	7.60 ± 0.12	6.27 ± 0.06	NT	1, H	2.8	60.0
18a	2,4-F (Trans, s.e. 1)	7.46 ± 0.08	6.17 ± 0.01	NT	1, H	2.8	60.0
18b	2,4-F (Trans, s.e. 2)	7.70 ± 0.12	6.02 ± 0.05	NT	1, H	2.8	60.0
19	2,4-F (Cis, rac.)	8.70 ± 0.01	6.53 ± 0.03	NT	1, H	2.8	60.0
19a	2,4-F (Cis, s.e. 1)	6.62 ± 0.01	NT	NT	1, H	2.8	60.0
19b	2,4-F (Cis, s.e. 2)	9.09 ± 0.01	6.59 ± 0.01	6.12 ± 0.10	1, H	2.8	60.0
20	2-F, 4-CF_3 (Trans, rac.)	8.03 ± 0.10	6.50 ± 0.07	NT	1, H	3.6	85.3
20a	2-F, 4-CF_3 (Trans, s.e. 1)	8.49 ± 0.15	6.51 ± 0.03	6.60 ± 0.18	1, H	3.6	85.3
20b	2-F, 4-CF_3 (Trans, s.e. 2)	8.21 ± 0.22	6.01 ± 0.04	6.35 ± 0.14	1, H	3.6	85.3
21	2-F, 4-CF_3 (Cis, rac.)	8.98 ± 0.22	6.48 ± 0.01	NT	1, H	3.6	85.3
21a	2-F, 4-CF_3 (Cis, s.e. 1)	7.14 ± 0.19	5.36 ± 0.02	6.16 ± 0.11	1, H	3.6	85.3
21b	2-F, 4-CF_3 (Cis, s.e. 2)	9.38 ± 0.09	6.65 ± 0.04	6.28 ± 0.02	1, H	3.6	85.3
22a	4-F, 2-CF_3 (Trans, s.e. 1)	8.98 ± 0.13	6.78 ± 0.02	5.92 ± 0.19	1, H	3.6	85.3
22b	4-F, 2-CF_3 (Trans, s.e. 2)	7.12 ± 0.01	5.66 ± 0.08	NT	1, H	3.6	85.3
23a	4-F, 2-CF_3 (Cis, s.e. 1)	7.05 ± 0.08	5.42 ± 0.01	NT	1, H	3.6	85.3
23b	4-F, 2-CF_3 (Cis, s.e. 2)	8.17 ± 0.05	5.89 ± 0.03	5.57 ± 0.24	1, H	3.6	85.3
24	4-CF_3 (Cis, rac.)	7.70 ± 0.12	5.76 ± 0.01	NT	1, OH	2.6	105.5
25	3,5-Cl (Trans, rac.)	9.38 ± 0.12	7.18 ± 0.08	> 7.0	1, H	3.7	85.3
26	3,5-Cl (Cis, rac.)	9.01 ± 0.02	7.21 ± 0.08	6.58 ± 0.11	1, H	3.7	85.3

* Literature data as reported in Ref. xx. DA D3 and DA D2 values are fpKis

rac.= racemate; s.e. 1= single enantiomer 1; s.e. 2= single enantiomer 2; NT= Not tested; NA= Not applicable; values shown are the average of three replicates and standard deviation.

Table 2. Affinity data at the D3R and D2R and potency data at the hERG ion channel for derivatives **27-39**

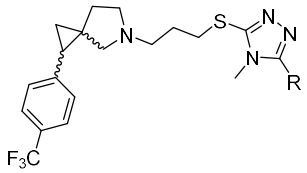

Entry	R	hD3 pKi	hD2 pKi	hERG pIC_{50}	cLogP	PSA
27	4-methyl-1,3-thiazol-5-yl (Trans, rac.)	7.82 ± 0.01	5.91 ± 0.08	NT	4.2	100.4
28	4-methyl-1,3-thiazol-5-yl (Cis, rac.)	8.44 ± 0.13	5.79 ± 0.01	6.10 ± 0.02	4.2	100.4
29	1,3-thiazol-2-yl (Trans, rac.)	8.00 ± 0.13	6.33 ± 0.06	NT	4.5	100.4
30	1,3-thiazol-2-yl (Cis, rac.)	8.86 ± 0.08	6.37 ± 0.01	6.35 ± 0.17	4.5	100.4
31	1,2,3-thiadiazol-4-yl (Trans, rac.)	8.56 ± 0.05	6.93 ± 0.09	6.95 ± 0.08	4.4	113.3
32	1,2,3-thiadiazol-4-yl (Cis, rac.)	8.50 ± 0.07	6.89 ± 0.14	< 5. 0	4.4	113.3
33	thiophen-2-yl (Cis, rac.)	9.22 ± 0.20	6.46 ± 0.11	> 7.0	5.2	72.4
34	thiophen-3-yl (Cis, rac.)	9.24 ± 0.17	6.48 ± 0.04	> 7.0	5.2	72.4
35	furan-2-yl (Cis, rac.)	8.86 ± 0.01	6.32 ± 0.08	NT	4.5	72.4
36	furan-3-yl (Cis, rac.)	8.78 ± 0.07	6.30 ± 0.11	6.82 ± 0.11	4.5	72.4
37	1-methyl-1H-pyrazol-4-yl (Cis, rac.)	8.62 ± 0.01	6.27 ± 0.01	6.33 ± 0.15	3.8	77.1
38	1-methyl-1H-pyrazol-5-yl (Cis, rac.)	8.76 ± 0.20	6.07 ± 0.05	6.21 ± 0.11	3.8	77.1
39	3-methyl-1,2-oxazol-5-yl (Cis, rac.)	8.57 ± 0.06	6.28 ± 0.05	6.69 ± 0.07	3.8	85.3

rac.= racemate; NT= Not tested; NA= Not applicable ; values shown are the average of three replicates and standard deviation.

Table 3. Affinity data at the D3R and D2R and potency data at the hERG ion channel for derivatives **40a**-**48a**

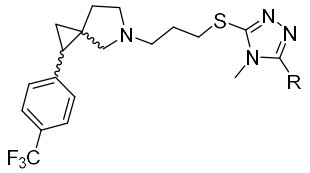

Entry	R	hD3 pKi	hD2 pKi	hERG pIC_{50}	cLogP	PSA
40a	4-benzamide (Cis, s.e.1)	9.80 ± 0.03	6.45 ± 0.01	6.09 ± 0.07	4.3	102.3
41a	3- benzamide (Cis, s.e.1)	9.33 ± 0.14	6.20 ± 0.01	5.55 ± 0.05	4.3	102.3
42a	2- benzamide (Cis, s.e.1)	7.82 ± 0.09	7.40 ± 0.01	NT	4.3	102.3
43a	4-phenyl-1-sulfonamide (Cis, s.e.1)	9.50 ± 0.01	6.66 ± 0.08	6.65 ± 0.10	4.0	127.8
44a	4-phenyl-ethan-1-one (Cis, s.e.1)	9.68 ± 0.01	6.35 ± 0.01	> 7.0	5.0	76.3
45a	4-benzonitrile (Cis, s.e.1)	9.58 ± 0.08	6.46 ± 0.03	> 7.0	5.3	83.0
46a	4-phenyl-1-acetamide (Cis, s.e.1)	9.07 ± 0.16	6.33 ± 0.08	5.12 ± 0.03	4.2	102.3
47a	4-(1,3-oxazol-2-yl)-phenyl (Cis, s.e.1)	10.17 ± 0.05	6.44 ± 0.01	6.82 ± 0.01	5.4	85.3
48a	3-(1,3-oxazol-2-yl)-phenyl (Cis, s.e.1)	9.74 ± 0.20	6.30 ± 0.07	6.92 ± 0.09	5.4	85.3

s.e. 1= single enantiomer 1; NT= Not tested; values shown are the average of three replicates and standard deviation.

Table 4. Affinity data at the D3R and D2R and potency data at the hERG ion channel for derivatives **49-62**

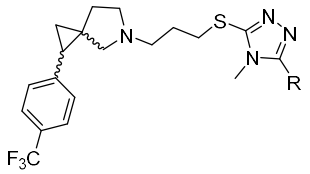

Entry	R	hD3 pKi	hD2 pKi	hERG pIC_{50}	cLogP	PSA
49	pyridin-4-yl (Trans, rac.)	8.10 ± 0.03	6.06 ± 0.07	6.65 ± 0.03	4.2	72.1
50	pyridin-4-yl (Cis, rac.)	8.96 ± 0.18	6.21 ± 0.01	6.53 ± 0.06	4.2	72.1
51	pyridin-3-yl (Trans, rac.)	7.70 ± 0.02	5.87 ± 0.04	NT	4.2	72.1
52	pyridin-3-yl (Cis, rac.)	8.74 ± 0.10	6.05 ± 0.02	5.91 ± 0.03	4.2	72.1
53	pyridin-2-yl (Trans, rac.)	8.11 ± 0.07	6.20 ± 0.06	NT	4.2	72.1
54	pyridin-2-yl (Cis, rac.)	9.10 ± 0.19	6.28 ± 0.02	6.68 ± 0.05	4.2	72.1
55	pyrazin-2-yl (Trans, rac.)	7.97 ± 0.01	5.84 ± 0.21	NT	3.4	85.0
56	pyrazin-2-yl (Cis, rac.)	8.90 ± 0.16	6.33 ± 0.07	6.59 ± 0.07	3.4	85.0
57	pyrimidin-4-yl (Trans, rac.)	8.29 ± 0.03	6.36 ± 0.12	NT	3.9	85.0
58	pyrimidin-4-yl (Cis, rac.)	8.99 ± 0.07	6.53 ± 0.02	6.84 ± 0.06	3.9	85.0
59	pyridazin-3-yl (Trans, rac.)	7.01 ± 0.02	5.75 ± 0.01	NT	3.6	85.0
60	pyridazin-3-yl (Cis, rac.)	7.78 ± 0.11	5.86 ± 0.01	NT	3.6	85.0
61	pyridazin-4-yl (Trans, rac.)	7.45 ± 0.14	5.59 ± 0.04	NT	3.2	85.0
62	pyridazin-4-yl (Cis, rac.)	8.40 ± 0.15	5.81 ± 0.01	5.60 ± 0.22	3.2	85.0

rac.= racemate; NT= Not tested; values shown are the average of three replicates and standard deviation.

Table 5. Affinity data at the D3R and D2R and potency data at the hERG ion channel for derivatives **63**-**66b**

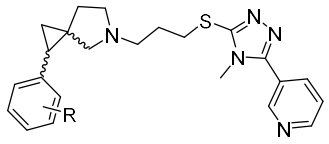

Entry	R	hD3 pKi	hD2 pKi	hERG pIC_{50}	cLogP	PSA
63	H (Cis, rac.)	7.53 ± 0.03	5.48 ± 0.04	NT	3.3	72.1
64b	2-F, 4-CF_3 (Cis, s.e.2)	8.93 ± 0.07	6.14 ± 0.01	6.03 ± 0.11	4.3	72.1
65b	2,4-F (Cis, s.e.2)	8.89 ± 0.08	6.28 ± 0.01	5.56 ± 0.17	3.6	72.1
66b	4-F (Cis, s.e.2)	8.70 ± 0.09	6.18 ± 0.01	5.68 ± 0.11	3.4	72.1

s.e. 2= single enantiomer 2; rac.= racemate; NT= Not tested; values shown are the average of three replicates and standard deviation.

Table 6. Affinity data at the D3R and D2R and potency data at the hERG ion channel for derivatives **67a-74a**

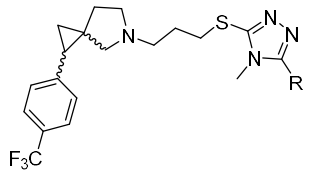

Entry	R	hD3 pKi	hD2 pKi	hERG pIC_{50}	cLogP	PSA
67a	2-methylpyridin-3-yl (Cis, s.e.1)	8.48 ± 0.13	5.83 ± 0.01	5.20 ± 0.05	4.3	72.1
68a	2-(trifluoromethyl)pyridin-3-yl (Cis, s.e.1)	8.15 ± 0.17	6.02 ± 0.03	5.88 ± 0.23	5.5	72.1
69a	2-methoxypyridin-3-yl (Cis, rac.)	8.59 ± 0.14	5.94 ± 0.05	6.22 ± 0.09	4.6	81.4
70a	2-cyano pyridin-5-yl (Cis, s.e.1)	8.84 ± 0.03	6.16 ± 0.01	> 7.0	4.4	95.9
71a	2-carboxamide pyridin-5-yl (Cis, s.e.1)	9.47 ± 0.18	6.26 ± 0.03	6.18 ± 0.13	3.4	115.2
72a	2,6-dimethylpyridin-3-yl (Cis, s.e.1)	8.48 ± 0.18	5.91 ± 0.04	6.03 ± 0.12	4.5	72.1
73a	2-carboxamide-6-methyl- pyridin-5-yl (Cis, s.e.1)	8.90 ± 0.08	5.94 ± 0.01	5.56 ± 0.17	3.6	115.2
74a	2-carboxy-6-methyl- pyridin-5-yl (Cis, s.e.1)	7.44 ± 0.17	5.12 ± 0.01	5.00 ± 0.01	4.4	109.4

s.e. 1= single enantiomer 1; rac.= racemate; NT= Not tested; values shown are the average of three replicates and standard deviation.

Table 7. Affinity data at the D3R and D2R and potency data at the hERG ion channel for derivatives **75-85a**

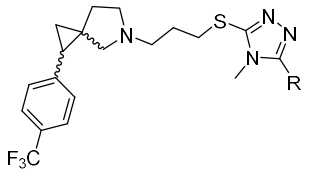

Entry	R	hD3 pKi	hD2 pKi	hERG pIC_{50}	cLogP	PSA
75	[1,2-dihydropyridin-2-one]-5-yl (Cis, rac.)	8.28 ± 0.02	6.12 ± 0.03	< 5.0	3.3	88.3
75a	[1,2-dihydropyridin-2-one]-5-yl (Cis, s.e.1)	8.66 ± 0.14	6.47 ± 0.04	5.02 ± 0.01	3.3	88.3
76	[1,2-dihydropyridin-2-one]-4-yl (Cis, rac.)	8.34 ± 0.10	5.84 ± 0.07	5.46 ± 0.08	3.3	88.3
77a	1-Me-[1,2-dihydropyridin-2-one]-5-yl (Cis, s.e.1)	8.76 ± 0.08	6.06 ± 0.01	5.50 ± 0.02	3.6	79.6
78a	1-Me-[1,2-dihydropyridin-2-one]-4-yl (Cis, s.e.1)	8.23 ± 0.05	5.65 ± 0.01	5.10 ± 0.08	3.6	79.6
79a	4-piperidinyl-2-one (Cis, s.e.1)	8.06 ± 0.19	5.87 ± 0.01	< 5.0	2.8	88.4
80a	1-Me-[4-piperidinyl-2-one] (Cis, s.e.1)	7.94 ± 0.15	5.77 ± 0.01	< 5.0	3.1	79.6
81a	[piperidin-4-yl]ethan-1-one (Cis, s.e.1)	8.13 ± 0.21	6.00 ± 0.04	5.48 ± 0.07	3.2	79.6
82a	4-cyclohexyl-yl-1-acetamide (Cis, s.e.1)	8.56 ± 0.13	6.34 ± 0.01	5.16 ± 0.01	3.9	88.3
83a	tetrahydropyran-4-yl (Cis, s.e.1)	8.78 ± 0.15	6.09 ± 0.02	5.53 ± 0.05	3.9	68.5
84a	8-oxabicyclo[3.2.1]octan-3-yl (Cis, s.e.1)	8.49 ± 0.10	6.13 ± 0.06	5.61 ± 0.07	4.5	68.5
85a	cyclohexyl (Cis, s.e.1)	9.56 ± 0.17	6.23 ± 0.15	6.53 ± 0.05	5.6	72.1

s.e. 1= single enantiomer 1; rac.= racemate; NT= Not tested; values shown are the average of three replicates and standard deviation.

Table 8. Affinity data at the D3R and D2R and functional data for selected derivatives

Entry	hD3 pKi	hD2 pKi	hD3 f-pKi	hD2 f-pKi
8b	8.26 ± 0.20	6.10 ± 0.11	8.18 ± 0.09	6.17 ± 0.16
10a	9.20 ± 0.12	6.67 ± 0.04	9.14 ± 0.11	7.13 ± 0.08
12	7.02 ± 0.20	6.28 ± 0.04	7.27± 0.09	6.30 ± 0.06
13	7.34 ± 0.04	6.01 ± 0.05	7.67± 0.22	5.87 ± 0.11
17b	9.04 ± 0.12	6.62 ± 0.01	9.28 ± 0.05	7.24 ± 0.08
19b	9.09 ± 0.01	6.59 ± 0.01	9.48 ± 0.17	7.18 ± 0.19
20b	8.21 ± 0.22	6.01 ± 0.04	8.18 ± 0.24	6.10 ± 0.10
21b	9.38 ± 0.09	6.65 ± 0.04	9.24 ± 0.02	7.59 ± 0.05
32	8.50 ± 0.07	6.89 ± 0.14	8.84 ± 0.13	6.21 ± 0.05
33	9.24 ± 0.20	6.48 ± 0.11	9.27 ± 0.03	6.79 ± 0.10
40a	9.80 ± 0.03	6.45 ± 0.01	9.41 ± 0.24	6.37 ± 0.01
41a	9.33 ± 0.14	6.20 ± 0.01	9.25 ± 0.08	6.47 ± 0.07
47a	10.17 ± 0.05	6.44 ± 0.01	9.72 ± 0.12	6.17 ± 0.05
48a	9.74 ± 0.20	6.30 ± 0.07	9.44 ± 0.10	5.93 ± 0.02
54	9.10 ± 0.19	6.28 ± 0.02	9.10 ± 0.05	6.97 ± 0.14
65b	8.89 ± 0.08	6.28 ± 0.01	8.83 ± 0.08	6.41± 0.07
71a	9.47 ± 0.18	6.26 ± 0.03	9.28 ± 0.03	6.32± 0.04
73a	8.90 ± 0.08	5.94 ± 0.01	9.17 ± 0.10	5.68± 0.09
78a	8.23 ± 0.05	5.65 ± 0.01	8.39 ± 0.18	5.73± 0.11
81a	8.13 ± 0.21	6.00 ± 0.04	8.58 ± 0.31	5.93 ± 0.10
83a	8.78 ± 0.15	6.09 ± 0.02	8.83 ± 0.11	6.16 ± 0.05
84a	8.49 ± 0.10	6.13 ± 0.06	8.68 ± 0.17	6.27 ± 0.07
85a	9.56 ± 0.17	6.23 ± 0.15	9.45 ± 0.05	6.91 ± 0.08

NT= Not tested; values shown are the average of three replicates and standard deviation.

Table 9. Selected *in vitro* PK parameters

Entry	rCli*	hCli*	Fu_{br} (%)	Fu_{bl} (%)
9a	161	22	4.8	12
10a	83	86	9.5	10.2
17b	73	37	27	38
19b	161	53	28	33
20b	23	20	4.4	7.9
21b	59	107	5.3	5.1
22a	51	65	8.9	12.3
23b	151	320	8.6	13.5
40a	41	155	4.4	14.1
41a	92	187	3.7	6.7
46a	22	58	5.2	14.1
47a	276	352	1.0	1.2
48a	100	447	0.7	0.4
64b	288	485	7.7	16.1
65b	253	257	24	> 50
66b	75	91	26	> 50
67a	103	80	6.2	18.6
68a	114	302	2.2	7.5
71a	29	106	5.2	18.4
72a	98	299	4.5	12.6
73a	38	299	7.8	19.0
74a	< 11	< 11	23	29.9
75a	14	28	8	19.1
77a	16	41	10.8	25
78a	27	40	14.6	16.7
79a	< 11	25	17.8	23.4

81a	17	61	11.8	20
83a	59	34	9.7	18.8
84a	21.3	50	5.6	12.4
85a	201	339	0.6	1.7

NT= Not tested; Data are reported ± s.d.

* μL/min/mg protein

Table 10. Selected *in vitro* PK parameters

Entry	F_a (%)	E_H	Cl_b(mL/min/kg)	V_{ss} (L/kg)	$T_{1/2}$ (h)	F (%)	AUC BB ratio
20b	70	0.31	32.9	4.9	2.3	49	1.6
21b	9	0.56	15.1	0.49	0.4	4	0.8
71a	40	0.35	19.4	3.2	2.2	26	0.3
73a	54	0.28	21.1	5.5	4.3	39	1.5
75a	1	NC	48.0	9.1	3.4	2	NC
77a	17	0.4	30.2	4.0	1.9	10	0.4
78a	41	0.3	34.6	3.5	1.5	30	0.2
81a	28	0.0	39.8	6.0	2.5	33	0.5
83a	57	0.8	87.3	3.7	0.6	11	0.3
84a	NT	NT	80.0	2.6	NT	NT	NT

NT= Not tested; Data are reported ± s.d. NC: not calculated

Table 11. Affinity data at the D3R and D2R, muscarinic M1 and M3 receptors and hERG channel, for selected derivatives

Entry	hD3 pKi	hD2 pKi	hERG	M1 fpKi	M3 fpKi
8b	8.26 ± 0.20	6.10 ± 0.11	5.33 ± 0.20	6.13 ± 0.11	5.69 ± 0.25
9a	8.40 ± 0.03	6.05 ± 0.08	6.72 ± 0.13	6.32 ± 0.15	5.94 ± 0.08
10a	9.20 ± 0.12	6.67 ± 0.04	6.39 ± 0.09	6.51 ± 0.04	6.56 ± 0.11
20b	8.21 ± 0.22	*6.10 ± 0.10*	6.35 ± 0.14	6.86 ± 0.04	6.26 ± 0.05
21b	9.38 ± 0.09	6.65 ± 0.04	6.65 ± 0.04	6.49± 0.06	6.37 ± 0.03
22a	8.98 ± 0.13	6.78 ± 0.02	5.92 ± 0.19	6.25 ± 0.01	5.68 ± 0.11
23b	8.17 ± 0.05	5.89 ± 0.03	5.57 ± 0.24	6.41 ± 0.01	5.83 ± 0.08
32	8.50 ± 0.07	6.89 ± 0.14	< 5.0	6.77 ± 0.18	6.56 ± 0.07
40a	9.80 ± 0.03	6.45 ± 0.01	6.09 ± 0.07	6.34 ± 0.05	6.37 ± 0.08
41a	9.33 ± 0.14	6.20 ± 0.01	5.55 ± 0.05	6.58 ± 0.16	6.42 ± 0.10
47a	10.17 ± 0.05	6.44 ± 0.01	6.82 ± 0.01	6.17 ± 0.01	6.52 ± 0.11
67a	8.48 ± 0.13	5.83 ± 0.01	5.20 ± 0.05	5.78 ± 0.14	5.91 ± 0.07
71a	9.47 ± 0.18	6.26 ± 0.03	6.18 ± 0.13	6.65 ± 0.05	6.72 ± 0.04
73a	8.90 ± 0.08	5.94 ± 0.01	5.56 ± 0.17	6.29 ± 0.08	6.73 ± 0.08
75a	8.66 ± 0.14	6.47 ± 0.04	5.02 ± 0.01	6.31 ± 0.01	6.20 ± 0.03
76	8.34 ± 0.10	5.84 ± 0.07	5.46 ± 0.08	6.43 ± 0.04	6.17 ± 0.22
78a	8.23 ± 0.05	5.65 ± 0.01	5.10 ± 0.08	6.52 ± 0.18	6.45 ± 0.16
81a	8.13 ± 0.21	6.00 ± 0.04	5.48 ± 0.07	7.18 ± 0.20	6.17 ± 0.22
82a	8.56 ± 0.13	6.34 ± 0.01	5.16 ± 0.01	6.76 ± 0.18	6.64 ± 0.01
83a	8.78 ± 0.15	6.09 ± 0.02	5.53 ± 0.05	6.60 ± 0.09	6.05 ± 0.06

Values shown are the average of three replicates and standard deviation.

FIGURE CAPTIONS

Figure 1. Structures of known and new D3R antagonists.

Figure 2. A schematic model of the D3R pharmacophore described in the early 2000 with aligned with derivative **1**.

Figure 3. Relevant interactions of derivative **2** (yellow) and **10a** (red) in docking to the D3R model. Portions of the backbone ribbon have been removed for clarity. The interaction of the basic nitrogen of the amine portion of the two compounds with $Asp^{3, 32}$ is clearly visible. The region of the thiotriazole and of the oxazole portion clearly points towards the EL. The new 5-Azaspiro[2.4]heptanes seem to direct the $–CF_3$ moiety of derivative **10a** in a similar hydrophobic region in common to compound **2**.

Figure 4. Derivatives **40a** (Cyan), **41a** (mustard) and **42a** (red) docking to the D3R model. Portions of the backbone ribbon have been removed for clarity. The interaction of the basic nitrogen of the amine portion of the two compounds with $Asp^{3,32}$ is clearly visible.

Figure 5. A) Left: asymmetric unit of 5-(4-methylbenzenesulfonyl)-(1R,3S)-[4-(trifluoromethyl)phenyl]-5-azaspiro[2.4]heptane (**87**) comprising four molecular entities, right: molecular structure of (**87**), with thermal ellipsoids drawn at the 50% probability level. B) Left: asymmetric unit of 5-(4-methylbenzenesulfonyl)-(1S,3R)-[4-(trifluoromethyl)phenyl]-5-azaspiro[2.4]heptane (**89**) comprising four molecular entities; right: molecular structure of (**89**), with thermal ellipsoids drawn at the 50% probability level.

SCHEME CAPTIONS

Scheme 1.

i: MnO_2, dioxane, RT; ii: 2M $LiAlH_4$ THF, reflux; iii: H_2, NH_4COOH, Pd/C, MeOH, reflux; iv: T3P in AcOEt, 4-methyl-3-thiosemicarbazide, NaOH; v: K_2CO_3/acetone, RT; vi: Na_2CO_3, NaI, DMF or CH_3CN, 60 ^0C.

Figure 1.

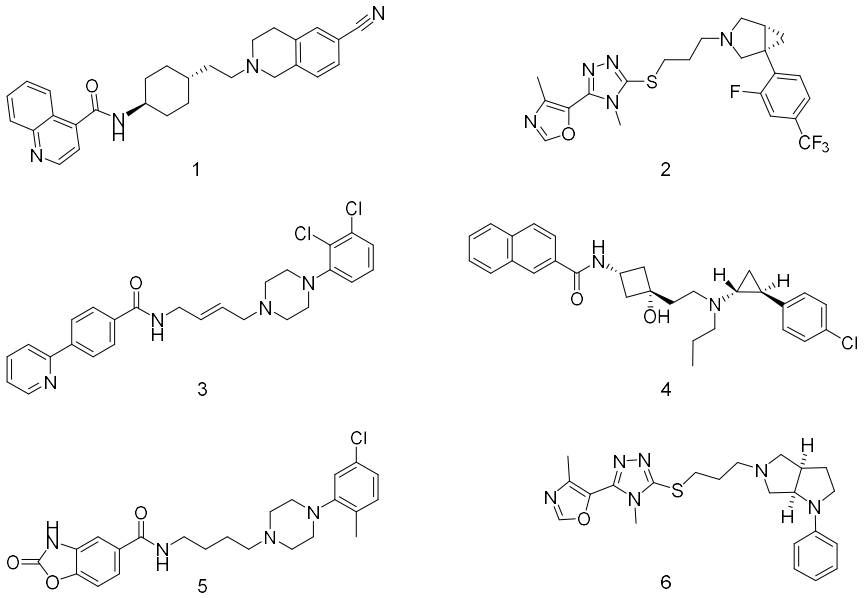

Figure 2

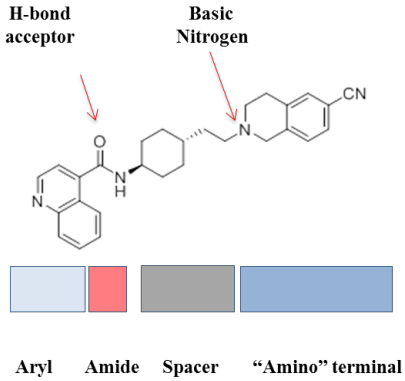
H-bond acceptor
Basic Nitrogen
CN
O
N
H
N
Aryl
Amide
Spacer
"Amino" terminal

Figure 3

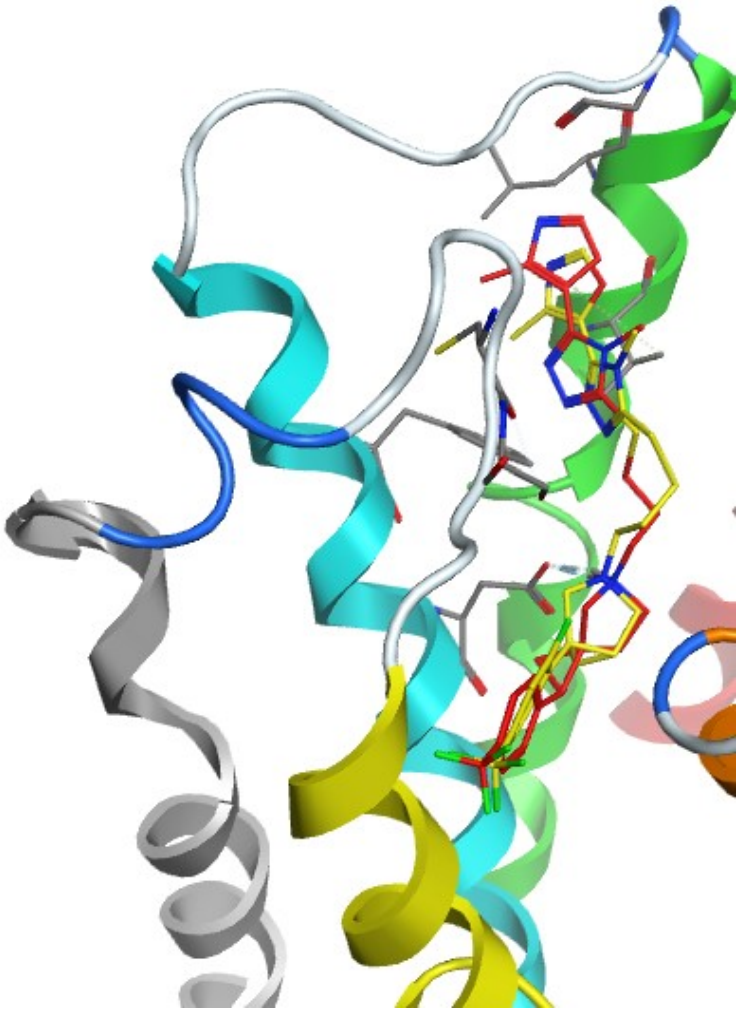

100

Figure 4

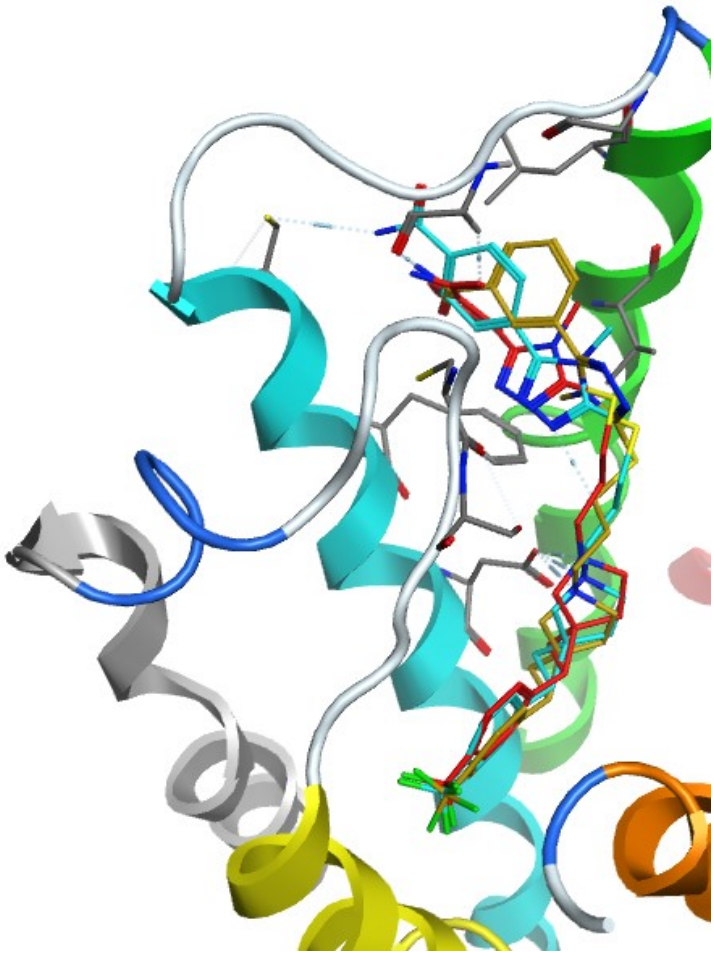

Figure 5

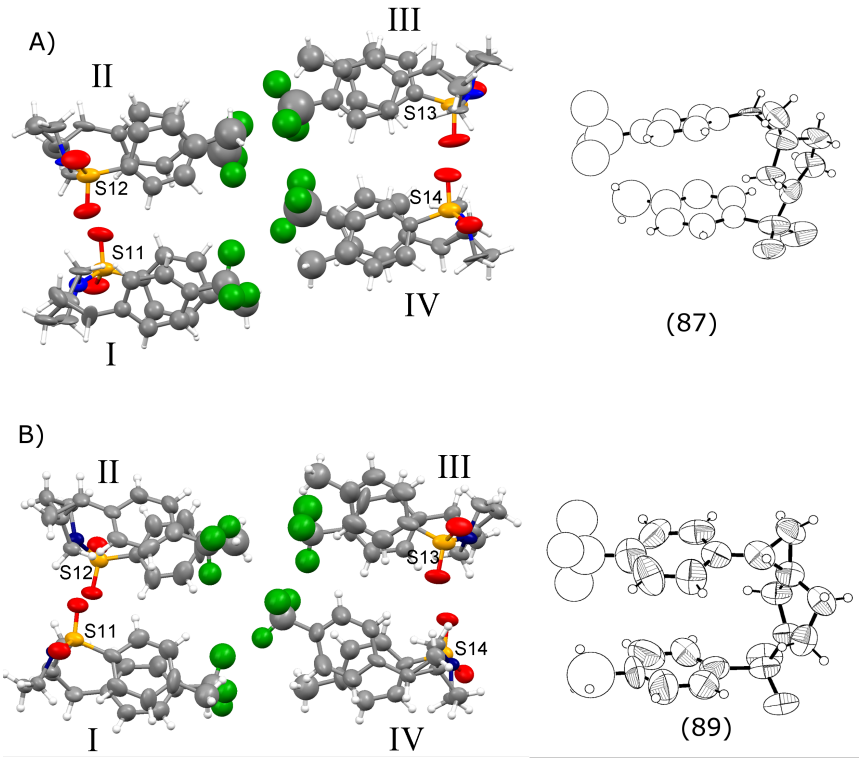

Scheme 1

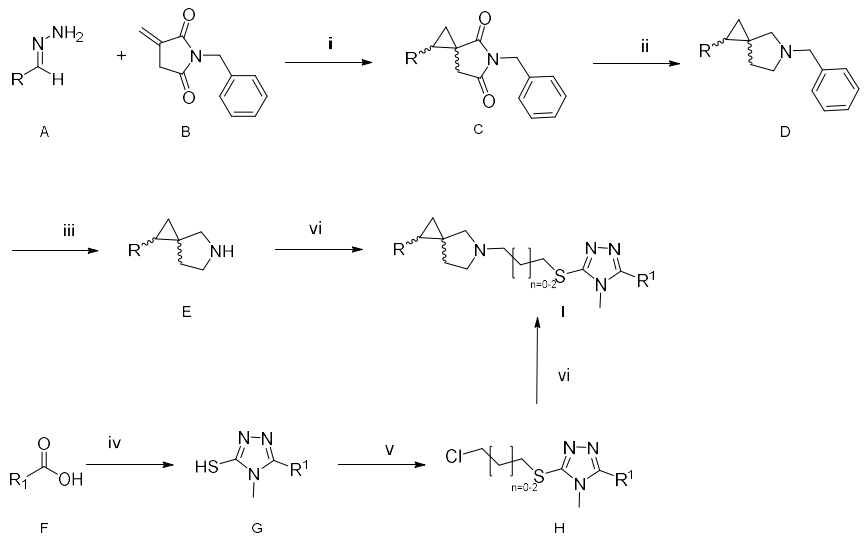

Table of Contents Graphic

1,2,4-Triazolyl 5-Azaspiro[2.4]heptanes: Lead Identification and Early Lead Optimization of a New Series of Potent and Selective Dopamine D3 Receptor Antagonists.

*Fabrizio Micheli**[a], Alessia Bacchi[#], Simone Braggio[a], Laura Castelletti[a], Palmina Cavallini[a], Paolo Cavanni[a], Susanna Cremonesi[a], Michele Dal Cin[a], Aldo Feriani[a], Sylvie Gehanne[a], Mahmoud Kajbaf[a], Luciano Marchió[#], Selena Nola[a], Beatrice Oliosi[a], Annalisa Pellacani[a], Elisabetta Perdona' [a], Anna Sava[a], Teresa Semeraro[a], Luca Tarsi[a], Silvia Tomelleri[a], Andrea Wong[a], Filippo Visentini[a], Laura Zonzini[a], and Christian Heidbreder[b].*